Published for SISSA by Springer

Received: *December 18, 2013*
Accepted: *February 1, 2014*
Published: *February 26, 2014*

331 models facing new $b \to s\mu^+\mu^-$ data

Andrzej J. Buras,[a,b] Fulvia De Fazio[c] and Jennifer Girrbach[a,b]

[a] *TUM Institute for Advanced Study, Lichtenbergstr. 2a, D-85747 Garching, Germany*
[b] *Physik Department, Technische Universität München, James-Franck-Straße, D-85747 Garching, Germany*
[c] *Istituto Nazionale di Fisica Nucleare, Sezione di Bari, Via Orabona 4, I-70126 Bari, Italy*

E-mail: andrzej.buras@tum.de, fulvia.defazio@ba.infn.it, jennifer.girrbach@tum.de

Abstract: We investigate how the 331 models, based on the gauge group $\mathrm{SU}(3)_C \times \mathrm{SU}(3)_L \times \mathrm{U}(1)_X$ face new data on $B_{s,d} \to \mu^+\mu^-$ and $B_d \to K^*(K)\mu^+\mu^-$ taking into account present constraints from $\Delta F = 2$ observables, low energy precision measurements, LEP-II and the LHC data. In these models new sources of flavour and CP violation originate dominantly through flavour violating interactions of ordinary quarks and leptons with a new heavy Z' gauge boson. The strength of the relevant couplings is governed by four new parameters in the quark sector and the parameter β which in these models determines the charges of new heavy fermions and gauge bosons. We study the implications of these models for $\beta = \pm n/\sqrt{3}$ with $n = 1, 2, 3$. The case $\beta = -\sqrt{3}$ leading to Landau singularities for $M_{Z'} \approx 4\,TeV$ can be ruled out when the present constraints on Z' couplings, in particular from LEP-II, are taken into account. For $n = 1, 2$ interesting results are found for $M_{Z'} < 4\,TeV$ with largest NP effects for $\beta < 0$ in $B_d \to K^*\mu^+\mu^-$ and the ones in $B_{s,d} \to \mu^+\mu^-$ for $\beta > 0$. As $\mathrm{Re}(\mathrm{C}_9^{\mathrm{NP}})$ can reach the values -0.8 and -0.4 for $n = 2$ and $n = 1$, respectively the $B_d \to K^*\mu^+\mu^-$ anomalies can be softened with the size depending on $\Delta M_s/(\Delta M_s)_{\mathrm{SM}}$ and the CP-asymmetry $S_{\psi\phi}$. A correlation between $\mathrm{Re}(\mathrm{C}_9^{\mathrm{NP}})$ and $\overline{\mathcal{B}}(B_s \to \mu^+\mu^-)$, identified for $\beta < 0$, implies for *negative* $\mathrm{Re}(\mathrm{C}_9^{\mathrm{NP}})$ uniquely suppression of $\overline{\mathcal{B}}(B_s \to \mu^+\mu^-)$ relative to its SM value which is favoured by the data. In turn also $S_{\psi\phi} < S_{\psi\phi}^{\mathrm{SM}}$ is favoured with $S_{\psi\phi}$ having dominantly opposite sign to $S_{\psi\phi}^{\mathrm{SM}}$ and closer to its central experimental value. Another triple correlation is the one between $\mathrm{Re}(\mathrm{C}_9^{\mathrm{NP}})$, $\overline{\mathcal{B}}(B_s \to \mu^+\mu^-)$ and $\mathcal{B}(B_d \to K\mu^+\mu^-)$. NP effects in $b \to s\nu\bar\nu$ transitions, $K^+ \to \pi^+\nu\bar\nu$ and $K_L \to \pi^0\nu\bar\nu$ turn out to be small. We find that the absence of $B_d \to K^*\mu^+\mu^-$ anomalies in the future data and confirmation of the suppression of $\overline{\mathcal{B}}(B_s \to \mu^+\mu^-)$ relative to its SM value would favour $\beta = 1/\sqrt{3}$ and $M_{Z'} \approx 3\,TeV$. Assuming lepton universality, we find an upper bound $|C_9^{\mathrm{NP}}| \le 1.1(1.4)$ from LEP-II data for *all* Z' models with only left-handed flavour violating couplings to quarks when NP contributions to ΔM_s at the level of 10%(15%) are allowed.

Keywords: Rare Decays, Beyond Standard Model, B-Physics

ArXiv ePrint: 1311.6729

doi:10.1007/JHEP02(2014)112

JHEP02(2014)112

Contents

1 Introduction

The great expectations to find New Physics (NP) at the LHC did not materialize until now. In particular the order of magnitude enhancements of the branching ratio for $B_s \to \mu^+\mu^-$ decay over its Standard Model (SM) value, possible in supersymmetric models and models with tree-level heavy neutral scalar and pseudoscalar exchanges, are presently ruled out. This is also the case of $\mathcal{O}(1)$ values of the CP-asymmetry $S_{\psi\phi}$ which could also be accommodated in these models. A recent review can be found in [1].

While for the models in question these new flavour data are a big disappointment, for other models like the ones with constrained minimal flavour violation (CMFV), 331 models [2] and Littlest Higgs Model with T-parity [3] they brought a relief as in these models NP effects were naturally predicted to be small. On the other hand the most recent data from LHCb and CMS bring new challenges for the latter models:

- The LHCb and CMS collaborations presented new results on $B_{s,d} \to \mu^+\mu^-$ [4–6]. While the branching ratio for $B_s \to \mu^+\mu^-$ as stated above turns out to be rather close to the SM prediction, although a bit lower than the latter, the central value for the one of $B_d \to \mu^+\mu^-$ is by a factor of 3.5 higher than its SM value. While this result invites us to speculate about NP behind it, the large experimental error precludes any clear cut conclusions.

- LHCb collaboration reported new results on angular observables in $B_d \to K^*\mu^+\mu^-$ that show departures from SM expectations [7, 8]. Moreover, new data on the observable F_L, consistent with LHCb value in [7] have been presented by CMS [9].

In particular the anomalies in $B_d \to K^*\mu^+\mu^-$ triggered two sophisticated analyses [10, 11] with the goal to understand the data and to indicate what type of NP could be responsible for these departures from the SM. Subsequently several other analyses of these data have been presented in [12–17] and very recently in [18].

The outcome of these efforts can be summarized briefly as follows. There seems to be a consensus among different groups that NP definitely affects the Wilson coefficient C_9 [10, 11, 13, 17, 18] with the value of the shift in C_9 depending on the analysis considered:

$$-1.9 \le C_9^{\rm NP} \le -0.5. \tag{1.1}$$

There is also a consensus that small negative NP contributions to the the Wilson coefficient $C_{7\gamma}$ could together with $C_9^{\rm NP}$ provide the explanation of the data [10, 11]. On the other hand as seen in the analyses in [11, 13, 17], a particularly successful scenario is the one with participation of right-handed currents

$$C_9^{\rm NP} < 0, \qquad C_9' > 0, \qquad C_9' \approx -C_9^{\rm NP}. \tag{1.2}$$

However a very recent analysis in [18] challenges this solution favouring the one with NP contributions dominantly represented by $C_9^{\rm NP} \approx -1.5$ with much smaller NP contributions to the remaining Wilson coefficients, in particular C_9'.

JHEP02(2014)112

For the models presented here sorting out these differences is important as in these models $C_9' = 0$ and as demonstrated in [2, 19] NP contributions to $C_{7\gamma}$ are totally negligible. Thus $C_9^{\rm NP}$ remains the only coefficient which could help in explaining the $B_d \to K^* \mu^+\mu^-$ anomalies. In our view this is certainly not excluded [10, 12–15, 18], in particular if these anomalies would soften with time. It should be emphasized at this point that these analyses are subject to theoretical uncertainties, which have been discussed at length in [10, 20–24] and it remains to be seen whether the observed anomalies are only result of statistical fluctuations and/or underestimated theoretical uncertainties.

Assuming that indeed NP is at work here, one of the physical mechanisms behind these deviations that seems to emerge from these studies is the presence of tree-level Z' exchanges. In [19] we have presented an anatomy of Z' contributions to flavour changing neutral current processes (FCNC) identifying various correlations between various observables characteristic for this NP scenario. Recently we have analyzed how this scenario faces the new data listed above [13] including the correlation with the values of $C_{B_q} = \Delta M_q/(\Delta M_q)_{\rm SM}$, $S_{\psi\phi}$ and $S_{\psi K_S}$ which should be precisely determined in this decade.

The dominant role in [13] was played by the so-called l.h.s. scenario in which the flavour violating couplings of Z' to quarks were purely left-handed. While, in agreement with [11] and recently with [17] it has been found that the presence of right-handed couplings leading to a non-vanishing C_9' gives a better description of the data than the l.h.s. scenario, it is clear that in view of theoretical and experimental uncertainties the l.h.s. scenario remains as a viable alternative.

The nice virtue of the l.h.s. scenario is that for certain choices of the Z' couplings the model resembles the structure of CMFV or models with $\mathrm{U(2)}^3$ flavour symmetry. Moreover as no new operators beyond those present in the SM are present, the non-perturbative uncertainties are the same as in the SM, still allowing for non-MFV contributions beyond those present in $\mathrm{U(2)}^3$ models. In particular the stringent CMFV relation between $\Delta M_{s,d}$ and $\mathcal{B}(B_{s,d} \to \mu^+\mu^-)$ [25] valid in the simplest $\mathrm{U(2)}^3$ models is violated in the l.h.s. scenario as analyzed in detail in [13]. Another virtue of the l.h.s. scenario is the paucity of its parameters that enter all flavour observables in a given meson system which should be contrasted with most NP scenarios outside the MFV framework. Indeed, if we concentrate on $B_s^0 - \bar B_s^0$ mixing, $b \to s\mu^+\mu^-$ and $b \to s\nu\bar\nu$ observables, for a given mass $M_{Z'}$ there are only four new parameters to our disposal: the three couplings (our normalizations of couplings are given in section 2)

$$\Delta_L^{sb}(Z'), \quad \Delta_A^{\mu\bar\mu}(Z'), \quad \Delta_V^{\mu\bar\mu}(Z'), \tag{1.3}$$

of which the first one is generally complex and the other two real. The couplings $\Delta_{A,V}^{\mu\bar\mu}(Z')$ are defined in (2.13) and due to $\mathrm{SU(2)}_L$ symmetry implying in l.h.s. $\Delta_L^{\nu\bar\nu}(Z') = \Delta_L^{\mu\bar\mu}(Z')$ one also has

$$\Delta_L^{\nu\bar\nu}(Z') = \frac{\Delta_V^{\mu\bar\mu}(Z') - \Delta_A^{\mu\bar\mu}(Z')}{2}. \tag{1.4}$$

Extending these considerations to B_d and K meson systems brings in four additional parameters, the complex couplings:

$$\Delta_L^{db}(Z'), \qquad \Delta_L^{sd}(Z'). \tag{1.5}$$

JHEP02(2014)112

Thus in this general l.h.s. scenario we deal with eight new parameters. Further reduction of parameters is only possible in a concrete dynamical model. In this context an interesting class of dynamical models representing l.h.s. scenario are the 331 models based on the gauge group $SU(3)_C \times SU(3)_L \times U(1)_X$ [26, 27]. A detailed analysis of FCNC processes in one of these models has been presented by us in [2]. Selection of earlier analyses of various aspects of these models related to our paper can be found in [28–37].

The nice feature of these models is a small number of free parameters which is lower than present in the general l.h.s. scenario considered in [13, 19]. This allows to find certain correlations between different meson systems which is not possible in the general case. Indeed the strength of the relevant Z' couplings to down-quarks is governed by two mixing parameters, two CP-violating phases and the parameter β which defines[1] a given 331 model and determines the charges of new heavy fermions and gauge bosons. Thus for a given $M_{Z'}$ and β there are only four free parameters to our disposal. In particular for a given β, the couplings of Z' to leptons are fixed. As evident from the general analysis of l.h.s. scenario in [13], knowing the latter couplings simplifies the analysis significantly, increasing simultaneously the predictive power of the theory.

In [2] the relevant couplings have been presented for arbitrary β but the detailed FCNC analysis has been only performed for $\beta = 1/\sqrt{3}$. While this model provides interesting results for $B_{s,d} \to \mu^+\mu^-$, it fails in the case of anomalies in $B_d \to K^*\mu^+\mu^-$ because in this model the coupling $\Delta_V^{\mu\bar{\mu}}(Z')$ and consequently the Wilson coefficient $C_9^{\rm NP}$ turn out to be very small.

It has been pointed out recently in [14] that for $\beta = -\sqrt{3}$ a very different picture arises. Indeed in this case $\Delta_V^{\mu\bar{\mu}}(Z')$ is much larger than for $\beta = 1/\sqrt{3}$ so that the $B_d \to K^*\mu^+\mu^-$ anomaly can be in principle successfully addressed. Simultaneously the coupling $\Delta_A^{\mu\bar{\mu}}(Z')$ turns out to be small so that NP contributions to $B_s \to \mu^+\mu^-$ are small in agreement with the data. Moreover aligning the new mixing matrix V_L with the CKM matrix, the authors end up with a very simple model in which the only new parameter relevant for their analysis is $M_{Z'}$ and the negative sign of $C_9^{\rm NP}$ required by the $B_d \to K^*\mu^+\mu^-$ anomaly is uniquely predicted.

Unfortunately this model has several problems, in particular in the MFV limit considered in [14], which in our view eliminates it as a valid description of the present flavour data. As discussed in appendix C these problems originate in the known fact that the 331 models with $\beta = \pm\sqrt{3}$ imply a Landau singularity for $\sin^2\theta_W = 0.25$ and this value is reached through the renormalization group evolution of the SM couplings for $M_{Z'}$ typically around 4 TeV, scales not much higher than the present lower bounds on $M_{Z'}$.

Yet, the observation of the authors of [14] that negative values of β could provide solution to $B_d \to K^*\mu^+\mu^-$ anomalies motivates us to generalize our phenomenological analysis of 331 model in [2] from $\beta = 1/\sqrt{3}$ to arbitrary values of β, both positive and negative, for which the Landau singularity in question is avoided up to the very high scales, even as high as GUTs scales. This generalization is in fact straight forward as in [2] we

[1] Up to the choice of the representation of the gauge group according to which the fermions should transform, as will be better clarified in the next section.

JHEP02(2014)112

have provided formulae for the Z' couplings to quarks and leptons for arbitrary β[2] and the expressions for various flavour observables as functions of β can be directly obtained from the formulae of that paper. In this context we will concentrate our analysis on the cases $\beta = \pm n/\sqrt{3}$ with $n = 1, 2$ choosing $M_{Z'} = 3\,\mathrm{TeV}$ in order to satisfy existing bounds from flavour conserving observables. A simple scaling law allows then to obtain predictions for other values of $M_{Z'}$.

However, in contrast to our numerical analysis in [2] which assumed certain fixed values of $\sqrt{\hat{B}_{B_s}}F_{B_s}$ and $\sqrt{\hat{B}_{B_d}}F_{B_d}$ we will investigate in the spirit of our recent paper [13] how our results depend on

$$C_{B_q} = \frac{\Delta M_q}{(\Delta M_q)_{\rm SM}}, \qquad S_{\psi\phi}, \qquad S_{\psi K_S} \tag{1.6}$$

which should be precisely determined in this decade.

Our paper is organized as follows. In section 2 we review very briefly the basic aspects of 331 models, recalling their free parameters and the general formulae for the couplings of Z' to quarks and leptons for arbitrary β. We also present a table with the values of flavour diagonal couplings of Z' to quarks and leptons for $n = 1, 2, 3$ which should facilitate other researchers to test precisely these models in processes not considered by us. In section 3 we collect formulae for various Wilson coefficients and one-loop master functions in terms of the couplings of section 2. This will allow us to identify certain properties and correlations between various observables that will be explicitly seen in our numerical analysis. As all relevant formulae for various branching ratios and other observables have been presented in [2] we recall in section 4 only crucial observables and their status in the SM and experiment. The strategy for our analysis is presented in section 5 and its execution in section 6. In section 7 we present predictions for low energy precision observables which could provide additional tests of the models considered and analyse also the bounds from LEP-II. We also comment on the bounds on $M_{Z'}$ from the LHC. We summarize the main results of our paper in section 8. Some useful information can also be found in three appendices.

2 The 331 models and their couplings

2.1 The 331 models

The name 331 encompasses a class of models based on the gauge group $\mathrm{SU}(3)_C \times \mathrm{SU}(3)_L \times \mathrm{U}(1)_X$ [26, 27], that is at first spontaneously broken to the SM group $\mathrm{SU}(3)_C \times \mathrm{SU}(2)_L \times \mathrm{U}(1)_Y$ and then undergoes the spontaneous symmetry breaking to $\mathrm{SU}(3)_C \times \mathrm{U}(1)_Q$. The extension of the gauge group with respect to SM leads to interesting consequences. The first one is that the requirement of anomaly cancellation together with that of asymptotic freedom of QCD implies that the number of generations must necessarily be equal to the number of colours, hence giving an explanation for the existence of three generations. Furthermore, quark generations should transform differently under the action of $\mathrm{SU}(3)_L$.

[2]See also [31].

In particular, two quark generations should transform as triplets, one as an antitriplet. Choosing the latter to be the third generation, this different treatment could be at the origin of the large top quark mass. This choice imposes that the leptons should transform as antitriplets. However, one could choose a different scenario in which the role of triplets and antitriplets is exchanged, provided that the number of triplets equals that of antitriplets, in order to fulfil the anomaly cancellation requirement. Therefore, different versions of the model are obtained according to the way one fixes the fermion representations. The fermion representations for specific 331 models analyzed in our paper are described in detail in [2].

A fundamental relation holds among some of the generators of the group:

$$Q = T_3 + \beta T_8 + X, \tag{2.1}$$

where Q indicates the electric charge, T_3 and T_8 are two of the SU(3) generators and X is the generator of $\mathrm{U}(1)_X$. β is a key parameter that defines a specific variant of the model. The 331 models comprise several new particles. There are new gauge bosons Y and V and new heavy fermions, all with electric charges depending on β. Also the Higgs system is extended.

As analyzed in detail in [31] and stated in that paper β can be arbitrary. Yet due to the fact that in 331 models

$$M_{Z'}^2 = \frac{g^2 u^2 c_W^2}{3[1-(1+\beta^2)s_W^2]} \tag{2.2}$$

where u is the vacuum expectation value related to the first symmetry breaking it is evident that only values of β satisfying

$$[1-(1+\beta^2)s_W^2] > 0 \tag{2.3}$$

are allowed. With the known value of s_W^2 this means that

$$|\beta| \le \sqrt{3} \tag{2.4}$$

and in fact the only explicit models analyzed in the literature are the ones with $\beta = \pm 1/\sqrt{3}$ and $\beta = \pm\sqrt{3}$. But only for $\beta = \pm 1/\sqrt{3}$ one can avoid the presence of exotic charges both in the fermion and gauge boson sectors. If one considers only

$$\beta = \pm\frac{n}{\sqrt{3}}, \qquad n = 1,2,3 \tag{2.5}$$

then for $n = 1$ there are singly charged $Y^\pm$ bosons and neutral ones $V^0(\bar{V}^0)$, while for $n = 3$ one finds instead two new singly charged bosons $V^\pm$ and two doubly charged ones $Y^{\pm\pm}$. For $n = 2$ exotic charges $\pm 1/2$ and $\pm 3/2$ for gauge bosons are found. From table 1 in [2] we also find that while for $n = 1$ no exotic charges for heavy fermions are present, for $n = 2$ heavy quarks carry exotic electric charges $\pm 5/6$ and $\pm 7/6$ while heavy leptons $\pm 1/2$ and $\pm 3/2$. Discovering such fermions at the LHC would be a spectacular event. We refer to [2] for further details. In principle β could be a continuous variable satisfying (2.4) but in the present paper we will only consider the cases $n = 1,2,3$.

Most importantly for our paper for all β a new neutral gauge boson Z' is present. This represents a very appealing feature, since Z' mediates tree level flavour changing neutral currents (FCNC) in the quark sector and could be responsible for the recent anomalies as indicated by their recent extensive analyses.

As in the SM, quark mass eigenstates are defined upon rotation of flavour eigenstates through two unitary matrices U_L (for up-type quarks) and V_L (for down-type quarks). The relation

$$V_{\rm CKM} = U_L^\dagger V_L \tag{2.6}$$

holds in analogy with the SM case. However, while in the SM $V_{\rm CKM}$ appears only in charged current interactions and the two rotation matrices never appear individually, this is not the case in this model and both U_L and V_L can generate tree-level FCNCs mediated by Z' in the up-quark and down-quark sector, respectively. But these two matrices have to satisfy the relation (2.6). A useful parametrization for V_L which we have used in [2] is

$$V_L = \begin{pmatrix} \tilde c_{12}\tilde c_{13} & \tilde s_{12}\tilde c_{23}e^{i\delta_3} - \tilde c_{12}\tilde s_{13}\tilde s_{23}e^{i(\delta_1-\delta_2)} & \tilde c_{12}\tilde c_{23}\tilde s_{13}e^{i\delta_1} + \tilde s_{12}\tilde s_{23}e^{i(\delta_2+\delta_3)} \\ -\tilde c_{13}\tilde s_{12}e^{-i\delta_3} & \tilde c_{12}\tilde c_{23} + \tilde s_{12}\tilde s_{13}\tilde s_{23}e^{i(\delta_1-\delta_2-\delta_3)} & -\tilde s_{12}\tilde s_{13}\tilde c_{23}e^{i(\delta_1-\delta_3)} - \tilde c_{12}\tilde s_{23}e^{i\delta_2} \\ -\tilde s_{13}e^{-i\delta_1} & -\tilde c_{13}\tilde s_{23}e^{-i\delta_2} & \tilde c_{13}\tilde c_{23} \end{pmatrix}. \tag{2.7}$$

This matrix implies through (2.6) new sources of flavour violation in the up-sector. However, when $U_L = \mathbb{1}$ as used in [14] $V_L = V_{\rm CKM}$ and we deal with a particular simple CMFV model.

With this parametrization, the Z' couplings to quarks, for the three meson systems, K, B_d and B_s

$$\Delta_L^{sd}(Z'), \qquad \Delta_L^{bd}(Z') \qquad \Delta_L^{bs}(Z') \tag{2.8}$$

being proportional to $v_{32}^*v_{31}$, $v_{33}^*v_{31}$ and $v_{33}^*v_{32}$, respectively, depend only on four new parameters (explicit formulae are given in [2]):

$$\tilde s_{13}, \quad \tilde s_{23}, \quad \delta_1, \quad \delta_2\,. \tag{2.9}$$

Here $\tilde s_{13}$ and $\tilde s_{23}$ are positive definite and δ_i in the range $[0, 2\pi]$. Therefore for fixed $M_{Z'}$ and β, the Z' contributions to all processes analyzed by us depend only on these parameters implying very strong correlations between NP effects to various observables. Indeed, as seen in (2.7) the B_d system involves only the parameters $\tilde s_{13}$ and δ_1 while the B_s system depends on $\tilde s_{23}$ and δ_2. Moreover, stringent correlations between observables in $B_{d,s}$ sectors and in the kaon sector are found since kaon physics depends on $\tilde s_{13}$, $\tilde s_{23}$ and $\delta_2 - \delta_1$. A very constraining feature of this models is that the diagonal couplings of Z' to quarks and leptons are fixed for a given β, except for a weak dependence on $M_{Z'}$ due to running of $\sin^2\theta_W$ provided β differs significantly from $\pm\sqrt{3}$.

2.2 The couplings

We will now recall those couplings for arbitrary β that are relevant for our paper. The expressions for other couplings and masses of new gauge bosons and fermions as well as expressions for their electric charges that depend on β can be found in [2].

Central for our analysis is the function

$$f(\beta) = \frac{1}{1-(1+\beta^2)s_W^2} > 0 \tag{2.10}$$

where the positivity of this function results from the reality of $M_{Z'}$ as stressed above.

The following properties should be noted:

- For $\beta \approx \sqrt{3}$ there is a Landau singularity for $s_W^2 = 0.25$. As at M_W one has $s_W^2 \approx 0.23$ (with exact number depending on its definition considered) and renormalization group evolution of weak couplings increases s_W^2 with increasing scale, $s_W^2(M_{Z'})$ reaches 0.25 and the singularity in question for $M_{Z'} \approx 4\,\text{TeV}$.

- For $|\beta| \leq \sqrt{3} - 0.20$ this problem does not arise even up to the GUTs scales.

While we will specifically consider only the cases $\beta = \pm n/\sqrt{3}$ with $n = 1, 2, 3$ we list here the formulae for the relevant couplings for arbitrary real $\beta \neq \sqrt{3}$ satisfying (2.4). The case $\beta = \sqrt{3}$ is considered separately in appendix A.

The important point which we would like to make here is that the couplings of Z' to quarks and leptons have to be evaluated at the scale μ at which Z' is integrated out, that is at $\mu = \mathcal{O}(M_{Z'})$ and not at M_W. For $n = 1$ this difference is irrelevant. For $n = 2$ it plays a role if acceptable precision is required and it is crucial for $n = 3$. The values of couplings listed by us and in appendix A correspond to $\mu = M_{Z'}$ with the latter specified below.

Denoting the elements of the matrix V_L in (2.7) by v_{ij}, the relevant couplings for quarks are then given as follows:

$$\Delta_L^{ij}(Z') = \frac{g}{\sqrt{3}} c_W \sqrt{f(\beta)} v_{3i}^* v_{3j}\,, \tag{2.11a}$$

$$\Delta_L^{ji}(Z') = \left[\Delta_L^{ij}(Z')\right]^\star, \qquad \Delta_L^{u\bar{u}}(Z') = \Delta_L^{d\bar{d}}(Z') \tag{2.11b}$$

$$\Delta_L^{d\bar{d}}(Z') = \frac{g}{2\sqrt{3}c_W}\sqrt{f(\beta)}\left[-1 + (1 + \frac{\beta}{\sqrt{3}})s_W^2\right], \tag{2.11c}$$

$$\Delta_R^{u\bar{u}}(Z') = \frac{g}{2\sqrt{3}c_W}\sqrt{f(\beta)}\frac{4}{\sqrt{3}}\beta s_W^2 = -2\Delta_R^{d\bar{d}}(Z')\,, \tag{2.11d}$$

$$\Delta_V^{d\bar{d}}(Z') = \frac{g}{2\sqrt{3}c_W}\sqrt{f(\beta)}\left[-1 + (1 - \frac{\beta}{\sqrt{3}})s_W^2\right], \tag{2.11e}$$

$$\Delta_A^{d\bar{d}}(Z') = \frac{g}{2\sqrt{3}c_W}\sqrt{f(\beta)}\left[1 - (1 + \sqrt{3}\beta)s_W^2\right], \tag{2.11f}$$

$$\Delta_V^{u\bar{u}}(Z') = \frac{g}{2\sqrt{3}c_W}\sqrt{f(\beta)}\left[-1 + (1 + \frac{5}{\sqrt{3}}\beta)s_W^2\right], \tag{2.11g}$$

$$\Delta_A^{u\bar{u}}(Z') = \frac{g}{2\sqrt{3}c_W}\sqrt{f(\beta)}\left[1 - (1 - \sqrt{3}\beta)s_W^2\right]. \tag{2.11h}$$

The diagonal couplings are valid for the first two generations of quarks neglecting the very small non-diagonal contributions in the matrices V_L and U_L. For the third generation there is an additional term which can be found in [2].

For leptons we have

$$\Delta_L^{\nu\bar{\nu}}(Z') = \frac{g}{2\sqrt{3}c_W}\sqrt{f(\beta)}\left[1 - (1 + \sqrt{3}\beta)s_W^2\right], \tag{2.12a}$$

$$\Delta_L^{\mu\bar{\mu}}(Z') = \Delta_L^{\nu\bar{\nu}}(Z')\,, \tag{2.12b}$$

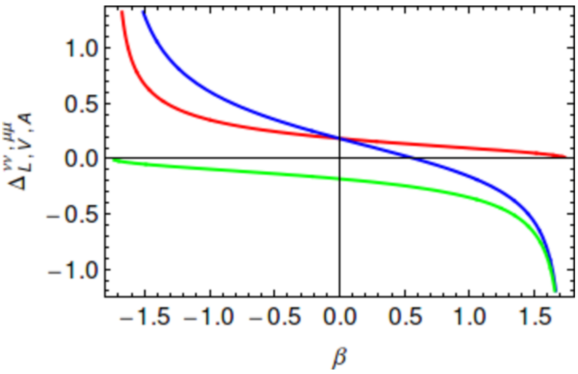

Figure 1. $\Delta_L^{\nu\bar{\nu}}(Z')$ (red), $\Delta_V^{\mu\bar{\mu}}(Z')$ (blue) and $\Delta_A^{\mu\bar{\mu}}(Z')$ (green) as functions of β for $s_W^2 = 0.249$ and $g = 0.633$. This plot applies to $\beta \neq \sqrt{3}$.

$$\Delta_R^{\mu\bar{\mu}}(Z') = \frac{-g\ \beta\ s_W^2}{c_W}\sqrt{f(\beta)} \tag{2.12c}$$

$$\Delta_V^{\mu\bar{\mu}}(Z') = \frac{g}{2\sqrt{3}c_W}\sqrt{f(\beta)}\ \left[1-(1+3\sqrt{3}\beta)s_W^2\right], \tag{2.12d}$$

$$\Delta_A^{\mu\bar{\mu}}(Z') = \frac{g}{2\sqrt{3}c_W}\sqrt{f(\beta)}\ \left[-1+(1-\sqrt{3}\beta)s_W^2\right] \tag{2.12e}$$

where we have defined

$$\begin{aligned}\Delta_V^{\mu\bar{\mu}}(Z') &= \Delta_R^{\mu\bar{\mu}}(Z') + \Delta_L^{\mu\bar{\mu}}(Z'),\\ \Delta_A^{\mu\bar{\mu}}(Z') &= \Delta_R^{\mu\bar{\mu}}(Z') - \Delta_L^{\mu\bar{\mu}}(Z').\end{aligned} \tag{2.13}$$

These definitions also apply to other leptons and quarks.

In figure 1 we show $\Delta_L^{\nu\bar{\nu}}(Z')$, $\Delta_V^{\mu\bar{\mu}}(Z')$ and $\Delta_A^{\mu\bar{\mu}}(Z')$ as functions of β for $s_W^2 = 0.249$ and $g = 0.633$ corresponding to $M_{Z'} = 3\,\mathrm{TeV}$. We observe the following features:

- $\Delta_L^{\nu\bar{\nu}}(Z')$ and $\Delta_A^{\mu\bar{\mu}}(Z')$ have definitive signs in the full range of β: *positive* and *negative*, respectively.

- $\Delta_V^{\mu\bar{\mu}}(Z')$ can have both signs and for fixed $|\beta|$ its magnitude is larger for $\beta < 0$. In fact the models with negative β are then favoured by the $B_d \to K^*\mu^+\mu^-$ anomalies. As noticed in [14] in this case in the limit of CMFV one automatically obtains $C_9^{\mathrm{NP}} < 0$ as required by experiment. If there are new sources of flavour violation represented by the matrix V_L then the region (*oasis*) in the space of new parameters has to be chosen for which in the case of negative β one still has $\mathrm{Re}(\mathrm{C}_9^{\mathrm{NP}}) < 0$. This will in turn have consequences for other processes as we will see below.

2.3 Various 331 models

It is instructive to list the values of the resulting couplings for the models with $n = 1, 2, 3$ in (2.5). We do this for flavour diagonal couplings in table 1 for $s_W^2 = 0.249$ and $g = 0.633$ valid at $M_{Z'} = 3\,\mathrm{TeV}$ except for $n = 3$, where we use $M_{Z'} = 2\,\mathrm{TeV}$ in order not to be too close to the Landau singularity. In appendix A we give explicit formulae for these couplings in terms of $\sin^2\theta_W$ as well as expressions for flavour violating couplings. Here and in appendix A we give also Z-couplings.

	β in Z' couplings						Z couplings
	$1/\sqrt{3}$	$-1/\sqrt{3}$	$2/\sqrt{3}$	$-2/\sqrt{3}$	$\sqrt{3}$	$-\sqrt{3}$	
$\Delta_L^{u\bar{u}}$	-0.172	-0.215	-0.191	-0.299	-0.849	-1.672	0.257
$\Delta_R^{u\bar{u}}$	0.086	-0.086	0.216	-0.216	1.645	-1.645	-0.115
$\Delta_V^{u\bar{u}}$	-0.087	-0.301	0.026	-0.515	0.796	-3.316	0.143
$\Delta_A^{u\bar{u}}$	0.258	0.130	0.407	0.082	2.494	0.027	-0.372
$\Delta_L^{d\bar{d}}$	-0.172	-0.215	-0.191	-0.299	-0.849	-1.672	-0.315
$\Delta_R^{d\bar{d}}$	-0.043	0.043	-0.108	0.108	-0.822	0.822	0.057
$\Delta_V^{d\bar{d}}$	-0.215	-0.172	-0.299	-0.191	-1.672	-0.849	-0.257
$\Delta_A^{d\bar{d}}$	0.130	0.258	0.082	0.407	0.027	2.494	0.372
$\Delta_L^{\mu\bar{\mu}}$	0.130	0.258	0.082	0.407	0.027	2.494	-0.199
$\Delta_R^{\mu\bar{\mu}}$	-0.128	0.128	-0.324	0.324	0.054	2.467	0.172
$\Delta_V^{\mu\bar{\mu}}$	0.001	0.386	-0.242	0.731	0.080	4.961	-0.028
$\Delta_A^{\mu\bar{\mu}}$	-0.258	-0.130	-0.407	-0.082	0.027	-0.027	0.372
$\Delta_L^{\nu\bar{\nu}}$	0.130	0.258	0.082	0.407	0.027	2.494	0.372

Table 1. Diagonal Z' couplings to fermions for different β and SM Z couplings to fermions (last column). We have used $\sin^2\theta_W = 0.249$ for $\beta = \pm 1/\sqrt{3}$ and $\beta = \pm 2/\sqrt{3}$, $\sin^2\theta_W = 0.246$ for $\beta = \pm\sqrt{3}$ and $\sin^2\theta_W = 0.231$ for Z-couplings.

3 Master formulae for one-loop functions and Wilson coefficients

3.1 New physics contributions

We collect here for completeness the corrections to SM one-loop functions and relevant Wilson coefficients as functions of the couplings listed in the previous section.

In the case of $\Delta F = 2$ transitions governed by the function S we have

$$\Delta S(B_q) = \left[\frac{\Delta_L^{bq}(Z')}{\lambda_t^{(q)}}\right]^2 \frac{4\tilde{r}}{M_{Z'}^2 g_{\rm SM}^2}, \qquad \Delta S(K) = \left[\frac{\Delta_L^{sd}(Z')}{\lambda_t^{(K)}}\right]^2 \frac{4\tilde{r}}{M_{Z'}^2 g_{\rm SM}^2} \tag{3.1}$$

where

$$g_{\rm SM}^2 = 4\frac{G_F}{\sqrt{2}}\frac{\alpha}{2\pi\sin^2\theta_W}, \qquad \lambda_i^{(K)} = V_{is}^* V_{id}, \qquad \lambda_t^{(q)} = V_{tb}^* V_{tq} \tag{3.2}$$

and $\tilde{r}$ is a QCD factor calculated in [2]. One finds $\tilde{r} = 0.965$, $\tilde{r} = 0.953$ and $\tilde{r} = 0.925$ for $M_{Z'} = 2,\ 3,\ 10\,\text{TeV}$, respectively. It should be remarked that $g_{\rm SM}^2$ and $\sin^2\theta_W$ appearing outside the Z' couplings, like in (3.7) and (3.8) below, should be evaluated at M_Z with input values given in table 3 as they are just related to the overall normalization of Wilson coefficients and rescale relative to SM contributions.

For decays $B_q \to \mu^+\mu^-$ with $q = d, s$ governed by the function Y one has

$$\Delta Y(B_q) = \left[\frac{\Delta_A^{\mu\bar{\mu}}(Z')}{M_{Z'}^2 g_{\rm SM}^2}\right]\frac{\Delta_L^{qb}(Z')}{V_{tq}^* V_{tb}} \tag{3.3}$$

and for $K_L \to \mu^+\mu^-$

$$\Delta Y(K) = \left[\frac{\Delta_A^{\mu\bar\mu}(Z')}{M_{Z'}^2 g_{\rm SM}^2}\right]\frac{\Delta_L^{sd}(Z')}{V_{ts}^* V_{td}}. \tag{3.4}$$

Similarly for $b \to q\nu\bar\nu$ transitions governed by the function X one finds

$$\Delta X(B_q) = \left[\frac{\Delta_L^{\nu\nu}(Z')}{g_{\rm SM}^2 M_{Z'}^2}\right]\frac{\Delta_L^{qb}(Z')}{V_{tq}^* V_{tb}} \tag{3.5}$$

and for $K^+ \to \pi^+\nu\bar\nu$ and $K_L \to \pi^0\nu\bar\nu$

$$\Delta X(K) = \left[\frac{\Delta_L^{\nu\bar\nu}(Z')}{g_{\rm SM}^2 M_{Z'}^2}\right]\frac{\Delta_L^{sd}(Z')}{V_{ts}^* V_{td}}. \tag{3.6}$$

The corrections from NP to the Wilson coefficients C_9 and C_{10} relevant for $b \to s\mu^+\mu^-$ transitions and used in the recent literature are given as follows[3]

$$\sin^2\theta_W C_9^{\rm NP} = -\frac{1}{g_{\rm SM}^2 M_{Z'}^2}\frac{\Delta_L^{sb}(Z')\Delta_V^{\mu\bar\mu}(Z')}{V_{ts}^* V_{tb}}, \tag{3.7}$$

$$\sin^2\theta_W C_{10}^{\rm NP} = -\frac{1}{g_{\rm SM}^2 M_{Z'}^2}\frac{\Delta_L^{sb}(Z')\Delta_A^{\mu\bar\mu}(Z')}{V_{ts}^* V_{tb}}. \tag{3.8}$$

3.2 Correlations

These formulae imply certain relations that are useful for the subsequent sections. First of all we have the ratio

$$R_1 = \frac{C_9^{\rm NP}}{C_{10}^{\rm NP}} = \frac{\mathrm{Re}(\mathrm{C}_9^{\rm NP})}{\mathrm{Re}(\mathrm{C}_{10}^{\rm NP})} = \frac{\mathrm{Im}(\mathrm{C}_9^{\rm NP})}{\mathrm{Im}(\mathrm{C}_{10}^{\rm NP})} = \frac{\Delta_V^{\mu\bar\mu}(Z')}{\Delta_A^{\mu\bar\mu}(Z')}, \tag{3.9}$$

which involves only leptonic couplings and depends only on β. This ratio is given in table 2 for different values of β and $s_W^2 = 0.249$ except for $\beta = \pm\sqrt{3}$ where we use $s_W^2 = 0.246$. We observe that for $\beta < 0$ these two coefficients are predicted to have opposite signs independently of the Z' couplings to quarks and as $C_{10}^{\rm SM}$ and $C_9^{\rm SM}$ have also opposite signs (see (4.13)). $\mathrm{Re}(\mathrm{C}_9^{\rm NP})$ and NP contributions to $\overline{\mathcal{B}}(B_s \to \mu^+\mu^-)$ are correlated with each other. This means that $\mathrm{Re}(\mathrm{C}_9^{\rm NP}) < 0$ required by $B_d \to K^*\mu^+\mu^-$ data implies for $\beta < 0$ uniquely suppression of $\overline{\mathcal{B}}(B_s \to \mu^+\mu^-)$ relative to its SM value which is favoured by the data. On the other hand for $\beta = 1/\sqrt{3}$ the ratio in (3.9) is tiny and for $\beta > 1/\sqrt{3}$ it is positive implying that NP contributions to $\overline{\mathcal{B}}(B_s \to \mu^+\mu^-)$ and $\mathrm{Re}(\mathrm{C}_9^{\rm NP})$ are anti-correlated with each other. Consequently in this case $\mathrm{Re}(\mathrm{C}_9^{\rm NP}) < 0$ required by $B_d \to K^*\mu^+\mu^-$ anomaly implies the enhancement of $\overline{\mathcal{B}}(B_s \to \mu^+\mu^-)$ which is presently not supported by the data but this could change in the future. We will see all this explicitly in section 6.

A complementary relation valid in any l.h.s. model that this time does not depend on the lepton couplings is [13]

$$\frac{\mathrm{Im}(\mathrm{C}_9^{\rm NP})}{\mathrm{Re}(\mathrm{C}_9^{\rm NP})} = \frac{\mathrm{Im}(\mathrm{C}_{10}^{\rm NP})}{\mathrm{Re}(\mathrm{C}_{10}^{\rm NP})} = \tan(\delta_2 - \beta_s). \tag{3.10}$$

[3] The coefficients C_V and C_A in [2] are obtained by multiplying C_9 and C_{10} by $\sin\theta_W^2$, respectively.

β	$1/\sqrt{3}$	$-1/\sqrt{3}$	$2/\sqrt{3}$	$-2/\sqrt{3}$	$\sqrt{3}$	$-\sqrt{3}$
R_1	-0.004	-2.98	0.59	-8.87	3.0	-185.5
R_2	-1.99	-0.50	-4.94	-0.20	1.0	-0.01
R_3	0.61	1.22	0.39	1.93	0.13	11.8
R_4	0.67	0.67	0.42	0.42	0.016	0.016
R_5	0.50	1.00	0.25	1.25	0.016	1.49
R_6	-1.00	-0.50	-1.25	-0.25	0.016	-0.016

Table 2. Values of the ratios R_i for different β setting $\sin^2\theta_W = 0.249$ except for $\beta = \pm\sqrt{3}$ where we use $s_W^2 = 0.246$.

JHEP02(2014)112

Two important points should be noticed here. These two ratios have to be equal to each other. Moreover they are the same in the two oases resulting from $\Delta F = 2$ constraint.

Next the ratios

$$R_2 = \frac{\Delta Y(B_q)}{\Delta X(B_q)} = \frac{\Delta Y(K)}{\Delta X(K)} = \frac{\Delta_A^{\mu\bar{\mu}}(Z')}{\Delta_L^{\nu\bar{\nu}}(Z')} \tag{3.11}$$

express the relative importance of Z' contributions within a given meson system to decays with muons and neutrinos in the final state. While investigating the numbers for R_2 in table 2 we should recall that in the SM $Y \approx 1.0$ while $X \approx 1.5$ which means that it is easier to make an impact on decays to muons. While from this ratio we cannot conclude whether a given branching ratio is enhanced or suppressed as the quark couplings cancel in this ratio, the message is clear:

- For $\beta > 0$ NP effects in decays to muons governed by axial-vector couplings are much larger than in decays to neutrinos, whereas the opposite is true for $\beta < 0$. Therefore in the latter case which is chosen by the $B_d \to K^*\mu^+\mu^-$ anomaly we can expect also measurable effects in decays to neutrinos.

- Very importantly in all models, except $\beta = \sqrt{3}$, considered NP effects in $B_s \to \mu^+\mu^-$ are anti-correlated with the ones in $b \to s\nu\bar{\nu}$ transitions.

Important are also the relations between the Z' contributions to $\Delta F = 1$ (X and Y functions) and $\Delta F = 2$ (S functions) observables. We have

$$\frac{\Delta X(B_q)}{\sqrt{\Delta S(B_q)^*}} = a_q \frac{\Delta_L^{\nu\bar{\nu}}(Z')}{2\sqrt{\tilde{r}}\, g_{\rm SM} M_{Z'}} = -a_q \frac{0.085}{\sqrt{\tilde{r}}} \left(\frac{3\,\text{TeV}}{M_{Z'}}\right) R_3 \tag{3.12}$$

where

$$R_3 = \frac{\left[1 - (1 + \sqrt{3}\beta) s_W^2\right]}{\sqrt{1 - (1 + \beta^2) s_W^2}}, \tag{3.13}$$

$a_d = 1$ and $a_s = -1$.

We also have

$$\frac{\Delta X(K)}{\sqrt{\Delta S(K)}} = \frac{\Delta X(B_s)}{\sqrt{\Delta S(B_s)^*}}. \tag{3.14}$$

As presently the constraints on 331 models are dominated by $\Delta F = 2$ transitions we observe that for a given allowed size of $\Delta S(B_q)$, NP effects in the functions in question are proportional to $1/M_{Z'}$ and this dependence is transfered to branching ratios in view of the fact that the dominant NP contributions are present there as interference between SM and NP contributions. That these effects are only suppressed like $1/M_{Z'}$ and not like $1/M_{Z'}^2$ is the consequence of the increase with $M_{Z'}$ of the allowed values of the couplings $\Delta_L^{ij}(Z')$ extracted from $\Delta F = 2$ observables, the point already stressed in [2]. In summary, denoting by $\Delta\mathcal{O}^{\rm NP}(M_{Z'}^{(i)})$ NP contributions to a given $\Delta F = 1$ observable in B_s and B_d decays at two $((i = 1, 2)$ different values $M_{Z'}^{(i)}$ we have a *scaling law*

$$\Delta\mathcal{O}^{\rm NP}(M_{Z'}^{(1)}) = \frac{M_{Z'}^{(2)}}{M_{Z'}^{(1)}}\Delta\mathcal{O}^{\rm NP}(M_{Z'}^{(2)}). \tag{3.15}$$

independently of β and C_{B_q}. However the size of NP effect will depend on these two parameters as seen already in the case of β in table 2 and we will see this more explicitly in section 6.

While this scaling law would apply in the case of the absence of correlations between B_q and K systems also to K decays, in the 331 models the situation is different as we will now demonstrate. Indeed in these models there is a correlation between the Z' effects in $\Delta F = 2$ master functions in different meson systems

$$\frac{\Delta S(K)}{\Delta S(B_d)\Delta S(B_s)^*} = \frac{M_{Z'}^2 g_{\rm SM}^2}{4\tilde{r}}\left[\frac{\Delta_L^{sd}(Z')}{\Delta_L^{bd}(Z')\Delta_L^{bs*}(Z')}\right]^2 = \frac{3.68}{\tilde{r}}\left(\frac{M_{Z'}}{3\,\text{TeV}}\right)^2 R_4 \tag{3.16}$$

where

$$R_4 = 1 - (1 + \beta^2)s_W^2. \tag{3.17}$$

Here and in following equations we set $|V_{tb}| = 1$ and $\tilde{c}_{13} = \tilde{c}_{23} = 1$ if necessary. As the present data and lattice results imply $|\Delta S(B_q)| < 0.25$ and $R_4 < 0.7$ in all models, NP effects in ε_K are typically below 10%, which is welcome as with input parameters in table 3 ε_K within the SM is in good agreement with the data.

Combining then relations (3.11), (3.12), (3.14) and (3.16) we find

$$\Delta X(K) = \frac{0.16}{\tilde{r}} R_5 \sqrt{\Delta S(B_d)\Delta S(B_s)^*}, \qquad R_5 = R_3\sqrt{R_4} \tag{3.18}$$

$$\Delta Y(K) = \frac{0.16}{\tilde{r}} R_6 \sqrt{\Delta S(B_d)\Delta S(B_s)^*}, \qquad R_6 = R_2 R_3\sqrt{R_4} \tag{3.19}$$

with the values of R_5 and R_6 given in table 2. We observe that $\Delta X(K)$ and $\Delta Y(K)$ do not depend on $M_{Z'}$ when the parameters in V_L are constrained through $B_{s,d}^0 - \bar{B}_{s,d}^0$ mixings. This fact has already been noticed in [2] but these explicit relations are new.

For the models considered in detail by us $R_5 < 1.3$ and as $|\Delta S(B_q)| < 0.25$ we find that $|\Delta X(K)| \leq 0.05$ which implies a correction to $K^+ \to \pi^+\nu\bar{\nu}$ and $K_L \to \pi^0\nu\bar{\nu}$ of at most 10% at the level of the branching ratios.

JHEP02(2014)112

As far as the Wilson coefficients $C_9^{\rm NP}$ and $C_{10}^{\rm NP}$ are concerned we have two important relations

$$(\Delta S(B_q))^* = 4\tilde r g_{\rm SM}^2 M_{Z'}^2 \sin^4\theta_W \left[\frac{C_9^{\rm NP}}{\Delta_V^{\mu\bar\mu}(Z')}\right]^2 = 0.327\left[\frac{C_9^{\rm NP}}{\Delta_V^{\mu\bar\mu}(Z')}\right]^2\left[\frac{M_{Z'}}{3\,{\rm TeV}}\right]^2, \tag{3.20}$$

$$(\Delta S(B_q))^* = 4\tilde r g_{\rm SM}^2 M_{Z'}^2 \sin^4\theta_W \left[\frac{C_{10}^{\rm NP}}{\Delta_A^{\mu\bar\mu}(Z')}\right]^2 = 0.327\left[\frac{C_{10}^{\rm NP}}{\Delta_A^{\mu\bar\mu}(Z')}\right]^2\left[\frac{M_{Z'}}{3\,{\rm TeV}}\right]^2, \tag{3.21}$$

which we have written in a form suitable for the analysis in section 6. We recall that $S_{\rm SM} = S_0(x_t) = 2.31$. Both relations are valid for B_s and B_d systems as indicated on the l.h.s. of these equations and the Wilson coefficients on the r.h.s. should be appropriately adjusted to the case considered.

The virtue of these relation is their independence of the new parameters in (2.9) so that for a given β the size of $C_9^{\rm NP}$ and $C_{10}^{\rm NP}$ allowed by the $\Delta F = 2$ constraints can be found. In particular in the case of a real $C_9^{\rm NP}$ and $C_{10}^{\rm NP}$, corresponding to $V_L = V_{\rm CKM}$, $\Delta S(B_q)$ and ΔM_q will be enhanced which is only allowed if the SM values of ΔM_q will turn out to be below the data. If this will not be the case the only solution is to misalign V_L and $V_{\rm CKM}$ which results in complex $C_9^{\rm NP}$ and $C_{10}^{\rm NP}$ and consequently novel CP-violating effects.

4 Crucial observables

4.1 $\Delta F = 2$ observables

The $B_s^0 - \bar B_s^0$ observables are fully described in 331 models by the function

$$S(B_s) = S_0(x_t) + \Delta S(B_s) \equiv |S(B_s)|e^{-i2\varphi_{B_s}}, \tag{4.1}$$

where $S_0(x_t)$ is the real one-loop SM box function and the additional generally complex term has been given in (3.1).

The two observables of interest, ΔM_s and $S_{\psi\phi}$ are then given by

$$\Delta M_s = \frac{G_F^2}{6\pi^2} M_W^2 m_{B_s} |V_{tb}^* V_{ts}|^2 F_{B_s}^2 \hat B_{B_s} \eta_B |S(B_s)| \tag{4.2}$$

and

$$S_{\psi\phi} = \sin(2|\beta_s| - 2\varphi_{B_s}), \qquad V_{ts} = -|V_{ts}|e^{-i\beta_s}. \tag{4.3}$$

with $\beta_s \simeq -1^\circ$. Here and in the rest of the paper we use the standard phase conventions for the elements of the CKM matrix [38].

In the case of B_d^0 system the corresponding formulae are obtained from (4.1) and (4.2) by replacing s by d. Moreover (4.3) is replaced by

$$S_{\psi K_S} = \sin(2\beta - 2\varphi_{B_d}), \qquad V_{td} = |V_{td}|e^{-i\beta}. \tag{4.4}$$

With the input for $|V_{ub}|$ and $|V_{cb}|$ in table 3 and $\gamma = 68^\circ$ there is a good agreement of the SM with data on $S_{\psi K_S}$ and ε_K.

JHEP02(2014)112

In the SM one has[4]

$$(\Delta M_s)_{\rm SM} = 18.8/{\rm ps}\cdot\left[\frac{\sqrt{\hat B_{B_s}}F_{B_s}}{266\,{\rm MeV}}\right]^2\left[\frac{S_0(x_t)}{2.31}\right]\left[\frac{|V_{ts}|}{0.0416}\right]^2\left[\frac{\eta_B}{0.55}\right], \tag{4.5}$$

$$(\Delta M_d)_{\rm SM} = 0.54/{\rm ps}\cdot\left[\frac{\sqrt{\hat B_{B_d}}F_{B_d}}{218\,{\rm MeV}}\right]^2\left[\frac{S_0(x_t)}{2.31}\right]\left[\frac{|V_{td}|}{8.8\cdot 10^{-3}}\right]^2\left[\frac{\eta_B}{0.55}\right]. \tag{4.6}$$

For the central values of the parameters in table 3 there is a good agreement with the very accurate data [40]:

$$\Delta M_s = 17.69(8)\,{\rm ps}^{-1}, \qquad \Delta M_d = 0.510(4)\,{\rm ps}^{-1}\,, \tag{4.7}$$

even if both central values are by $5-6\%$ above the data. With the most recent values from the Twisted Mass Collaboration [41]

$$\sqrt{\hat B_{B_s}}F_{B_s} = 262(10)\,{\rm MeV}, \qquad \sqrt{\hat B_{B_d}}F_{B_d} = 216(10)\,{\rm MeV}, \tag{4.8}$$

that are not yet included in the FLAG average, the central value of ΔM_s would go down to 18.2/ps.

Concerning $S_{\psi\phi}$ and $S_{\psi K_S}$ we have

$$S_{\psi\phi} = -\left(0.04^{+0.10}_{-0.13}\right), \qquad S_{\psi K_S} = 0.679(20) \tag{4.9}$$

with the second value known already for some time [40] and the first one being the most recent average from HFAG [40] close to the earlier result from the LHCb [42]. The first value is consistent with the SM expectation of 0.04. This is also the case of $S_{\psi K_S}$ for the values of $|V_{ub}|$ and $|V_{cb}|$ used by us.

4.2 $b \to s\mu^+\mu^-$ observables

The two Wilson coefficients that receive NP contributions in 331 models are C_9 and C_{10}. We decompose them into the SM and NP contributions:[5]

$$C_9 = C_9^{\rm SM} + C_9^{\rm NP}, \qquad C_{10} = C_{10}^{\rm SM} + C_{10}^{\rm NP}, \tag{4.10}$$

where NP contributions have been given in (3.7) and (3.8) and the SM contributions are given as follows

$$\sin^2\theta_W C_9^{\rm SM} = \sin^2\theta_W P_0^{\rm NDR} + [\eta_{\rm eff}Y_0(x_t) - 4\sin^2\theta_W Z_0(x_t)], \tag{4.11}$$

$$\sin^2\theta_W C_{10}^{\rm SM} = -\eta_{\rm eff}Y_0(x_t) \tag{4.12}$$

with all the entries given in [13, 19] except for $\eta_{\rm eff}$ which is new and given below. We have then

$$C_9^{\rm SM} \approx 4.1, \qquad C_{10}^{\rm SM} \approx -4.1\,. \tag{4.13}$$

[4]The central value of $|V_{ts}|$ corresponds roughly to the central $|V_{cb}| = 0.0424$ obtained from tree-level inclusive decays [39].

[5]These coefficients are defined as in [19] and the same definitions are used in [10, 11].

In the case of $B_s \to \mu^+\mu^-$ decay one has [43–45]

$$\frac{\overline{\mathcal{B}}(B_s \to \mu^+\mu^-)}{\overline{\mathcal{B}}(B_s \to \mu^+\mu^-)_{\rm SM}} = \left[\frac{1+\mathcal{A}^{\mu\mu}_{\Delta\Gamma}\, y_s}{1+y_s}\right] |P|^2, \qquad P = \frac{C_{10}}{C_{10}^{\rm SM}} \equiv |P| e^{i\varphi_P}, \tag{4.14}$$

where

$$\overline{\mathcal{B}}(B_s \to \mu^+\mu^-)_{\rm SM} = \frac{1}{1-y_s}\mathcal{B}(B_s \to \mu^+\mu^-)_{\rm SM}\,, \tag{4.15}$$

$$\mathcal{B}(B_s \to \mu^+\mu^-)_{\rm SM} = \tau_{B_s}\frac{G_F^2}{\pi}\left(\frac{\alpha}{4\pi\sin^2\theta_W}\right)^2 F_{B_s}^2 m_\mu^2 m_{B_s}\sqrt{1-\frac{4m_\mu^2}{m_{B_s}^2}}\,|V_{tb}^*V_{ts}|^2\,\eta_{\rm eff}^2 Y_0(x_t)^2\,, \tag{4.16}$$

$$\mathcal{A}^{\mu\mu}_{\Delta\Gamma} = \cos(2\varphi_P - 2\varphi_{B_s}), \qquad y_s \equiv \tau_{B_s}\frac{\Delta\Gamma_s}{2} = 0.062 \pm 0.009 \tag{4.17}$$

with the later value being the latest world average [40]. The *bar* indicates that $\Delta\Gamma_s$ effects have been taken into account. In the SM and CMFV $\mathcal{A}^{\mu\mu}_{\Delta\Gamma} = 1$ but in the 331 models it is slightly smaller and we take this effect into account. Generally as shown in [45] $\mathcal{A}^{\mu\mu}_{\Delta\Gamma}$ can serve to test NP models as it can be determined in time-dependent measurements [43, 44]. Of interest is also the CP asymmetry

$$S^s_{\mu\mu} = \sin(2\varphi_P - 2\varphi_{B_s}), \tag{4.18}$$

which has been studied in detail in [19, 45] in the context of Z' models. In the case of $B_d \to \mu^+\mu^-$ decay the formulae given above apply with s replaced by d and $y_d \approx 0$. Explicit formulae for $B_d \to \mu^+\mu^-$ can be found in [19].

Concerning the the status of the branching ratios for $B_{s,d} \to \mu^+\mu^-$ decays we have

$$\overline{\mathcal{B}}(B_s \to \mu^+\mu^-)_{\rm SM} = (3.65 \pm 0.23)\times 10^{-9}, \quad \overline{\mathcal{B}}(B_s \to \mu^+\mu^-) = (2.9 \pm 0.7)\times 10^{-9}, \tag{4.19}$$

$$\mathcal{B}(B_d \to \mu^+\mu^-)_{\rm SM} = (1.06 \pm 0.09)\times 10^{-10}, \quad \mathcal{B}(B_d \to \mu^+\mu^-) = \left(3.6^{+1.6}_{-1.4}\right)\times 10^{-10}. \tag{4.20}$$

The SM values are based on [46] in which NLO corrections of electroweak origin [47] and QCD corrections up to NNLO [48] have been taken into account. These values are rather close to the ones presented previously by us [45, 49] but the inclusion of these new higher order corrections that were missing until now reduced significantly various scale uncertainties so that non-parametric uncertainties in both branching ratios are below 2%. The experimental data are the most recent averages of the results from LHCb and CMS [4–6].

The calculations performed in [47, 48] are very involved and in analogy to the QCD factors, like η_B and η_{1-3} in $\Delta F = 2$ processes, we find it useful to include all QCD and electroweak corrections into $\eta_{\rm eff}$ introduced in (4.12) that without these corrections would be equal to unity. Inspecting the analytic formulae in [46] one finds then

$$\eta_{\rm eff} = 0.9882 \pm 0.0024\ . \tag{4.21}$$

The small departure of $\eta_{\rm eff}$ from unity was already anticipated in [49, 50] but only the calculations in [46–48] could put these expectations and conjectures on firm footing.

Indeed, in order to end up with such a simple result it was crucial to perform such involved calculations as these small corrections are only valid for particular definitions of the top-quark mass and of other electroweak parameters involved. In particular one has to use in $Y_0(x_t)$ the $\overline{\rm MS}$-renormalized top-quark mass $m_t(m_t)$ with respect to QCD but on-shell with respect to electroweak interactions. This means $m_t(m_t) = 163.5\,\text{GeV}$ as calculated in [46]. Moreover, in using (4.21) to calculate observables like branching ratios it is important to have the same normalization of effective Hamiltonian as in the latter paper. There this normalization is expressed in terms of G_F and M_W only. Needless to say one can also use directly the formulae in [46].

In the present paper we follow the normalization of effective Hamiltonian in [51] which uses G_F, $\alpha(M_Z)$ and $\sin^2\theta_W$ and in order to be consistent with the calculation in [46] our $\eta_{\rm eff} = 0.991$ with $m_t(m_t)$ unchanged. Interestingly also in the case of $K^+\to\pi^+\nu\bar\nu$ and $K_L\to\pi^0\nu\bar\nu$ the analog of $\eta_{\rm eff}$, multiplying this time $X_0(x_t)$, is found with the normalizations of effective Hamiltonian in [51] and definition of m_t as given above to be within 1% from unity [52].

In the case of $B\to K^*\mu^+\mu^-$ we will concentrate our discussion on the Wilson coefficient $C_9^{\rm NP}$ which can be extracted from the angular observables, in particular $\langle F_L\rangle$, $\langle S_5\rangle$ and $\langle A_8\rangle$, in which within the 331 models NP contributions enter exclusively through this coefficient. On the other hand $\text{Im}(\text{C}_{10}^{\rm NP})$ governs the CP-asymmetry $\langle A_7\rangle$. Useful approximate expressions for these angular observables at low q^2 in terms of $C_9^{\rm NP}$, $C_{10}^{\rm NP}$ and other Wilson coefficients have been provided in [11]. Specified to 331 models they are given as follows

$$\langle F_L\rangle \approx 0.77 + 0.05\ \text{Re}\,\text{C}_9^{\rm NP}, \tag{4.22}$$

$$\langle S_4\rangle \approx 0.29, \tag{4.23}$$

$$\langle S_5\rangle \approx -0.14 - 0.09\ \text{Re}\,\text{C}_9^{\rm NP}. \tag{4.24}$$

$$\langle A_7\rangle \approx 0.07\ \text{Im}\,\text{C}_{10}^{\rm NP}, \tag{4.25}$$

$$\langle A_8\rangle \approx 0.04\ \text{Im}\,\text{C}_9^{\rm NP}, \tag{4.26}$$

$$\langle A_9\rangle \approx 0. \tag{4.27}$$

Note that NP contributions to $\langle S_4\rangle$ and $\langle A_9\rangle$ vanish in 331 models due to the absence of right-handed currents in these models.

Eliminating $\text{Re}\,\text{C}_9^{\rm NP}$ from these expressions in favour of $\langle S_5\rangle$ one finds [13]

$$\langle F_L\rangle = 0.69 - 0.56\langle S_5\rangle, \tag{4.28}$$

which shows analytically the point made in [10, 11] that NP effects in F_L and S_5 are anti-correlated as observed in the data.

Indeed, the recent $B\to K^*\mu^+\mu^-$ anomalies imply the following ranges for $C_9^{\rm NP}$ [10, 11] respectively

$$C_9^{\rm NP} = -(1.6\pm 0.3), \qquad C_9^{\rm NP} = -(0.8\pm 0.3)\ . \tag{4.29}$$

As $C_9^{\rm SM}\approx 4.1$ at $\mu_b = 4.8\,\text{GeV}$, these are very significant suppressions of this coefficient. We note that C_9 remains real as in the SM but the data do not yet preclude a significant

$G_F = 1.16637(1) \times 10^{-5}\,\mathrm{GeV}^{-2}$	[55]	$m_{B_d} = m_{B^+} = 5279.2(2)\,\mathrm{MeV}$	[38]
$M_W = 80.385(15)\,\mathrm{GeV}$	[55]	$m_{B_s} = 5366.8(2)\,\mathrm{MeV}$	[38]
$\sin^2\theta_W = 0.23116(13)$	[55]	$F_{B_d} = (190.5 \pm 4.2)\,\mathrm{MeV}$	[56]
$\alpha(M_Z) = 1/127.9$	[55]	$F_{B_s} = (227.7 \pm 4.5)\,\mathrm{MeV}$	[56]
$\alpha_s(M_Z) = 0.1184(7)$	[55]	$F_{B^+} = (185 \pm 3)\,\mathrm{MeV}$	[57]
$m_u(2\,\mathrm{GeV}) = (2.1 \pm 0.1)\,\mathrm{MeV}$	[58]	$\hat{B}_{B_d} = 1.27(10)$, $\hat{B}_{B_s} = 1.33(6)$	[56]
$m_d(2\,\mathrm{GeV}) = (4.73 \pm 0.12)\,\mathrm{MeV}$	[58]	$\hat{B}_{B_s}/\hat{B}_{B_d} = 1.01(2)$	[41]
$m_s(2\,\mathrm{GeV}) = (93.4 \pm 1.1)\,\mathrm{MeV}$	[58]	$F_{B_d}\sqrt{\hat{B}_{B_d}} = 216(15)\,\mathrm{MeV}$	[56]
$m_c(m_c) = (1.279 \pm 0.013)\,\mathrm{GeV}$	[59]	$F_{B_s}\sqrt{\hat{B}_{B_s}} = 266(18)\,\mathrm{MeV}$	[56]
$m_b(m_b) = 4.19^{+0.18}_{-0.06}\,\mathrm{GeV}$	[55]	$\xi = 1.268(63)$	[56]
$m_t(m_t) = 163.5(9)\,\mathrm{GeV}$	[38]	$\eta_B = 0.55(1)$	[60]
$M_t = 173.1(9)\,\mathrm{GeV}$	[61]	$\Delta M_d = 0.510(4)\,\mathrm{ps}^{-1}$	[40]
$m_K = 497.614(24)\,\mathrm{MeV}$	[55]	$\Delta M_s = 17.69(8)\,\mathrm{ps}^{-1}$	[40]
$F_K = 156.1(11)\,\mathrm{MeV}$	[58]	$S_{\psi K_S} = 0.679(20)$	[55]
$\hat{B}_K = 0.766(10)$	[56]	$S_{\psi\phi} = -(0.04^{+0.10}_{-0.13})$	[40]
$\kappa_\epsilon = 0.94(2)$	[62, 63]	$\Delta\Gamma_s/\Gamma_s = 0.123(17)$	[40]
$\eta_{cc} = 1.87(76)$	[64]	$\tau_{B_s} = 1.516(11)\,\mathrm{ps}$	[40]
$\eta_{tt} = 0.5765(65)$	[60]	$\tau_{B_d} = 1.519(7)\,\mathrm{ps}$	[40]
$\eta_{ct} = 0.496(47)$	[65]	$\tau_{B^\pm} = 1.641(8)\,\mathrm{ps}$	[40]
$\Delta M_K = 0.5292(9) \times 10^{-2}\,\mathrm{ps}^{-1}$	[55]	$\lvert V_{us}\rvert = 0.2252(9)$	[40]
$\lvert\epsilon_K\rvert = 2.228(11) \times 10^{-3}$	[55]	$\lvert V_{cb}\rvert = (42.4(9)) \times 10^{-3}$	[39]
$\mathcal{B}(B^+ \to \tau^+\nu) = (0.96 \pm 0.26) \times 10^{-4}$	[40]	$\lvert V_{ub}\rvert = (3.6 \pm 0.3) \times 10^{-3}$	[38]

Table 3. Values of the experimental and theoretical quantities used as input parameters.

imaginary part for this coefficient. The details behind these two results that differ by a factor of two is discussed in [11]. In fact inspecting figures 3 and 4 of the latter paper one sees that if the constraints from $A_{\rm FB}$ and $B \to K\mu^+\mu^-$ were not taken into account $C_9^{\rm NP} \approx -1.4$ alone could explain the anomalies in the observables F_L and S_5. But the inclusion of these constraints reduces the size of this coefficient. Yet values of $C_9^{\rm NP} \approx -(1.2 - 1.0)$ seem to give reasonable agreement with all data and the slight reduction of departure of F_L and S_5 from their SM values in the future data would allow to explain the two anomalies with the help of $C_9^{\rm NP}$ only as suggested originally in [10].

Similarly a very recent comprehensive Bayesian analysis of the authors of [53, 54] in [15] finds that although SM works well, if one wants to interpret the data in extensions of the SM then NP scenarios with dominant NP effect in C_9 are favoured although the inclusion of chirality-flipped operators in agreement with [11] would help to reproduce the data. This is also confirmed in [13, 17]. However, as we remarked at the beginning of our paper, a very recent analysis in [18] challenges the solution with significant right-handed currents and we are looking forward to the consensus on this point in the future. References to earlier papers on $B \to K^*\mu^+\mu^-$ by all these authors can be found in [10, 11, 54] and [1].

JHEP02(2014)112

5 Strategy for numerical analysis

In our numerical analysis we will follow our recent strategy applied to general l.h.s. models in [13] with the following significant simplification in the case of 331 models. The leptonic couplings of Z' are fixed for a given β and this allows us to avoid a rather involved numerical analysis that in [13] had as a goal finding the optimal values of these couplings. Even if β is not fixed and varying it changes the leptonic couplings in question, the $\Delta_V^{\mu\bar\mu}$, $\Delta_A^{\mu\bar\mu}$ and $\Delta_L^{\nu\bar\nu}$ couplings are correlated with each other and finding one day their optimal values in 331 models will also select the optimal value of β fixing the electric charges of new heavy gauge bosons and fermions. Of course also quark couplings will play a prominent role in this analysis, although even if they depend on β, their correlation with leptonic couplings is washed out by the new parameters in (2.9).

Clearly NP contributions in any extension of the SM are constrained by $\Delta F = 2$ processes which presently are subject to theoretical and experimental uncertainties. However, it is to be expected that in the flavour precision era ahead of us, which will include both advances in experiment and theory, in particular lattice calculations, it will be possible to decide with high precision whether ΔM_s and ΔM_d within the SM agree or disagree with the data. For instance already the need for enhancements or suppressions of these observables would be an important information. Similar comments apply to $S_{\psi\phi}$ and $S_{\psi K_S}$ as well as to the branching ratios $\mathcal{B}(B_{s,d} \to \mu^+\mu^-)$ and angular observables in $B_d \to K^*\mu^+\mu^-$. In particular correlations and anti-correlations between suppressions and enhancements allow to distinguish between various NP models as can be illustrated with the DNA charts proposed in [1].

In order to monitor this progress in the context of the 331 models we will consider similarly to [13] the following five bins for C_{B_s} and C_{B_d} in (1.6)

$$\begin{aligned} C_{B_s} &= 0.90 \pm 0.01 \text{ (yellow)}, \quad 0.96 \pm 0.01 \text{ (green)}, \quad 1.00 \pm 0.01 \text{ (red)}, \\ C_{B_s} &= 1.04 \pm 0.01 \text{ (blue)}, \quad 1.10 \pm 0.01 \text{ (purple)} \end{aligned} \tag{5.1}$$

and similarly for C_{B_d}. This strategy avoids variations over non-perturbative parameters like $F_{B_s}\sqrt{\hat{B}_{B_s}}$ and can be executed here because in 331 models these ratios have a very simple form

$$C_{B_s} = \frac{|S(B_s)|}{S_0(x_t)}, \qquad C_{B_d} = \frac{|S(B_d)|}{S_0(x_t)} \tag{5.2}$$

and thanks to the presence of a single operator do not involve any non-perturbative uncertainties. Of course in order to find out the experimental values of these ratios one has to handle these uncertainties but this is precisely what we want to monitor in the coming years. The most recent update from Utfit collaboration reads

$$C_{B_s} = 1.08 \pm 0.09, \qquad C_{B_d} = 1.10 \pm 0.17\ . \tag{5.3}$$

However, it should be stressed that such values are sensitive to the CKM input and in fact as seen in (4.5) and (4.6) with the central values of CKM parameters in table 3 we would rather expect the central values of C_{B_s} and C_{B_d} to be below unity. In order to have full picture we will not use the values in (5.3) but rather investigate how the results depend on the bins in (5.1).

Concerning $S_{\psi\phi}$ and $S_{\psi K_S}$ we will vary them in the ranges

$$-0.14 \leq S_{\psi\phi} \leq 0.09, \qquad 0.639 \leq S_{\psi K_S} \leq 0.719 \tag{5.4}$$

corresponding to 1σ and 2σ ranges around the central experimental values for $S_{\psi\phi}$ and $S_{\psi K_S}$, respectively.

Finally, in order to be sure that the lower bounds from LEP-II and LHC on $M_{Z'}$ are satisfied we will present the results for $\beta = \pm 1/\sqrt{3}$ and $\beta = \pm 2/\sqrt{3}$ for $M_{Z'} = 3\,\text{TeV}$. We will return to this issue in section 7. The scaling law in (3.15) allows to translate our results for observables in B_s and B_d decays into results for other choices of $M_{Z'}$. As we have shown in (3.18) and (3.19) the $M_{Z'}$ dependence cancels out in $\Delta X(K)$ and $\Delta Y(K)$.

6 Numerical analysis

6.1 CMFV case

It will be instructive to begin our numerical analysis with a particular case, considered in [14], in which

$$V_L = V_{\text{CKM}}. \tag{6.1}$$

In this case the CP-asymmetries $S_{\psi\phi}$ and $S_{\psi K_S}$ equal the SM ones and the Wilson coefficients C_9^{NP} and C_{10}^{NP} remain real as in the SM. Moreover, having only two new variables to our disposal, β and $M_{Z'}$, we find very concrete predictions and a number of correlations.

In presenting our results in this section we choose the following colour coding for β:

$$\beta = -\frac{2}{\sqrt{3}}\ \text{(red)}, \quad \beta = -\frac{1}{\sqrt{3}}\ \text{(blue)}, \quad \beta = \frac{1}{\sqrt{3}}\ \text{(green)}, \quad \beta = \frac{2}{\sqrt{3}}\ \text{(yellow)}. \tag{6.2}$$

The cases of $\beta = \pm\sqrt{3}$ will be considered separately.

In figure 2 we show C_{B_s}, C_{B_d}, $\overline{\mathcal{B}}(B_s \to \mu^+\mu^-)$ and $\mathcal{B}(B_d \to \mu^+\mu^-)$ as functions of $M_{Z'}$ for the four chosen values of β. The values below 1.5 TeV are presented only for illustration as such low masses appear rather unrealistic on the basis of messages from the LHC. In figure 3 we show the correlations C_{B_s} versus C_9^{NP} and $\overline{\mathcal{B}}(B_s \to \mu^+\mu^-)$ versus C_9^{NP} for different values of β, varying $M_{Z'}$ in the range $2-5$ TeV.

We observe:

- As already pointed out in [13] and known from CMFV scenario C_{B_s} and C_{B_d} are bound to be above unity but this enhancement for the values of β in (6.2) is not as severe as in the $\beta = -\sqrt{3}$ case considered in [14]. It should be noted that the sign of β does not matter in these plots and the red and blue lines shown there are equivalent to yellow and green lines, respectively.

- The case of $\beta = \pm\sqrt{3}$ is shown separately in figure 4 for fixed $s_W^2 = 0.246$, corresponding to $M_{Z'} = 2\,\text{TeV}$ only as an illustration. Only values of $M_{Z'}$ away from singularity are shown and to bring C_{B_s} and C_{B_d} down to the acceptable values $M_{Z'}$

JHEP02(2014)112

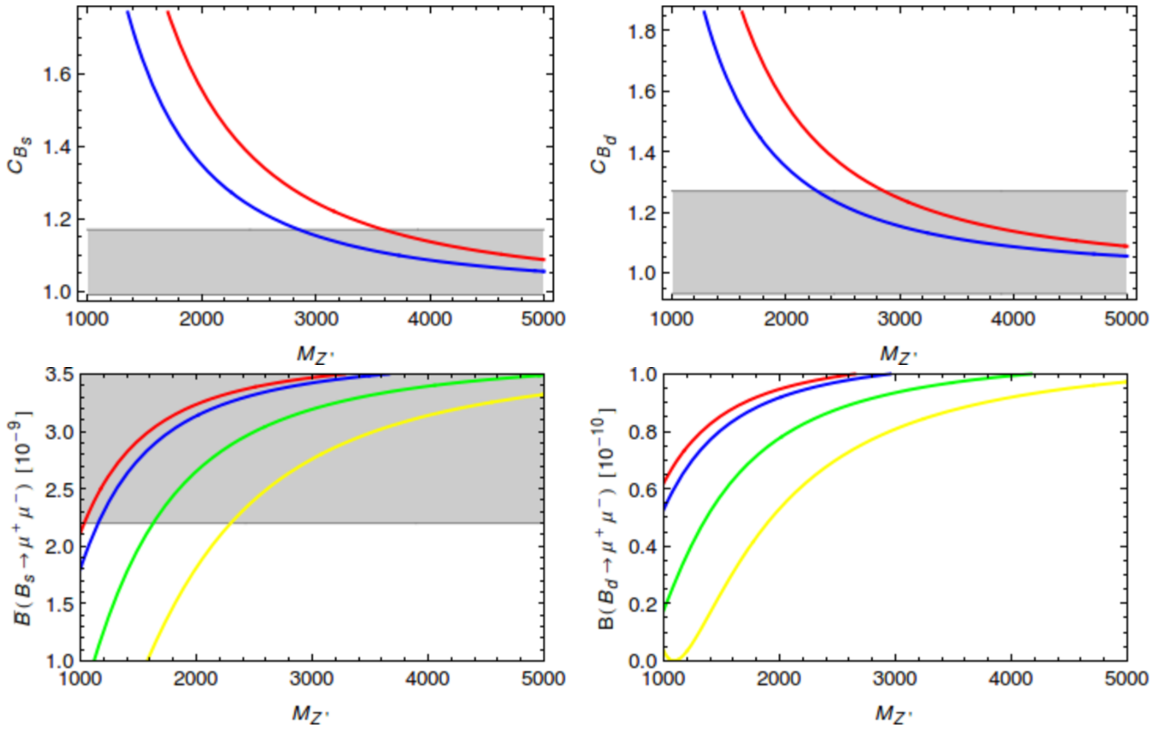

Figure 2. C_{B_s}, C_{B_d}, $\overline{\mathcal{B}}(B_s \to \mu^+\mu^-)$ and $\mathcal{B}(B_d \to \mu^+\mu^-)$ in the CMFV limit as functions of $M_{Z'}$ for the four chosen values of β with the colour coding given in (6.2). The gray regions show the UTfit range from eq. (5.3) and the experimental range $\overline{\mathcal{B}}(B_s \to \mu^+\mu^-) = (2.9 \pm 0.7) \cdot 10^{-9}$. The region for $B_d \to \mu^-\mu^-$ is outside the range of the plot.

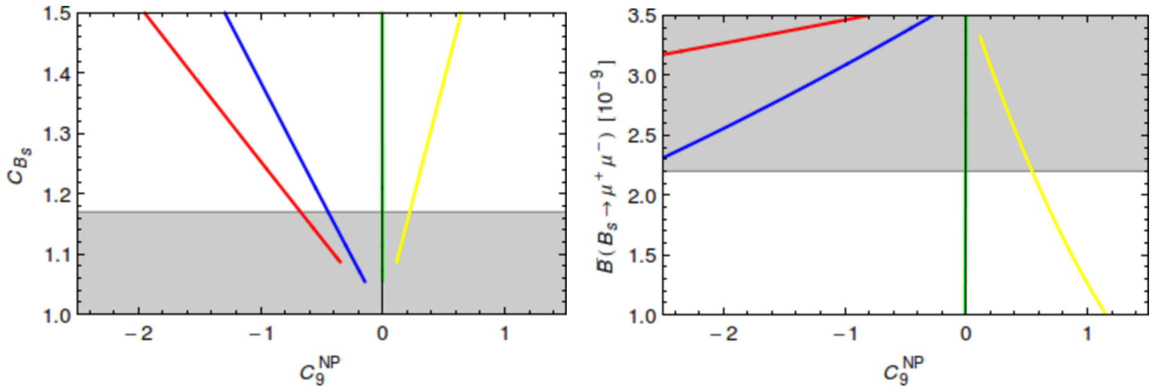

Figure 3. Correlations C_{B_s} versus $C_9^{\rm NP}$ and $\overline{\mathcal{B}}(B_s \to \mu^+\mu^-)$ versus $C_9^{\rm NP}$ in the CMFV limit for different values of β, varying $M_{Z'}$ in the range $2-5$ TeV. Colour coding in (6.2). The gray regions show the UTfit range from eq. (5.3) and the experimental range $\overline{\mathcal{B}}(B_s \to \mu^+\mu^-) = (2.9 \pm 0.7) \cdot 10^{-9}$.

has to be increased well above $M_{Z'} = 4\,\text{TeV}$ at which Landau singularity is present, that is beyond the range of validity of this model. The authors of [14] working with $s_W^2 = 0.231$ could not see these large enhancements of C_{B_s} and C_{B_d} . One can also check that for $\beta = -\sqrt{3}$ and $M_{Z'} < 3.5\,\text{TeV}$, in order to stay away from the

JHEP02(2014)112

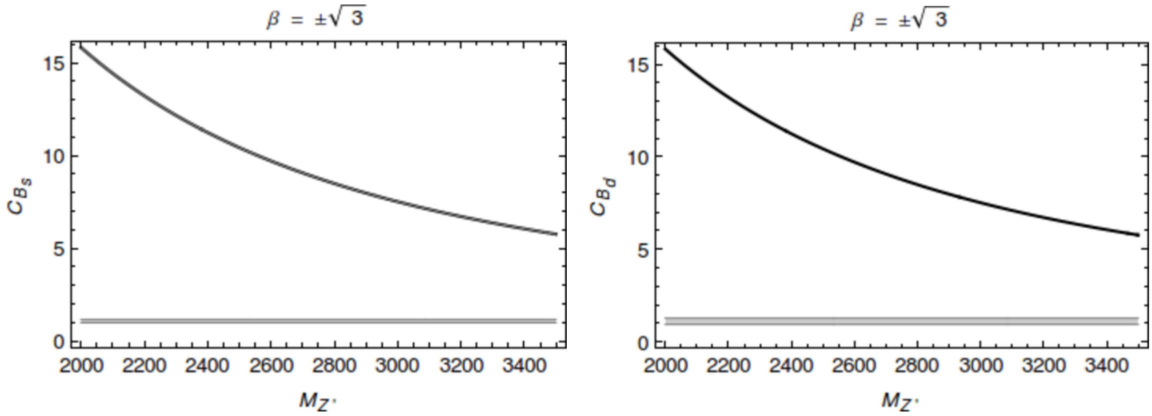

Figure 4. C_{B_s} and C_{B_d} as functions of $M_{Z'}$ for $\beta = \pm\sqrt{3}$ in the CMFV limit. The gray regions show the UTfit range from eq. (5.3).

singularity, $|C_9^{\rm NP}|$ is much larger than indicated by the data. Clearly, as suggested in [66, 67] one could improve this situation by shifting the singularity above 4 TeV through addition of other matter but then the model is a different one and one would have to investigate what impact this additional matter has for observables considered here.

- As evident from our formulae for the $\Delta_A^{\mu\bar\mu}(Z')$ couplings in the case of CMFV the branching ratios $\overline{\mathcal{B}}(B_s \to \mu^+\mu^-)$ and $\mathcal{B}(B_d \to \mu^+\mu^-)$ can only be suppressed with respect to the SM. This is welcome in the case of $\overline{\mathcal{B}}(B_s \to \mu^+\mu^-)$ but not for $\mathcal{B}(B_d \to \mu^+\mu^-)$ where the present data would favour an enhancement. But even in the case of $\overline{\mathcal{B}}(B_s \to \mu^+\mu^-)$ not all values of $M_{Z'}$ are consistent with the 1σ experimental range for $\overline{\mathcal{B}}(B_s \to \mu^+\mu^-)$. In fact for the case $\beta = 2/\sqrt{3}$ (yellow) values $M_{Z'} \le 2$ TeV are outside this range.

- The requirement of $C_9^{\rm NP} < 0$ excludes in the CMFV case $\beta > 0$. The case of $\beta = -2/\sqrt{3}$ is clearly favoured as then the coupling $\Delta_V^{\mu\bar\mu}(Z')$ is largest and values $C_{B_s} \approx 1.2$ would be sufficient to soften significantly the $B_d \to K^*\mu^+\mu^-$ anomaly. For $\beta = -2/\sqrt{3}$ and $M_{Z'} \ge 2$ TeV NP effects in $\overline{\mathcal{B}}(B_s \to \mu^+\mu^-)$ and $\mathcal{B}(B_d \to \mu^+\mu^-)$ are small, in the ballpark of $5-10\%$ of the SM values.

To summarize, in this scenario for quark couplings the case $\beta = -2/\sqrt{3}$ is performing best as due to large value of $\Delta_V^{\mu\bar\mu}(Z')$ it allows to obtain $C_9^{\rm NP} \approx -1.0$ for $C_{B_s} \approx 1.2$. Yet a value $C_{B_s} \approx 1.2$ could be problematic when the data improve. For $\beta = -1/\sqrt{3}$ which does not introduce exotic charges the required values of C_{B_s} to get sufficiently negative $C_9^{\rm NP}$ are even larger and the positive values of β are excluded by the required sign of the latter coefficient.

Thus on the whole the idea of the authors of [14] to consider negative values of β was a good one but their choice $\beta = -\sqrt{3}$ is excluded on the basis of the constraints on C_{B_s} and C_{B_d} when the correct values of $\sin\theta_W^2$ at $M_{Z'}$ are used. Moreover LEP-II data on leptonic Z' couplings exclude this case as we will see in the next section.

It should finally be noted that NP physics effects in figures 2 and 3 appear to be significantly larger than found by us in [2]. One reason for this are different values of β considered here but the primary reason is that the constraints from ΔM_s and ΔM_d require the matrix V_L to be even more hierarchical than $V_{\rm CKM}$ and $V_L = V_{\rm CKM}$ in 331 models appears to be problematic as we have just seen. The case $V_L \neq V_{\rm CKM}$ is much more successful as we will demonstrate now.

6.2 Non-CMFV case (B_s-system)

6.2.1 Preliminaries

Assuming next that the matrix V_L in (2.7) differs from the CKM matrix one has to find first the ranges of parameters (oases) for which a given 331 model agrees with the $\Delta F = 2$ data. The outcome of this search, for a given C_{B_s} (or C_{B_d} below), are two oases in the space $(\tilde{s}_{23}, \delta_2)$ for B_s-system and in the space $(\tilde{s}_{13}, \delta_1)$ for the B_d-system. We will not show these oases as they have structure similar to the ones shown in [2, 19]. We only recall that the two oases differ by a 180° shift in the phases $\delta_{1,2}$ which implies flips of signs of NP contributions to various $\Delta F = 1$ observables. As the $\Delta F = 2$ observables do not change under this shift of phases, the correlation of a given $\Delta F = 2$ observable like $S_{\psi\phi}$ and $\Delta F = 1$ observable like $\overline{\mathcal{B}}(B_s \to \mu^+\mu^-)$ in one oasis is changed to the anti-correlation in another oasis and vice versa. Measuring these two observables one can then determine the favoured oasis and subsequently make predictions for other observables.

We will next investigate what happens for the four different values of β considered by us and how the correlations between observables depend on the value of C_{B_s} using the colour coding in (5.1). We recall that all results for $\beta = \pm 1/\sqrt{3}$ and $\beta = \pm 2/\sqrt{3}$ are obtained for $M_{Z'} = 3\,\text{TeV}$ in order to be sure that the LHC lower bound on $M_{Z'}$ is satisfied, although as we will discuss in the next section, for $\beta = \pm 1/\sqrt{3}$ also values $M_{Z'} \approx 2.5\,\text{TeV}$ are consistent with these bounds. The results for $\Delta F = 1$ observables for $M_{Z'} \neq 3\,\text{TeV}$ can be obtained by using the scaling law in (3.15). Then NP effects in $\beta = \pm 1/\sqrt{3}$ could still be by a factor 1.2 larger than shown in the plots below.

Concerning the case of $\beta = -\sqrt{3}$, the problem with too a large C_{B_s} can now be avoided by properly choosing V_L but the other problems of this scenario, mentioned at the beginning of our paper and listed in appendix C, cannot be avoided in this manner and we will not discuss this case any more.

6.2.2 Results

In figure 5 we show $\overline{\mathcal{B}}(B_s \to \mu^+\mu^-)$ versus $\text{Re}(\text{C}_9^{\text{NP}})$ for the four models considered. These four plots exhibit the structure identified through the ratio R_1 in (3.9) for which numerical values have been given in table 2. In particular we observe the following features:[6]

- For a given $C_{B_s} \neq 1$, one can always find an oasis in which $\text{Re}(\text{C}_9^{\text{NP}})$ is negative softening significantly the $B_d \to K^*\mu^+\mu^-$ anomalies. However while for $\beta = -2/\sqrt{3}$

[6]We do not show the SM point in the plots as it corresponds to the point where various curves cross each other and in any case for coefficients that vanish in the SM it is obvious where the SM point is placed in the plot.

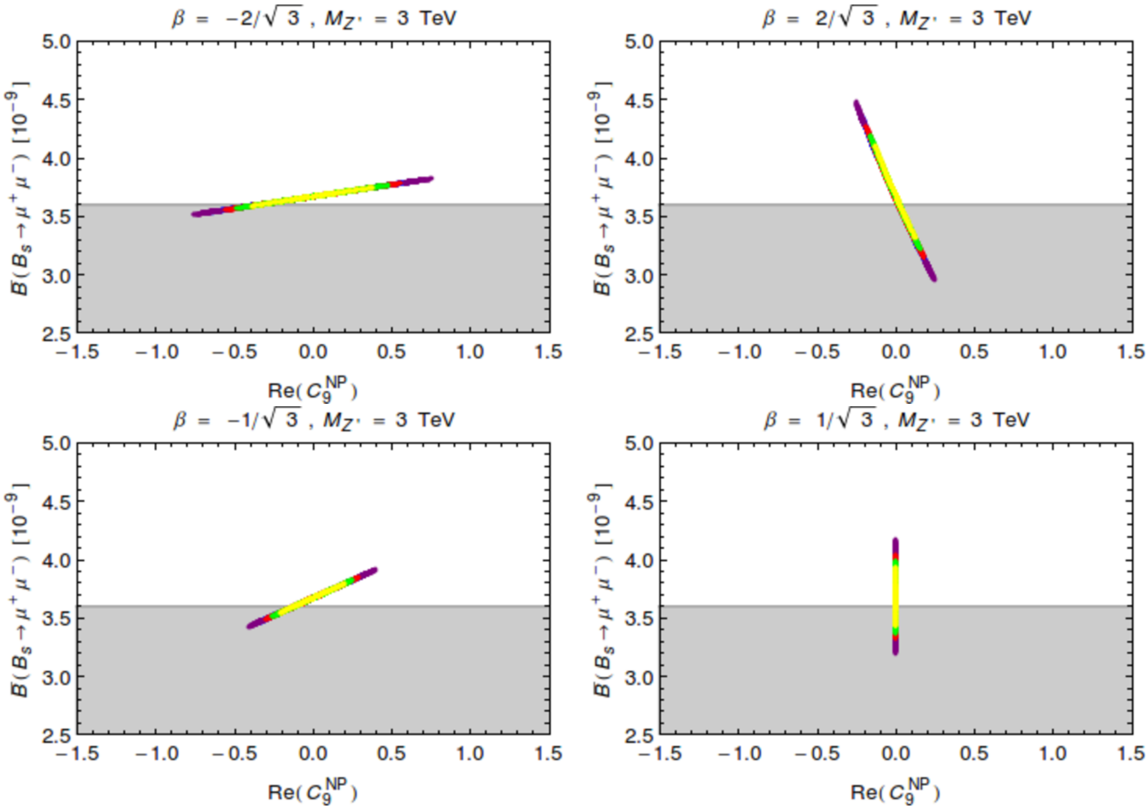

Figure 5. Correlation $\overline{\mathcal{B}}(B_s \to \mu^+\mu^-)$ versus $\mathrm{Re}(\mathrm{C}_9^{\mathrm{NP}})$ for $\beta = \pm 1/\sqrt{3}$ and $\beta = \pm 2/\sqrt{3}$ setting $M_{Z'} = 3\,\mathrm{TeV}$ and different values of C_{B_s} with their colour coding in (5.1). The gray regions show the experimental range $\overline{\mathcal{B}}(B_s \to \mu^+\mu^-) = (2.9 \pm 0.7) \cdot 10^{-9}$.

and $\beta = -1/\sqrt{3}$ the values $\mathrm{Re}(\mathrm{C}_9^{\mathrm{NP}}) = -0.8$ and $\mathrm{Re}(\mathrm{C}_9^{\mathrm{NP}}) = -0.4$ can be reached respectively, this is not possible for models with $\beta > 0$.

- For $\beta < 0$ the branching ratio $\overline{\mathcal{B}}(B_s \to \mu^+\mu^-)$ remains SM-like although in accordance with the relation (3.9) it is suppressed relative to its SM value for negative $\mathrm{Re}(\mathrm{C}_9^{\mathrm{NP}})$. For the largest values of C_{B_s} (purple and blue lines) this suppression can reach for most negative values of $\mathrm{Re}(\mathrm{C}_9^{\mathrm{NP}})$ 4% and 7% for $\beta = -2/\sqrt{3}$ and $\beta = -1/\sqrt{3}$, respectively. The slope of the strict correlation between these two observables depends on β. This correlation is presently supported by the data for both observables even if the effects in $\overline{\mathcal{B}}(B_s \to \mu^+\mu^-)$ are small.

- Looking at these four plots simultaneously we note that going from negative to positive values of β the correlation line moves counter clock-wise with the center of the clock placed at the SM value. This of course means that with increasing beta the correlation $\overline{\mathcal{B}}(B_s \to \mu^+\mu^-)$ versus $\mathrm{Re}(\mathrm{C}_9^{\mathrm{NP}})$ observed for $\beta < 0$ changes into anti-correlation for $\beta > 0$, which is rather pronounced in the case of $\beta = 2/\sqrt{3}$. Consequently the suppression of $\overline{\mathcal{B}}(B_s \to \mu^+\mu^-)$ implies positive values of $\mathrm{Re}(\mathrm{C}_9^{\mathrm{NP}})$ which is not what we want to understand $B_d \to K^*\mu^+\mu^-$ data. We also note that for $\beta > 0$ $\mathrm{Re}(\mathrm{C}_9^{\mathrm{NP}})$ remains small but the effects in $\overline{\mathcal{B}}(B_s \to \mu^+\mu^-)$ can be larger

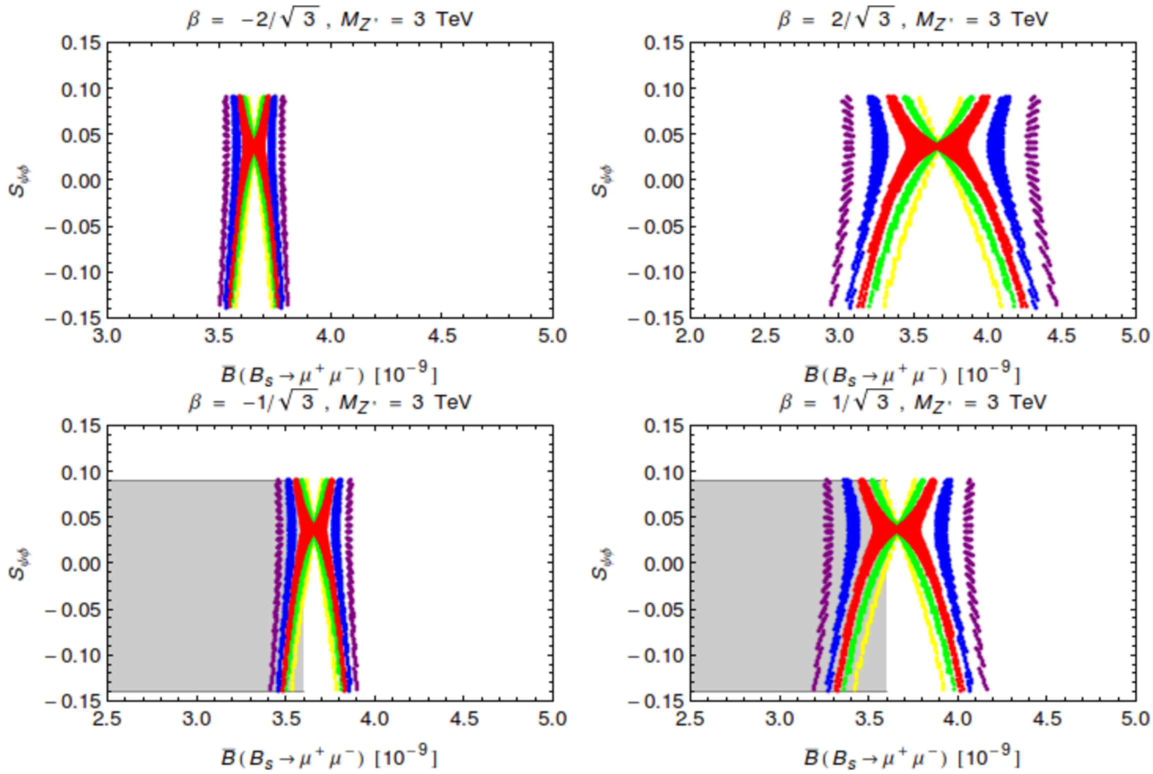

Figure 6. Correlations $S_{\psi\phi}$ versus $\overline{\mathcal{B}}(B_s \to \mu^+\mu^-)$ for $\beta = \pm 1/\sqrt{3}$ and $\beta = \pm 2/\sqrt{3}$ setting $M_{Z'} = 3\,\text{TeV}$ and different values of C_{B_s} with their colour coding in (5.1). The gray regions show the experimental range for $\overline{\mathcal{B}}(B_s \to \mu^+\mu^-)$ and $S_{\psi\phi}$.

than for $\beta < 0$. These scenarios would be the favorite ones if the $B_d \to K^*\mu^+\mu^-$ anomalies decreased or disappeared in the future while the experimental branching ratio $\overline{\mathcal{B}}(B_s \to \mu^+\mu^-)$ turned out to be indeed by 20% suppressed below its SM value as present central experimental and SM values seem to indicate. In this case the model with $\beta = 1/\sqrt{3}$ would be the winner.

This pattern of effects for negative and positive values of β is also seen in figures 6 and 7 where we show the correlations between $S_{\psi\phi}$ versus $\overline{\mathcal{B}}(B_s \to \mu^+\mu^-)$ and $S_{\psi\phi}$ versus $\text{Re}(\text{C}_9^{\text{NP}})$, respectively. In particular we find that for models with $\beta < 0$ for most negative values of $\text{Re}(\text{C}_9^{\text{NP}})$ and smallest values of $\overline{\mathcal{B}}(B_s \to \mu^+\mu^-)$ the negative values of $S_{\psi\phi}$ are favoured. But as the values of $S_{\psi\phi}$ are rather sensitive for a given value of C_{B_s} to the value of $\overline{\mathcal{B}}(B_s \to \mu^+\mu^-)$, away from the lower bound on this branching ratio also positive values of $S_{\psi\phi}$ are allowed. This is in particular the case for largest values of C_{B_s}.

Bearing this ambiguity in mind, we identify therefore for a given C_{B_s} a triple correlation between $\text{Re}(\text{C}_9^{\text{NP}})$, $\overline{\mathcal{B}}(B_s \to \mu^+\mu^-)$ and $S_{\psi\phi}$ that is an important test of this model. Interestingly the requirement of a most negative $\text{Re}(\text{C}_9^{\text{NP}})$ shifts automatically the other two observables closer to the data.

While the departure of $S_{\psi\phi}$ from its SM value is already a clear signal of new sources of CP-violation in $\Delta F = 2$ transitions, non-vanishing imaginary parts of C_9 and C_{10} are

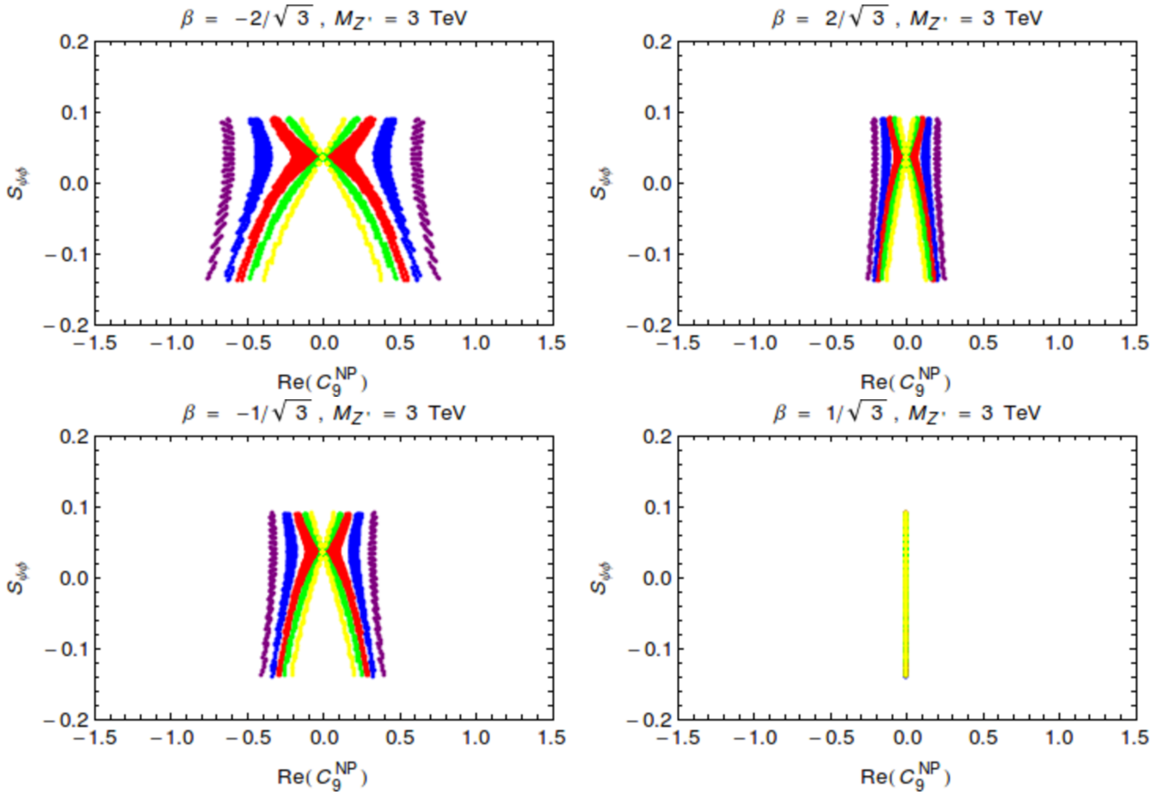

Figure 7. Correlations $S_{\psi\phi}$ versus $\mathrm{Re}(C_9^{\rm NP})$ for $\beta = \pm 1/\sqrt{3}$ and $\beta = \pm 2/\sqrt{3}$ setting $M_{Z'} = 3\,\mathrm{TeV}$ and different values of C_{B_s} with their colour coding in (5.1).

signals of such new effects in $\Delta F = 1$ transitions. In figures 8 and 9 we show the correlations $\mathrm{Im}(C_9^{\rm NP})$ versus $\mathrm{Re}(C_9^{\rm NP})$ and $\mathrm{Im}(C_{10}^{\rm NP})$ versus $\mathrm{Re}(C_{10}^{\rm NP})$, respectively. The fact that the pattern in both figures for a given β is the same, even if the size of NP effects differs, is related to the relation (3.10).

We again observe that for $\beta < 0$ NP effects are mainly seen in $\mathrm{Im}(C_9^{\rm NP})$ while for $\beta > 0$ in $\mathrm{Im}(C_{10}^{\rm NP})$. In particular for $\beta = 1/\sqrt{3}$ NP effects in C_9 practically vanish which is a good test of this model. Dependently on the values of C_{B_s} and $|\beta|$, the CP-asymmetry $\langle A_8 \rangle$ could reach $(2-3)\%$ and the asymmetry $\langle A_7 \rangle$ even $(3-4)\%$ for $\beta < 0$ and $\beta > 0$, respectively.

Finally in figures 10 and 11 we show the correlations $\mathrm{Re}(C_{10}^{\rm NP})$ versus $\mathrm{Re}(C_9^{\rm NP})$ and $\mathrm{Im}(C_{10}^{\rm NP})$ versus $\mathrm{Im}(C_9^{\rm NP})$ for the four 331 models considered by us. These results follow from (3.9).

New sources of CP-violation can also be tested in $B_s \to \mu^+\mu^-$ through the asymmetry $S_{\mu\mu}$ defined in (4.18) and studied in detail in [19, 45] in the context of general Z' models. In figure 12 we show the correlation of $S_{\mu\mu}^s$ versus $\overline{\mathcal{B}}(B_s \to \mu^+\mu^-)$ in 331 model considered. As expected the effects in the models with $\beta > 0$ are larger than for $\beta < 0$. Similar to the case of $S_{\psi\phi}$ the required suppression of $\overline{\mathcal{B}}(B_s \to \mu^+\mu^-)$ favours negative values of $S_{\mu\mu}^s$ in all models.

As stressed in [11] the Wilson coefficient $C_9^{\rm NP}$ by itself has difficulty in removing completely the anomalies in $B_d \to K^*\mu^+\mu^-$ due to the constraint from $B_d \to K\mu^+\mu^-$. We

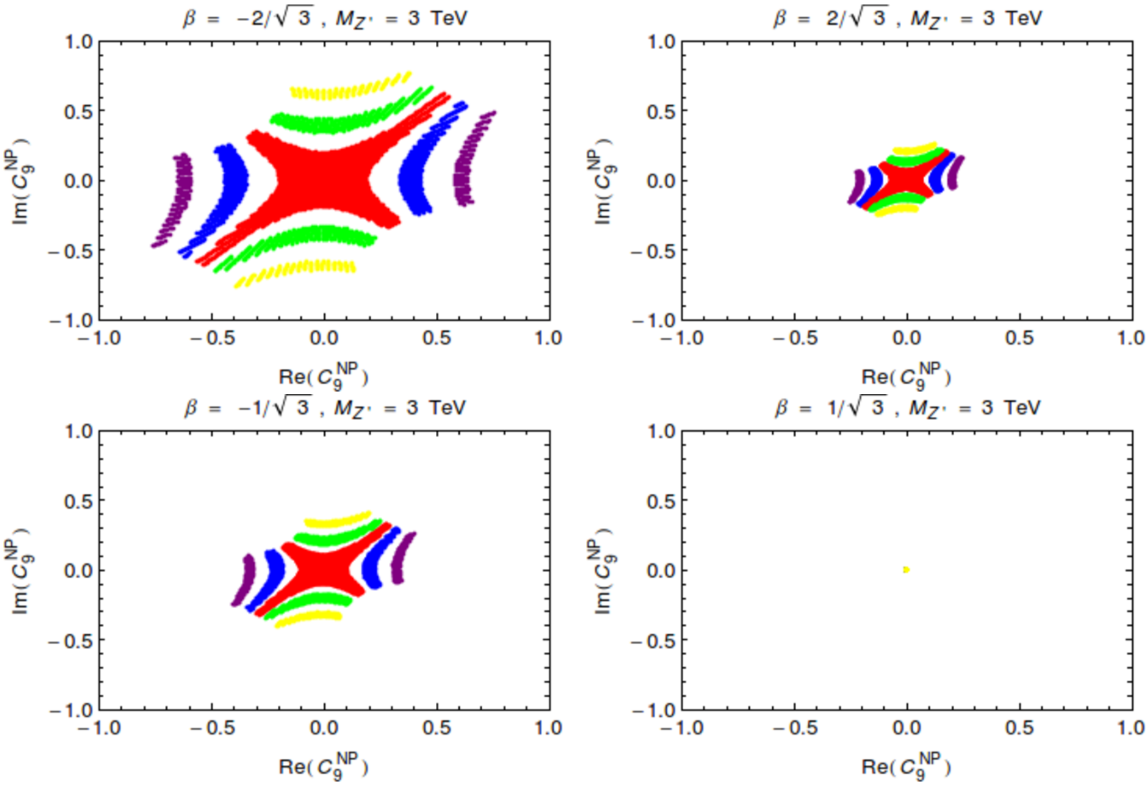

Figure 8. Correlations $\mathrm{Im}(\mathrm{C}_9^{\mathrm{NP}})$ versus $\mathrm{Re}(\mathrm{C}_9^{\mathrm{NP}})$ for $\beta = \pm 1/\sqrt{3}$ and $\beta = \pm 2/\sqrt{3}$ setting $M_{Z'} = 3\,\mathrm{TeV}$ and different values of C_{B_s} with their colour coding in (5.1).

have seen that even without this constraint the values of Re $\mathrm{C}_9^{\mathrm{NP}}$ have to be larger than -0.8 but this could turn out to be sufficient to reproduce the data when they improve. Still it is of interest to have a closer look at $B_d \to K\mu^+\mu^-$ within the four 331 models analysed by us.

To this end the approximate formula for the branching ratio confined to large q^2 region by the authors of [11] is very useful. Lattice calculations of the relevant form factors are making significant progress here [68, 69] and the importance of this decay will increase in the future. Neglecting the interference between NP contributions the formula of [11] reduces in 331 models to

$$10^7 \times \mathcal{B}(B_d \to K\mu^+\mu^-)_{[14.2,22]} = 1.11 + 0.27\ \mathrm{Re}(\mathrm{C}_9^{\mathrm{NP}}) \left(1 - \frac{1}{\mathrm{R}_1}\right), \tag{6.3}$$

where we have used (3.9) to express $\mathrm{Re}(\mathrm{C}_{10}^{\mathrm{NP}})$ in terms of $\mathrm{Re}(\mathrm{C}_9^{\mathrm{NP}})$. The error on the first SM term is estimated to be 10% [68, 69]. This should be compared with the LHCb result

$$10^7 \times \mathcal{B}(B_d \to K\mu^+\mu^-)_{[14.2,22]} = 1.04 \pm 0.12 \qquad \text{(LHCb)}. \tag{6.4}$$

Using (6.3) we show in figure 13 the correlation between $\mathcal{B}(B_d \to K\mu^+\mu^-)_{[14.2,22]}$ and $\mathrm{Re}(\mathrm{C}_9^{\mathrm{NP}})$ for the four 331 models in question.

We observe that the pattern of the correlations is similar to the ones in figure 5 which originates in the fact that $\mathcal{B}(B_d \to K\mu^+\mu^-)_{[14.2,22]}$ is strongly correlated with $\overline{\mathcal{B}}(B_s \to$

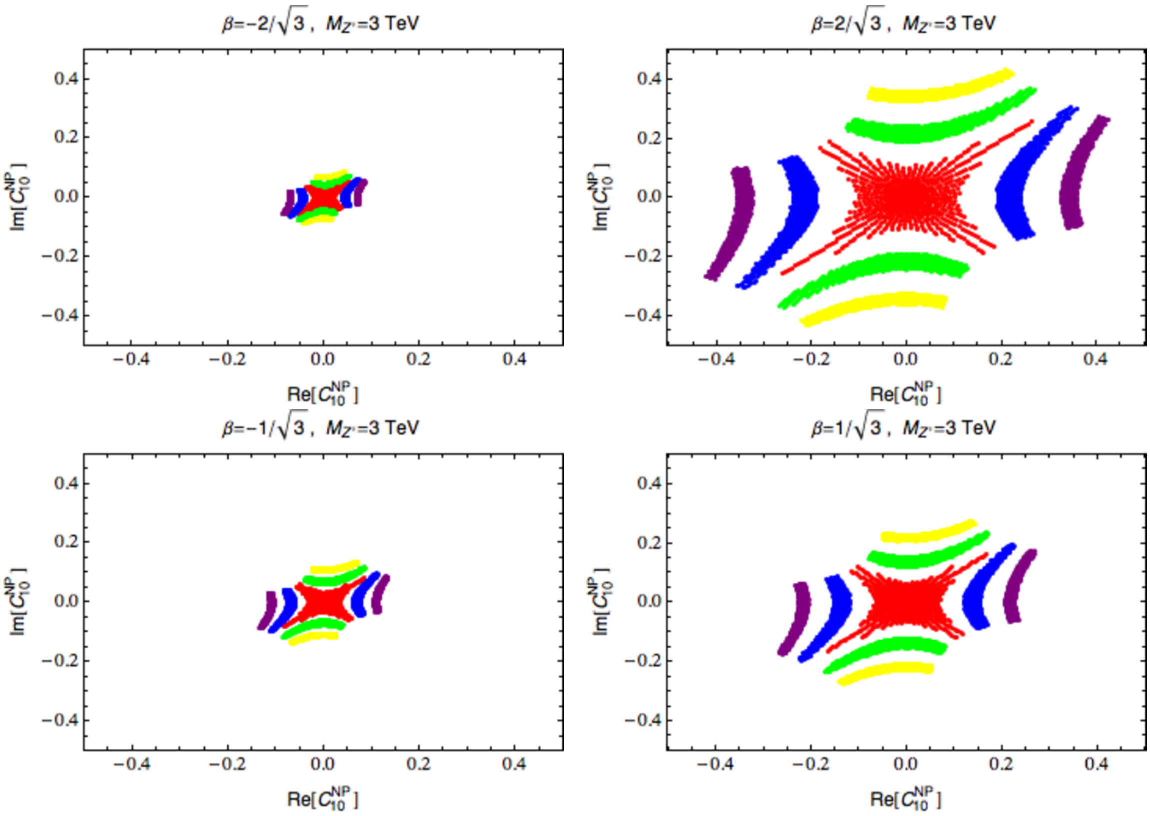

Figure 9. $\mathrm{Im}(\mathrm{C}_{10}^{\mathrm{NP}})$ versus $\mathrm{Re}(\mathrm{C}_{10}^{\mathrm{NP}})$ for $\beta = \pm 1/\sqrt{3}$ and $\beta = \pm 2/\sqrt{3}$ setting $M_{Z'} = 3\,\mathrm{TeV}$ and different values of C_{B_s} with their colour coding in (5.1).

$\mu^+\mu^-$) within l.h.s. models as already shown in [13] for a general l.h.s. model. Moreover, as R_1 is fixed in a given model and its values have been collected in table 2 the straight lines in figure 5 can be easily understood.

There are two messages from this exercise:

- Our results for $\mathrm{Re}(\mathrm{C}_9^{\mathrm{NP}})$ are fully in accordance with the present data on $\mathcal{B}(B_d \to K\mu^+\mu^-)_{[14.2,22]}$.
- On the basis of figures 5 and 13 there is a triple correlation between $\mathcal{B}(B_d \to K\mu^+\mu^-)_{[14.2,22]}$, $\mathrm{Re}(\mathrm{C}_9^{\mathrm{NP}})$ and $\overline{\mathcal{B}}(B_s \to \mu^+\mu^-)$ which constitutes an important test for the models in question. We indicate this correlation in figure 13 by showing when the latter branching ratio is suppressed (*black*) or enhanced (*yellow*) with respect to its SM value in accordance with the colour coding in DNA-charts of [1].

6.3 Non-CMFV case (B_d-system)

We have seen in the case of the MFV limit that $\mathcal{B}(B_d \to \mu^+\mu^-)$ is predicted to be suppressed relative to its SM value when $\mathrm{Re}(\mathrm{C}_9^{\mathrm{NP}})$ is negative. This moves the theory away from the central value of the experimental branching ratio. However, in the non-MFV case we can choose the particular oasis in the space $(\tilde{s}_{13}, \delta_1)$ in which $\mathcal{B}(B_d \to \mu^+\mu^-)$ is enhanced.

JHEP02(2014)112

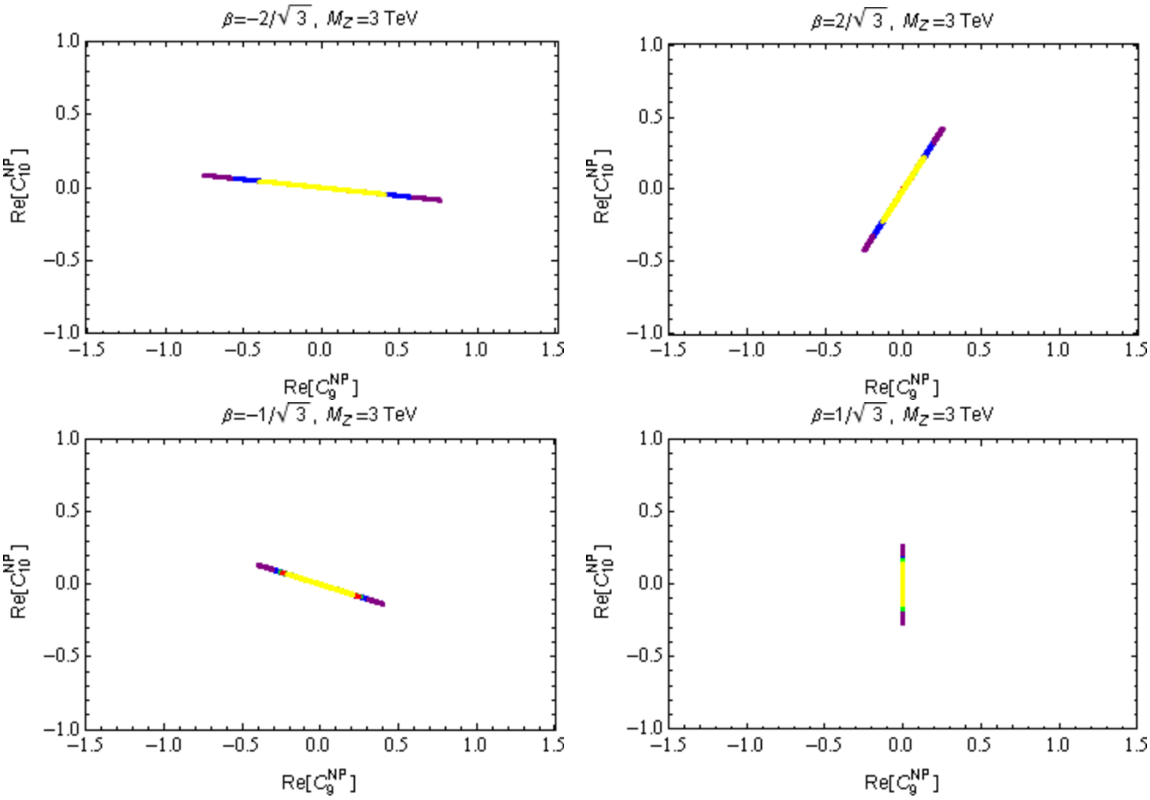

Figure 10. $\mathrm{Re}(\mathrm{C}_{10}^{\mathrm{NP}})$ versus $\mathrm{Re}(\mathrm{C}_9^{\mathrm{NP}})$ for $\beta = \pm 1/\sqrt{3}$ and $\beta = \pm 2/\sqrt{3}$ setting $M_{Z'} = 3\,\mathrm{TeV}$ and different values of C_{B_s} with their colour coding in (5.1).

In the left upper panel of figure 14 we show $\mathcal{B}(B_d \to \mu^+\mu^-)$ versus $S_{\psi K_S}$ again for $\beta = -2/\sqrt{3}$ and different bins of C_{B_d}. We observe that the values of $\mathcal{B}(B_d \to \mu^+\mu^-)$ are SM-like and as already expected from the values of $\Delta_A^{\mu\bar{\mu}}$ the central experimental value of this branching ratio cannot be reproduced in this model.

More interesting results are found for $\beta > 0$. In the right upper panel of figure 14 we show $\mathcal{B}(B_d \to \mu^+\mu^-)$ versus $S_{\psi K_S}$ for $\beta = 2/\sqrt{3}$. We observe that now enhancement of $\mathcal{B}(B_d \to \mu^+\mu^-)$ can reach 20% over its SM value but still far away from the central experimental value. For $\beta = -1/\sqrt{3}$ and $\beta = 1/\sqrt{3}$ NP effects turn out to be larger and smaller relative to $\beta = \mp 2/\sqrt{3}$ respectively, as one could deduce from the values of the axial-vector couplings.

Next in figure 15 we show $\mathcal{B}(B_d \to \mu^+\mu^-)$ versus $\overline{\mathcal{B}}(B_s \to \mu^+\mu^-)$ for the four models considered with the colour coding for β given in (6.2). We also show the CMFV line. As the uncertainty in the latter line should be reduced to a few percent in this decade, this plot could turn out to be useful for testing and distinguishing the four 331 models.

6.4 Non-CMFV case for $b \to s\nu\bar{\nu}$, $K^+ \to \pi^+\nu\bar{\nu}$ and $K_L \to \pi^0\nu\bar{\nu}$

6.4.1 Preliminaries

Finally, we turn our discussion to decays with neutrinos in the final state. We recall that for given β, C_{B_d}, C_{B_s} and the chosen oases in B_d and B_s systems the corresponding oasis

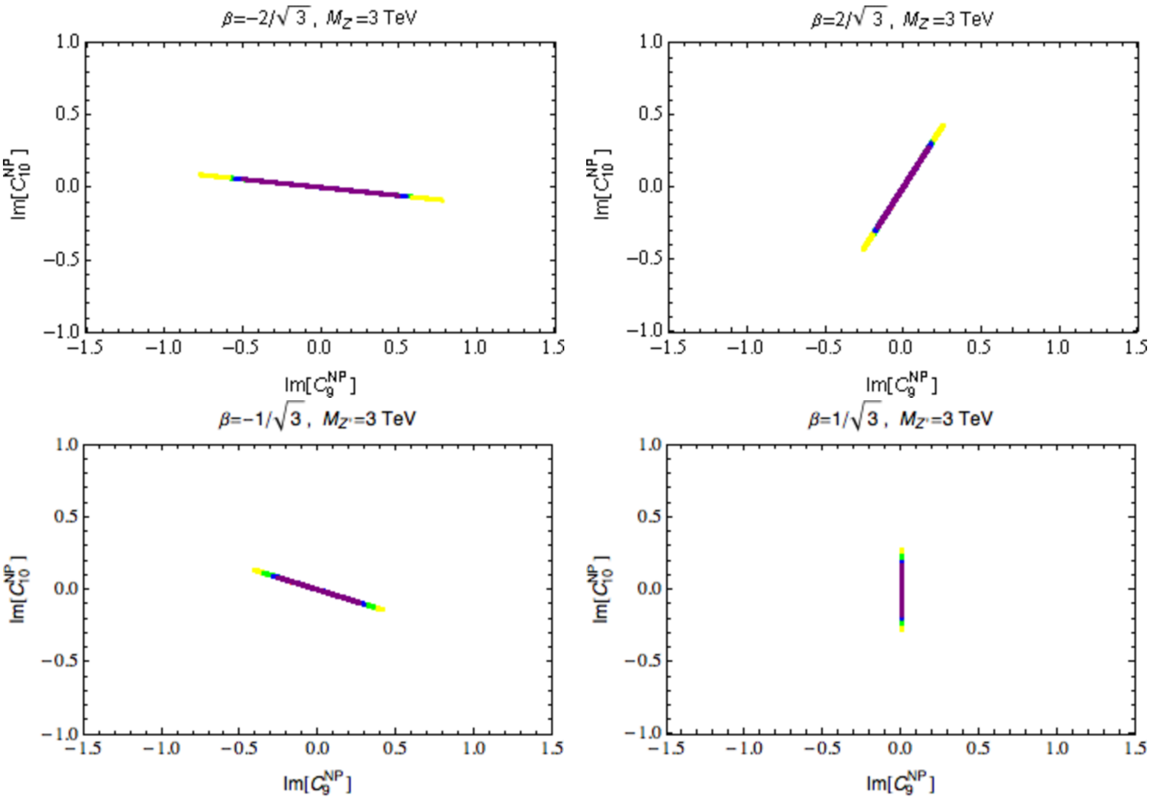

Figure 11. $\mathrm{Im}(C_{10}^{\mathrm{NP}})$ versus $\mathrm{Im}(C_9^{\mathrm{NP}})$ for $\beta = \pm 1/\sqrt{3}$ and $\beta = \pm 2/\sqrt{3}$ setting $M_{Z'} = 3\,\mathrm{TeV}$ and different values of C_{B_s} with their colour coding in (5.1).

including its size is fixed so that definite predictions for $b \to s\nu\bar{\nu}$ transition, $K^+ \to \pi^+\nu\bar{\nu}$ and $K_L \to \pi^0\nu\bar{\nu}$ can be made.

The inspection of the correlations presented in section 4 teaches us about the following facts:

- NP effects in ε_K are small but this is not a problem as with our nominal values of $|V_{ub}|$, $|V_{cb}|$ and γ SM value of ε_K agrees well with the data.
- For $\beta > 0$ NP effects in these decays are found to be small but are larger in the cases with $\beta < 0$ where Z' couplings to neutrinos are largest.
- Similarly NP effects in $K^+ \to \pi^+\nu\bar{\nu}$ and $K_L \to \pi^0\nu\bar{\nu}$ are small as we have already expected on the basis of the relation (3.18).

6.4.2 The $b \to s\nu\bar{\nu}$ transitions

In the absence of right-handed currents one finds [70]

$$R_{\nu\bar{\nu}} = \frac{\mathcal{B}(B \to K\nu\bar{\nu})}{\mathcal{B}(B \to K\nu\bar{\nu})_{\mathrm{SM}}} = \frac{\mathcal{B}(B \to K^*\nu\bar{\nu})}{\mathcal{B}(B \to K^*\nu\bar{\nu})_{\mathrm{SM}}} = \frac{\mathcal{B}(B \to X_s\nu\bar{\nu})}{\mathcal{B}(B \to X_s\nu\bar{\nu})_{\mathrm{SM}}} = \frac{|X_{\mathrm{L}}(B_s)|^2}{|\eta_X X_0(x_t)|^2}\,, \quad (6.5)$$

with

$$X_{\mathrm{L}}(B_s) = \eta_X X_0(x_t) + \Delta X(B_s) \quad (6.6)$$

JHEP02(2014)112

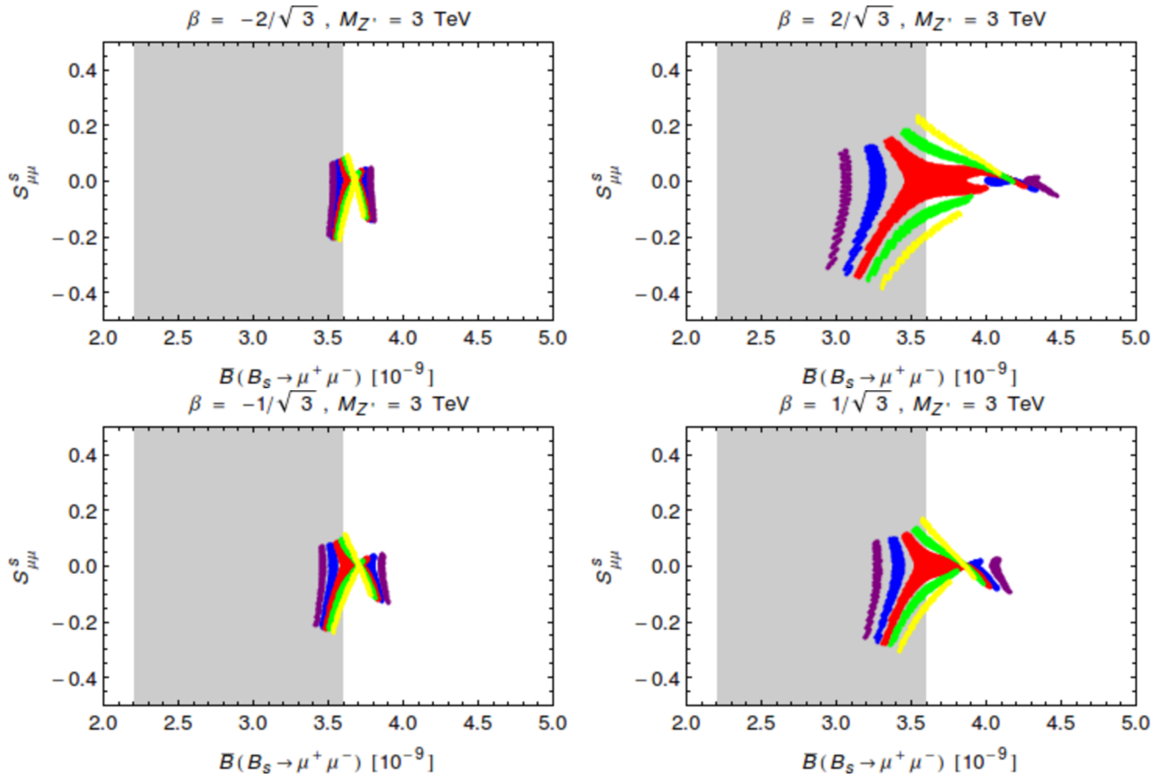

Figure 12. $S^s_{\mu\mu}$ versus $\overline{\mathcal{B}}(B_s \to \mu^+\mu^-)$ for $\beta = \pm 1/\sqrt{3}$ and $\beta = \pm 2/\sqrt{3}$ setting $M_{Z'} = 3\,\text{TeV}$ and different values of C_{B_s} with their colour coding in (5.1). The gray regions show the experimental range for $\overline{\mathcal{B}}(B_s \to \mu^+\mu^-)$.

and $\Delta X(B_s)$ given in (3.5). The QCD factor $\eta_X = 0.994$ [71]. In this case the NLO electroweak corrections are of the order of one per mil [52] when similarly to our discussion of η_{eff} in the context of $B_{s,d} \to \mu^+\mu^-$ decays one uses the normalization of effective Hamiltonian in [51] and the top quark mass is evaluated in the $\overline{\text{MS}}$ scheme for QCD and on-shell with respect to electroweak interactions. Thus accidentally η_{eff} that includes both QCD and electroweak corrections turns out in this scheme to be practically the same for $K \to \pi\nu\bar{\nu}$ and $B_{s,d} \to \mu^+\mu^-$ decays.

The equality of these three ratios is an important test of any l.h.s. scenario. The violation of them would imply the presence of right-handed couplings at work [70, 72, 73]. In the context of Z' models this is clearly seen in figure 20 of [19].

The $\text{SU}(2)_L$ relation in (1.4) satisfied in any l.h.s. model, therefore also in the 331 models presented by us, implies a correlation between $R_{\nu\bar{\nu}}$, $\overline{\mathcal{B}}(B_s \to \mu^+\mu^-)$ and C_9^{NP} as shown for a general l.h.s. model in figure 9 of [13].

In figure 16 we show one of these ratios versus $\overline{\mathcal{B}}(B_s \to \mu^+\mu^-)$ for the models considered. We observe that in all models considered we have an anti-correlation between these two observables. But the predicted NP effects in all models are rather small. The same conclusion has been reached for general l.h.s. models in [11, 13].

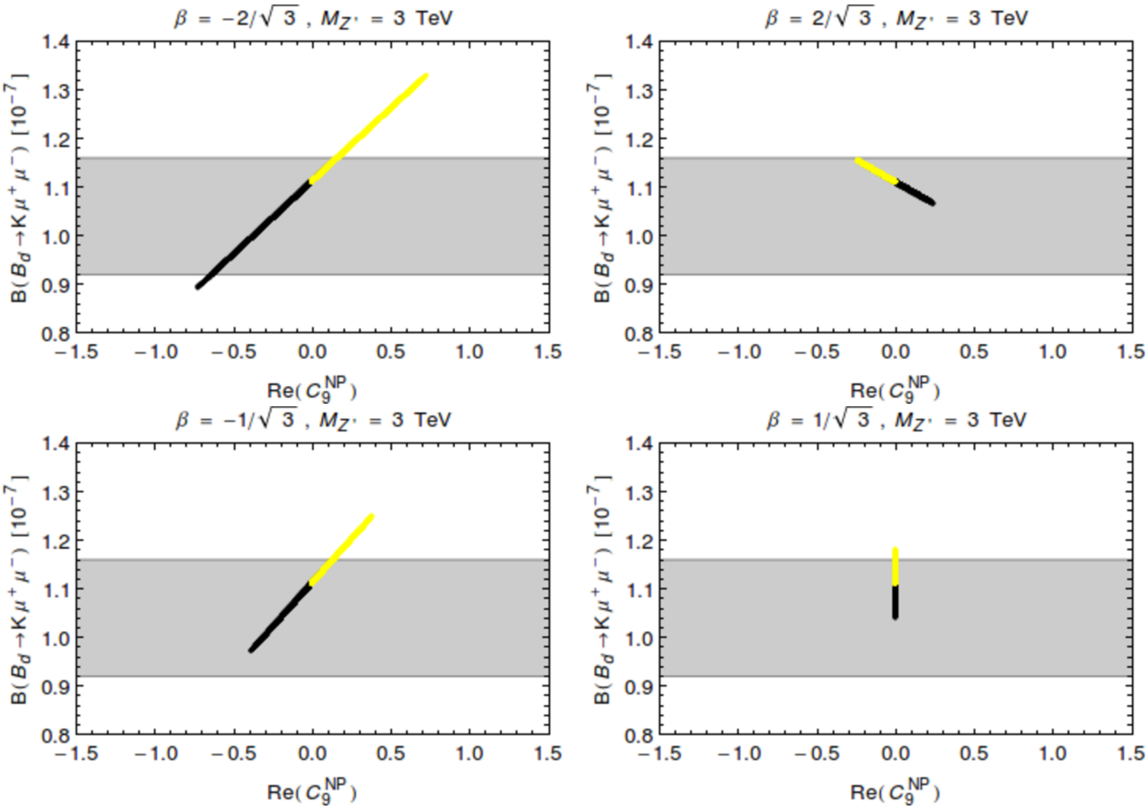

Figure 13. Correlation $\mathcal{B}(B_d \to K\mu^+\mu^-)_{[14.2,22]}$ versus $\mathrm{Re}(C_9^{\mathrm{NP}})$ for $\beta = \pm 1/\sqrt{3}$ and $\beta = \pm 2/\sqrt{3}$ setting $M_{Z'} = 3\,\mathrm{TeV}$, $\overline{\mathcal{B}}(B_s \to \mu^+\mu^-) \leq \overline{\mathcal{B}}(B_s \to \mu^+\mu^-)_{\mathrm{SM}}$ (black) and $\overline{\mathcal{B}}(B_s \to \mu^+\mu^-) \geq \overline{\mathcal{B}}(B_s \to \mu^+\mu^-)_{\mathrm{SM}}$ (yellow) . The gray regions show the experimental range for $\mathcal{B}(B_d \to K\mu^+\mu^-)_{[14.2,22]}$ in (6.4).

6.4.3 $K^+ \to \pi^+\nu\bar{\nu}$, $K_L \to \pi^0\nu\bar{\nu}$ and $K_L \to \mu^+\mu^-$ decays

The formulae for these decays have been given in [19] and will not be repeated here. In figure 17 we show the correlation between $\mathcal{B}(K^+ \to \pi^+\nu\bar{\nu})$ and $\mathcal{B}(K_L \to \pi^0\nu\bar{\nu})$ and the one between $\mathcal{B}(K^+ \to \pi^+\nu\bar{\nu})$ and $\mathcal{B}(K_L \to \mu^+\mu^-)$ for the four models considered. The effects are rather small. What is interesting are the SM values in the middle of both plots that are enhanced over the usual values quoted as a consequence of inclusive value of $|V_{cb}|$ used by us.

7 Low and high energy constraints

7.1 Low energy precision observables

Low energy precision observables provide additional bounds on the parameters of the models considered, in particular on the allowed range of $M_{Z'}$ as investigated recently in the context of $\beta = -\sqrt{3}$ model in [14]. We want to add that in concrete models studied here the signs of deviations from SM predictions for these observables are fixed providing additional tests beyond the lower bounds on $M_{Z'}$. In what follows we will present the predictions for

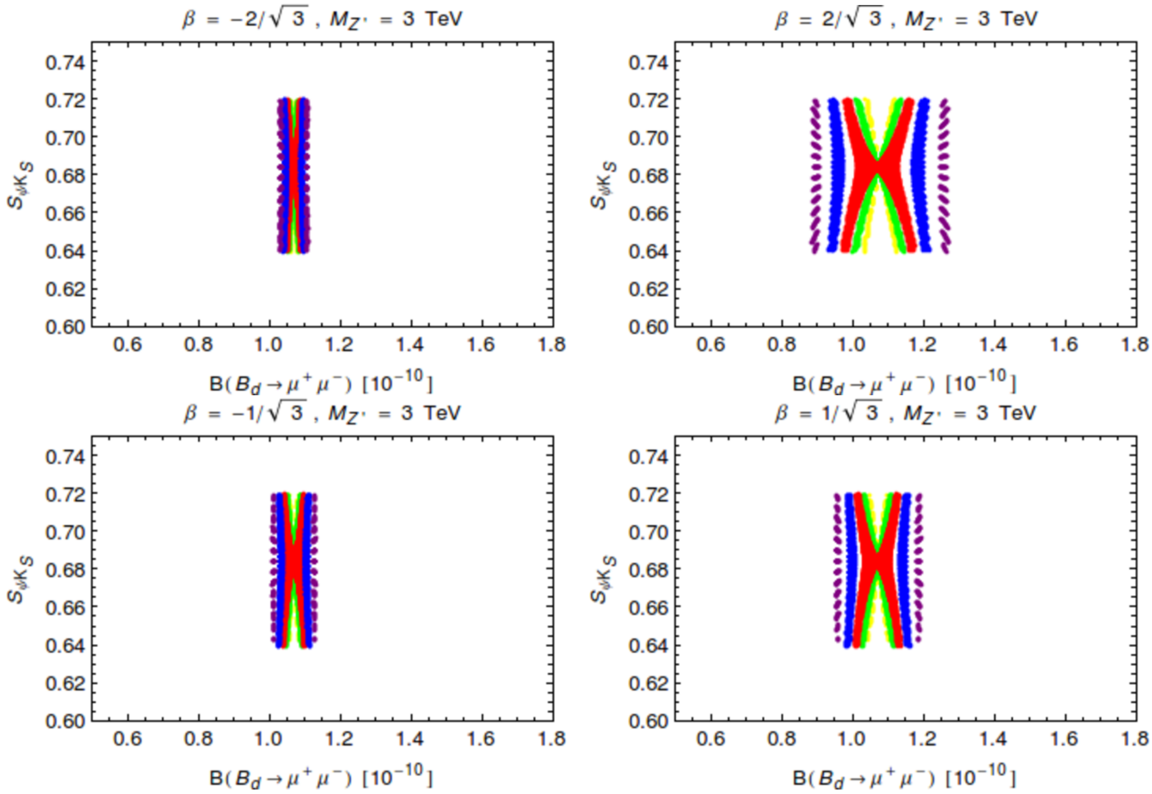

Figure 14. Correlation $\mathcal{B}(B_d \to \mu^+\mu^-)$ versus $S_{\psi K_S}$ for $\beta = \pm 1/\sqrt{3}$ and $\beta = \pm 2/\sqrt{3}$ setting $M_{Z'} = 3\,\text{TeV}$ and different values of C_{B_s} with their colour coding in (5.1).

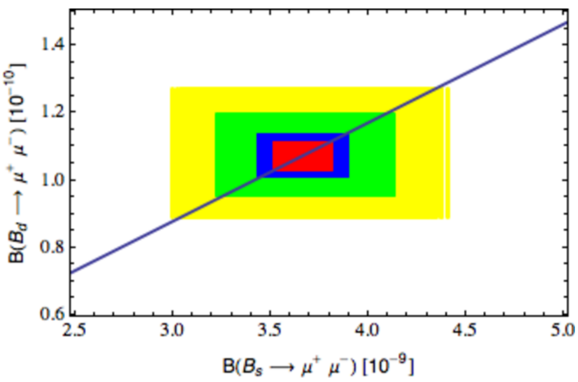

Figure 15. Correlation $\mathcal{B}(B_d \to \mu^+\mu^-)$ versus $\overline{\mathcal{B}}(B_s \to \mu^+\mu^-)$ for the four models considered in the paper. The colour coding for β is given in (6.2). The straight line represents CMFV.

three such observables, considered also in [14], separately in each model from which the lower bounds on $M_{Z'}$ follow.

We begin with the effect due to a Z' gauge boson on the weak charge of a nucleus consisting of Z protons and N neutrons calculated in [74]. In translating this result into our notation one should note that the vector and axial-vector couplings $f_{V,A}$ defined in [74]

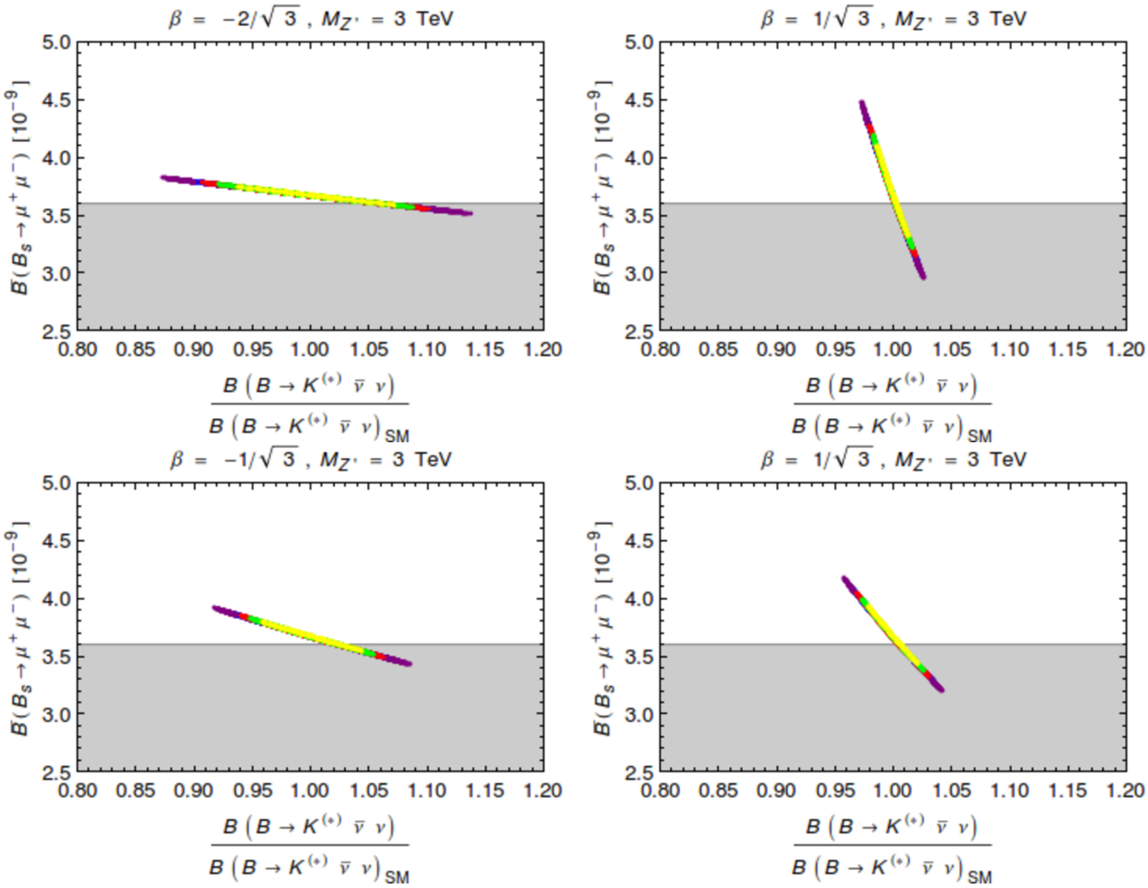

Figure 16. $\overline{\mathcal{B}}(B_s \to \mu^+\mu^-)$ versus the ratio in (6.5) for all four $\beta = \pm\frac{2}{\sqrt{3}}, \pm\frac{1}{\sqrt{3}}$.

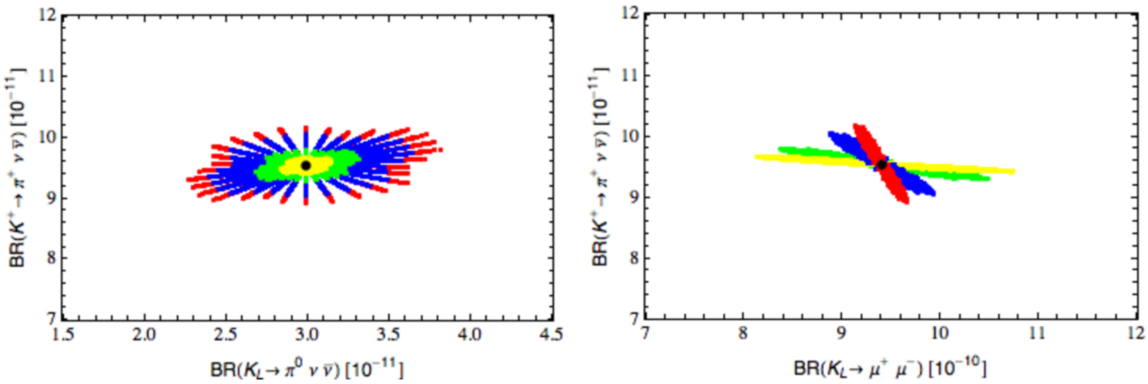

Figure 17. Correlations between rare K decays for different values of β using the colour coding in (6.2).

are not equal to our couplings $\Delta_{V,A}(Z')$ but are related through

$$f_V = \frac{\Delta_V(Z')}{2}, \qquad f_A = -\frac{\Delta_A(Z')}{2}. \tag{7.1}$$

JHEP02(2014)112

We find then $(\Delta_A^{e\bar{e}}(Z') = \Delta_A^{\mu\bar{\mu}}(Z'))$

$$\Delta Q_W(Z,N) = \frac{1}{\sqrt{2}G_F}\frac{\Delta_A^{e\bar{e}}(Z')}{M_{Z'}^2}\left[(2Z+N)\Delta_V^{u\bar{u}}(Z') + (Z+2N)\Delta_V^{d\bar{d}}(Z')\right] \tag{7.2}$$

which has an additional overall factor of $-1/4$ relative to the corresponding expression in [14] where $f_{V,A} = \Delta_{V,A}$ have been used.[7] We have then

$$\Delta Q_W(Z,N) = (0.67)\,10^{-2}\left[\frac{3\,\text{TeV}}{M_{Z'}}\right]^2 \Delta_A^{e\bar{e}}(Z')\left[(2Z+N)\Delta_V^{u\bar{u}}(Z') + (Z+2N)\Delta_V^{d\bar{d}}(Z')\right]. \tag{7.3}$$

Similarly for the effective shift in the weak charge of electron that can be studied in Møller scattering we find

$$\Delta Q_W^e = (0.67)\,10^{-2}\left[\frac{3\,\text{TeV}}{M_{Z'}}\right]^2 \Delta_A^{e\bar{e}}(Z')\Delta_V^{e\bar{e}}(Z'). \tag{7.4}$$

For the violation of the first row CKM unitarity expressed through

$$\tilde{\Delta}_{\text{CKM}} \equiv 1 - \sum_{q=d,s,b}|V_{uq}|^2 \tag{7.5}$$

one has for $M_{Z'} \gg M_W$ [12–14, 75]

$$\tilde{\Delta}_{\text{CKM}} = \frac{3}{4\pi^2}\frac{M_W^2}{M_{Z'}^2}\ln\frac{M_{Z'}^2}{M_W^2}\Delta_L^{\mu\bar{\mu}}(Z')\left[\Delta_L^{\mu\bar{\mu}}(Z') - \Delta_L^{d\bar{d}}(Z')\right]. \tag{7.6}$$

In table 4 we show predictions for these shifts in four models considered by us and in each case the lower bound on $M_{Z'}$ that follows from present experimental bounds. In the first case we use, as in [14], Cesium nucleus with $Z = 55$ and $N = 78$. We observe that the 90% CL experimental bounds [38, 76]

$$|\Delta Q_W^{\text{Cs}}| \le 0.6, \qquad |\Delta Q_W^{\text{e}}| \le 0.016, \qquad |\tilde{\Delta}_{\text{CKM}}| \le 0.001 \tag{7.7}$$

are well satisfied and the lower bounds on $M_{Z'}$ are significantly below the values used by us. We indicated by dashes lower bounds on $M_{Z'}$ below 1 TeV. In order to obtain these bounds we neglected running of $\sin^2\theta_W$ from 3 TeV down to these bounds. Including it would further weaken these bound but this effect is minor.

7.2 LEP-II constraints

Recently the final analysis of LEP-II data by the LEP electroweak working group appeared in [77] which allows us to check whether the values for $M_{Z'}$ for the six 331 models considered by us are consistent with these data. The data relevant for us correspond to the range of center of mass energy $189\,\text{GeV} \le \sqrt{s} \le 207\,\text{GeV}$. In our numerical calculations we will set $\sqrt{s} = 200\,\text{GeV}$.

[7] The authors of [14] confirm our findings.

β	$1/\sqrt{3}$	$-1/\sqrt{3}$	$2/\sqrt{3}$	$-2/\sqrt{3}$
$\Delta Q_W^{\rm Cs}$	0.106	0.080	0.158	0.075
$\mathrm{Min}(M_{Z'})[\,\mathrm{TeV}]$	1.26	1.10	1.54	1.06
$10^3 \times \Delta Q_W^e$	-0.002	-0.334	0.656	-0.402
$\mathrm{Min}(M_{Z'})[\,\mathrm{TeV}]$	–	–	–	–
$10^4 \times \tilde\Delta_{\rm CKM}$	0.154	0.482	0.088	1.13
$\mathrm{Min}(M_{Z'})[\,\mathrm{TeV}]$	–	–	–	1.01

Table 4. Prediction for various observables for different β setting $M_{Z'} = 3\,\mathrm{TeV}$. Only lower bounds on $M_{Z'}$ above 1 TeV resulting from present constraints on these observables are shown.

The fundamental for this analysis is the formula (3.8) in this paper [78][8]

$$\mathcal{L}_{\rm eff} = \frac{4\pi}{\Lambda_\pm^2} \sum_{i,j=L,R} \eta_{ij} \bar e_i \gamma_\mu e_i \bar f_j \gamma^\mu f_j, \qquad (f \neq e). \tag{7.8}$$

In this formula $\eta_{ij} = \pm 1$ or $\eta_{ij} = 0$. The different signs of η_{ij} allow to distinguish between constructive $(+)$ and destructive $(-)$ interference between the SM and NP contribution. $\Lambda_\pm$ is the scale of the contact interaction which can be related to $M_{Z'}$ after proper rescaling of η_{ij}. The lower bounds on $\Lambda_\pm$ presented in table 3.15 of [77] apply to certain choices of η_{ij} that are defined in table 3.14 of that paper.

In the models considered by us there is the overall minus sign due to Z' propagator relative to the SM contribution which we include in the definition of η_{ij} so that with

$$\eta_{ij}^{ef}(Z') = -\Delta_i^{e\bar e}(Z')\Delta_j^{f\bar f}(Z'), \tag{7.9}$$

we obtain the relation

$$M_{Z'} = \frac{\Lambda_\pm}{\sqrt{4\pi}} \sqrt{|\Delta_i^{e\bar e}(Z')\Delta_j^{f\bar f}(Z')|}. \tag{7.10}$$

As we know the signs of η_{ij} in each model we know in each case whether the bound on Λ_+ or Λ_- should be used. In tables 5–7 we list the values of the couplings η_{ij} for the six models considered by us together with the corresponding values for $\eta_{ij}(Z)$ for which the minus sign in (7.9) should be omitted as the energies involved at LEP-II $\sqrt{s} > M_Z$.

The case of $\beta = -\sqrt{3}$ is easy to test in the case of $e^+e^- \to \mu^+\mu^-$ as in this case we deal with the model VV^- of [77]. We find then the lower bound for $M_{Z'}$ of 11 TeV, well above the validity of this model. We would like to emphasize that this bound is quoted here only as an illustration. As discussed in appendix C the coupling α_X at scales above 1 TeV is too large to trust perturbation theory and calculating only tree diagrams misrepresents the real situation. Whether a non-perturbative dynamics would cure this model remains to be seen.

Before turning to explicit four models analyzed by us let us note that in the LL^-, RR^- and VV^- models for couplings in [77], which correspond to $\Delta_R^{l\bar l}(Z') = 0$, $\Delta_L^{l\bar l}(Z') = 0$

[8]We prefer not to use $e^+e^- \to e^+e^-$ due to other contributions like Babha scattering.

JHEP02(2014)112

and $\Delta_L^{l\bar{l}}(Z') = \Delta_R^{l\bar{l}}(Z')$, respectively, the combination of (7.10) and (3.20) allows to derive upper bounds on $|C_9^{\rm NP}|$ that go beyond the 331 models and apply to l.h.s. scenario for Z' generally. Indeed for the case $e^+e^- \to \mu^+\mu^-$ we obtain from (7.10) the bound

$$\frac{M_{Z'}}{\Delta_V^{\mu\bar{\mu}}} \geq a\frac{\Lambda_-}{\sqrt{4\pi}} \equiv K \tag{7.11}$$

with a=1 for LL^- and RR^- and $a = 1/2$ for VV^-. From table 3.15 in [77] we find then

$$K = 2.77\,\text{TeV (LL}^-), \qquad K = 2.62\,\text{TeV (RR}^-), \qquad K = 2.30\,\text{TeV (VV}^-). \tag{7.12}$$

Therefore (3.20) can be rewritten as an upper bound on $|C_9^{\rm NP}|$ as follows:

$$|C_9^{\rm NP}| \leq \frac{2.52\,\text{TeV}}{K}\sqrt{\frac{|\Delta S|}{0.231}}. \tag{7.13}$$

The last factor becomes unity for a 10% contribution from NP to ΔM_s and consequently in this case the maximal by LEP-II allowed values for $|C_9^{\rm NP}|$ read: 0.91, 0.96 and 1.10, for LL^-, RR^- and VV^-, respectively. The latter case is the one considered in [10] and also has similar structure to $\beta = -\sqrt{3}$ model without specification of actual values of the muon couplings.

We conclude that for a 10% shift in S it is impossible in these models to obtain $C_9^{\rm NP} = -1.5$ as found in [10]. Only for effects S in the ballpark of 20% could such large negative values of $C_9^{\rm NP}$ be obtained. While these results look similar to the ones shown in figure 3, they are more general as they do not assume CMFV and 331 models at work and moreover take into account LEP-II data. Needless to say these LEP-II bounds can be significantly weakened by breaking lepton universality in Z' couplings and suppressing Z' couplings to electrons relative to the muon ones.

As far as the bound on $|C_{10}^{\rm NP}|$ is concerned the bounds obtained for LL^- and RR^- apply also to this coefficient with Δ_V replaced by Δ_A. For VV^- this coefficient vanishes. But for the case AA^- in [77] that corresponds to $\Delta_L^{l\bar{l}}(Z') = -\Delta_R^{l\bar{l}}(Z')$, we find the analogue of the ratio K to be 1.89 TeV and slightly weaker bound than for $|C_9^{\rm NP}|$ in the VV^- case. Thus LEP-II bounds on $|C_{10}^{\rm NP}|$ are weaker than the bounds presently available from $B_s \to \mu^+\mu^-$.

For the remaining models considered by us a complication arises due to the fact that the values of η_{ij} in the simple models studied in [77] and listed in table 3.14 of that paper do not correspond to our models in which generally all combinations of L and R contribute.

However, even without new global fits in these models, which would be beyond the scope of our paper we have checked by using the tables 5–7, the formulae in appendix B and the table 3.15 of [77] that the four models considered in detail by us satisfy all LEP-II bounds. In fact our findings are as follows:

- For the cases $n = -1, 1, 2$ the lower bounds on $M_{Z'}$ are significantly below 2 TeV, typically close to 1 TeV.
- For $\beta = -2\sqrt{3}$ the lower bound on $M_{Z'}$ is below 2 TeV but its precise value would require a more sophisticated analysis. In any case it appears that the LHC bound of approximately 3 TeV in this model is stronger that LEP-II bounds.

β	$1/\sqrt{3}$	$-1/\sqrt{3}$	$2/\sqrt{3}$	$-2/\sqrt{3}$	$\sqrt{3}$	$-\sqrt{3}$	Z couplings
LL	-0.168	-0.666	-0.068	-1.65	-0.01	-62.0	0.396
RR	-0.165	-0.165	-1.05	-1.05	-0.03	-60.5	0.296
LR	0.166	-0.331	0.267	-1.32	-0.02	-61.2	-0.342
RL	0.166	-0.331	0.267	-1.32	-0.02	-61.2	-0.342

Table 5. Values of $10 \times \eta_{ij}$ for different β relevant for $e^+e^- \to \ell^+\ell^-$ using $\sin^2\theta_W = 0.249$ for $\beta = \pm 1/\sqrt{3}$ and $\beta = \pm 2/\sqrt{3}$ and $\sin^2\theta_W = 0.246$ for $\beta = \sqrt{3}$. $\sin^2\theta_W = 0.231$ for Z-couplings.

Concerning the LHC bounds on $M_{Z'}$ from ATLAS and in particular CMS [79], the authors of [14] using MAdGraph5 and CTEQ611 parton distribution functions derived for the $\beta = -\sqrt{3}$ model a 95% CL bound of $M_{Z'} > 3.9\,\text{TeV}$. As these bounds are based on the Drell-Yan process and are dominated by Z' couplings to up-quarks and muons that in 331 models equal to those of electrons, the values of η_{ij} in table 7 can give us a hint what happens in the models considered by us.

As the relevant η_{ij} in the models considered in detail by us are much lower than the ones in the $\beta = -\sqrt{3}$ model, the lower bounds on $M_{Z'}$ in these models must be significantly lower than 3.9 TeV. On the other hand the couplings in the $\beta = \pm 2/\sqrt{3}$ models are comparable, even if slightly larger than the ones of Z boson. Therefore, we expect that lower bound on $M_{Z'}$ could be slightly larger than the one reported by CMS ($M_{Z'} > 2.9\,\text{TeV}$) and our choice of $M_{Z'} = 3.0\,\text{TeV}$ could be consistent with LHC bounds. Yet in order to find it out a dedicated analysis would be necessary.[9] As far as the LHC bounds for $\beta = \pm 1/\sqrt{3}$ are concerned the analysis in [81] indicates that in these models one could still have $M_{Z'} \approx 2.5\,\text{TeV}$. This would allow to enhance NP effects in all $\Delta F = 1$ observables in these models by roughly a factor of 1.2 A complementary lower bound $M_{Z'} \geq 1\,\text{TeV}$ for 331 models with $\beta = -1/\sqrt{3}$ was derived in [82] using dark matter data. However, this bound is based on further assumptions regarding the relevance of 331 models to the cosmological dark matter abundance and is not on the same footing as the other bounds discussed by us.

As we have provided all information on the couplings necessary to perform such an analysis in the $\beta = \pm 2/\sqrt{3}$ and $\beta = \pm 1/\sqrt{3}$ models, collider experimentalists and phenomenologists having the relevant codes could derive precise lower bounds on $M_{Z'}$ in the models in question. If these bounds turn out in the future to be stronger or weaker than $M_{Z'} = 3.0\,\text{TeV}$ our *scaling law* in (3.15) will allow us to translate all results presented in our paper into the new ones.

8 Summary and conclusions

We have generalized our phenomenological analysis of flavour observables in the particular 331 model with $\beta = 1/\sqrt{3}$ presented in [2] to the cases $\beta = -1/\sqrt{3}$, $\beta = \pm 2/\sqrt{3}$ and $\beta = \pm\sqrt{3}$ and confronted these models with the most recent data on $B_{s,d} \to \mu^+\mu^-$ and

[9]Recently the bound $M_{Z'} \geq 3.2\,\text{TeV}$ in this model resulting from the LHC has been derived in [80].

β	$1/\sqrt{3}$	$-1/\sqrt{3}$	$2/\sqrt{3}$	$-2/\sqrt{3}$	$\sqrt{3}$	$-\sqrt{3}$	Z couplings
LL	0.223	0.555	0.157	1.22	0.23	-41.6	0.626
RR	-0.055	-0.055	-0.351	-0.351	0.44	-20.2	0.098
LR	0.055	-0.110	0.089	-0.440	0.22	-20.5	-0.113
RL	-0.221	0.276	-0.618	0.969	0.45	41.1	-0.542

Table 6. Values of $10 \times \eta_{ij}$ for different β relevant for $e^+e^- \to d\bar{d}$ using $\sin^2\theta_W = 0.249$ for $\beta = \pm 1/\sqrt{3}$ and $\beta = \pm 2/\sqrt{3}$ and $\sin^2\theta_W = 0.246$ for $\beta = \sqrt{3}$. $\sin^2\theta_W = 0.231$ for Z-couplings.

β	$1/\sqrt{3}$	$-1/\sqrt{3}$	$2/\sqrt{3}$	$-2/\sqrt{3}$	$\sqrt{3}$	$-\sqrt{3}$	Z couplings
LL	0.223	0.555	0.157	1.22	0.23	-41.6	-0.511
RR	0.110	0.110	0.702	0.702	-0.88	40.5	-0.198
LR	-0.111	0.221	-0.178	0.86	-0.44	41.0	0.229
RL	-0.221	0.276	-0.618	0.969	0.45	41.1	0.442

Table 7. Values of $10 \times \eta_{ij}$ for different β relevant for $e^+e^- \to u\bar{u}$ using $\sin^2\theta_W = 0.249$ for $\beta = \pm 1/\sqrt{3}$ and $\beta = \pm 2/\sqrt{3}$ and $\sin^2\theta_W = 0.246$ for $\beta = \sqrt{3}$. $\sin^2\theta_W = 0.231$ for Z-couplings.

$B_d \to K^*\mu^+\mu^-$. We have also presented predictions of these models for $b \to s\nu\bar{\nu}$ transitions and decays $K^+ \to \pi^+\nu\bar{\nu}$, $K_L \to \pi^0\nu\bar{\nu}$ and $K_L \to \mu^+\mu^-$.

Our three most important messages from this analysis are as follows:

- The 331 models analyzed by us do not account for the $B_d \to K^*\mu^+\mu^-$ anomalies if the latter require $\mathrm{Re}(\mathrm{C}_9^{\mathrm{NP}}) \leq -1.3$ as indicated by the model independent analysis in [10]. On the other hand, these models could be in accordance with the outcome of the analyses in [11, 13, 15, 17] provided the required size of C_9' in some of these papers will decrease with time (see also [18] where the impact of a NP contribution to C_9' on these anomalies is discussed).

- Going beyond 331 models and assuming lepton universality we find an upper bound $|C_9^{\mathrm{NP}}| \leq 1.1(1.4)$ from LEP-II data for all Z' models within l.h.s. scenario, when NP contributions to ΔM_s at the level of 10%(15%) are allowed. We conclude therefore that it is unlikely that values like $\mathrm{Re}(\mathrm{C}_9^{\mathrm{NP}}) = -1.5$ can be accommodated in Z' models of l.h.s. type when lepton universality is assumed. As the 331 models not analyzed by us belong to this class of models, this finding applies to them as well.

- The central experimental value of $\mathcal{B}(B_d \to \mu^+\mu^-)$ from LHCb and CMS cannot be reproduced in the 331 models, although an enhancement by 20% over its SM value is possible. A general l.h.s. scenario can do much better as demonstrated in [13]. But then the universality in lepton couplings has to be broken to satisfy LEP-II constraints and the diagonal Z' couplings to quarks must be smaller than in 331 models considered by us to avoid the bounds on $M_{Z'}$ from LHC.

In more detail our findings are as follows:

- Analyzing the models with $\beta = \pm 1/\sqrt{3}$ and $\beta = \pm 2/\sqrt{3}$ we find that for $\beta > 0$ measurable NP effects are allowed in $B_{s,d} \to \mu^+\mu^-$, sufficient to suppress $\overline{\mathcal{B}}(B_s \to \mu^+\mu^-)$ down to its central experimental value. On the other hand as mentioned above $\mathcal{B}(B_d \to \mu^+\mu^-)$ even if reaching values 20% above SM result, is still well below the experimental central value. Thus we expect that the experimental value of $\mathcal{B}(B_d \to \mu^+\mu^-)$ must go down if these models should stay alive. For $\beta > 0$, the $B_d \to K^*\mu^+\mu^-$ anomaly cannot be explained and in fact the anti-correlation between $\overline{\mathcal{B}}(B_s \to \mu^+\mu^-)$ and $\mathrm{Re}(\mathrm{C}_9^{\mathrm{NP}})$ predicted in this case is not in accordance with the present data. On the other hand in the case of the absence of $B_d \to K^*\mu^+\mu^-$ anomalies in the future data and confirmation of the suppression of $\mathcal{B}(B_s \to \mu^+\mu^-)$ relative to its SM value the model with $\beta = 1/\sqrt{3}$ and $M_{Z'} \approx 3\,\mathrm{TeV}$ would be favoured.

- Presently, more interesting appear models with $\beta < 0$ where NP effects in $\overline{\mathcal{B}}(B_s \to \mu^+\mu^-)$ and $\mathrm{Re}(\mathrm{C}_9^{\mathrm{NP}})$ bring the theory closer to the data. Moreover we identified a triple correlation between $\mathrm{Re}(\mathrm{C}_9^{\mathrm{NP}})$, $\overline{\mathcal{B}}(B_s \to \mu^+\mu^-)$ and $S_{\psi\phi}$ that for $\mathrm{Re}(\mathrm{C}_9^{\mathrm{NP}}) < -0.5$ required by $B_d \to K^*\mu^+\mu^-$ anomalies implies uniquely suppression of $\overline{\mathcal{B}}(B_s \to \mu^+\mu^-)$ relative to its SM value which is favoured by the data. In turn also $S_{\psi\phi} < S_{\psi\phi}^{\mathrm{SM}}$ is favoured with $S_{\psi\phi}$ having dominantly opposite sign to $S_{\psi\phi}^{\mathrm{SM}}$ and closer to its central experimental value. Figures 5–7 show these correlations in explicit terms.

- Another important triple correlation is the one between $\mathrm{Re}(\mathrm{C}_9^{\mathrm{NP}})$, $\overline{\mathcal{B}}(B_s \to \mu^+\mu^-)$ and $B_d \to K\mu^+\mu^-$. It can be found in figure 13.

- Our study of $b \to s\nu\bar{\nu}$ transitions, $K^+ \to \pi^+\nu\bar{\nu}$ and $K_L \to \mu^+\mu^-$ shows that NP effects in these decays in the models considered are typically below 10% at the level of the branching ratios. NP effects in $K_L \to \pi^0\nu\bar{\nu}$ can reach 20%.

- We have demonstrated how the effects found by us are correlated with the departures of C_{B_s} and C_{B_d} from unity. As the latter departures depend sensitively on the precision of lattice non-perturbative calculations, the future of 331 models does not only depend on experimental progress but also on progress of latter calculations.

- As a by-product we have presented bounds on 331 models from low energy precision experiments and provided enough information on the couplings of Z' to quarks and leptons that a sophisticated analyses of LEP-II observables and of LHC constraints could be performed in the future.

- Finally, the model with $\beta = -\sqrt{3}$ can be ruled out on the basis of the data for various observables, in particular the final results from LEP-II. But even if renormalization group effects in $\sin^2\theta_W$ are not taken into account, the resulting lower bounds on $M_{Z'}$ are higher than the upper bounds implied by the Landau singularity. On the other hand the model with $\beta = \sqrt{3}$ does not predict significant departures from the SM.

Whether the models with $\beta = -1/\sqrt{3}$ and $\beta = -2/\sqrt{3}$ or with $\beta = 1/\sqrt{3}$ and $\beta = 2/\sqrt{3}$ will be favoured by the data will depend on the future of the experimental results for

JHEP02(2014)112

$B_{s,d} \to \mu^+\mu^-$, $B_d \to K^*(K)\mu^+\mu^-$ and future values of C_{B_q}. The numerous plots presented in our paper should allow to monitor these developments. Most importantly, the values of $M_{Z'}$ considered in our paper are sufficiently low that this new gauge boson could be discovered in the next run of the LHC and its properties could even be studied at a future ILC [80].

Acknowledgments

We thank in particular Francois Richard for informative discussions on the bounds on Z' couplings from LEP-II data, Christoph Bobeth, Martin Gorbahn and Mikolaj Misiak for discussions related to $B_s \to \mu^+\mu^-$ and David Straub in connection with the decay $B_d \to K^*(K)\mu^+\mu^-$. Extensive E-mail exchanges with Ulrich Haisch in the context of the $\beta = -\sqrt{3}$ model were very enjoyable. Thanks go also to Quim Matias. This research was done and financed in the context of the ERC Advanced Grant project "FLAVOUR"(267104) and was partially supported by the DFG cluster of excellence "Origin and Structure of the Universe".

A Expressions for couplings in various 331 models

In obtaining the results below we use for $\beta = \pm 1/\sqrt{3}$ and $\beta = \pm 2/\sqrt{3}$ the values $\sin^2\theta_W = 0.249$ and $g = 0.633$ corresponding to $M_{Z'} = 3\,\text{TeV}$. We stress that for these models the dependence of the couplings on $M_{Z'}$ for $1\,\text{TeV} \le M_{Z'} \le 5\,\text{TeV}$, unless they are very small, is basically negligible assuring the scaling law (3.15).

$\beta = \pm 1/\sqrt{3}$. For both signs we have

$$\Delta_L^{ij}(Z') = \frac{g}{\sqrt{3}} c_W \sqrt{f(1/\sqrt{3})}\, v_{3i}^* v_{3j} = 0.388\ v_{3i}^* v_{3j} \tag{A.1}$$

Next for $\beta = 1/\sqrt{3}$ we have

$$\Delta_V^{d\bar{d}}(Z') = \frac{g}{2\sqrt{3}c_W}\sqrt{f(1/\sqrt{3})}\ \left[-1 + \frac{2}{3}s_W^2\right] = -0.215\,, \tag{A.2a}$$

$$\Delta_A^{d\bar{d}}(Z') = \frac{g}{2\sqrt{3}c_W}\sqrt{f(1/\sqrt{3})}\ \left[1 - 2s_W^2\right] = 0.130\,, \tag{A.2b}$$

$$\Delta_V^{u\bar{u}}(Z') = \frac{g}{2\sqrt{3}c_W}\sqrt{f(1/\sqrt{3})}\ \left[-1 + \frac{8}{3}s_W^2\right] = -0.087\,, \tag{A.2c}$$

$$\Delta_A^{u\bar{u}}(Z') = \frac{g}{2\sqrt{3}c_W}\sqrt{f(1/\sqrt{3})}\ [1] = 0.258\,, \tag{A.2d}$$

$$\Delta_L^{\nu\bar{\nu}}(Z') = \frac{g}{2\sqrt{3}c_W}\sqrt{f(1/\sqrt{3})}\,\left[1 - 2s_W^2\right] = 0.130\,, \tag{A.2e}$$

$$\Delta_V^{\mu\bar{\mu}}(Z') = \frac{g}{2\sqrt{3}c_W}\sqrt{f(1/\sqrt{3})}\ \left[1 - 4s_W^2\right] = 0.001\,, \tag{A.2f}$$

$$\Delta_A^{\mu\bar{\mu}}(Z') = \frac{g}{2\sqrt{3}c_W}\sqrt{f(1/\sqrt{3})}\ [-1] = -0.258 \tag{A.2g}$$

JHEP02(2014)112

and for $\beta = -1/\sqrt{3}$

$$\Delta_V^{d\bar{d}}(Z') = \frac{g}{2\sqrt{3}c_W}\sqrt{f(1/\sqrt{3})}\ \left[-1 + \frac{4}{3}s_W^2\right] = -0.172\,, \tag{A.3a}$$

$$\Delta_A^{d\bar{d}}(Z') = \frac{g}{2\sqrt{3}c_W}\sqrt{f(1/\sqrt{3})}\ [1] = 0.258\,, \tag{A.3b}$$

$$\Delta_V^{u\bar{u}}(Z') = \frac{g}{2\sqrt{3}c_W}\sqrt{f(1/\sqrt{3})}\ \left[-1 - \frac{2}{3}s_W^2\right] = -0.301\,, \tag{A.3c}$$

$$\Delta_A^{u\bar{u}}(Z') = \frac{g}{2\sqrt{3}c_W}\sqrt{f(1/\sqrt{3})}\ \left[1 - 2s_W^2\right] = 0.130\,, \tag{A.3d}$$

$$\Delta_L^{\nu\bar{\nu}}(Z') = \frac{g}{2\sqrt{3}c_W}\sqrt{f(1/\sqrt{3})}\,[1] = 0.258\,, \tag{A.3e}$$

$$\Delta_V^{\mu\bar{\mu}}(Z') = \frac{g}{2\sqrt{3}c_W}\sqrt{f(1/\sqrt{3})}\ \left[1 + 2s_W^2\right] = 0.386\,, \tag{A.3f}$$

$$\Delta_A^{\mu\bar{\mu}}(Z') = \frac{g}{2\sqrt{3}c_W}\sqrt{f(1/\sqrt{3})}\ \left[-1 + 2s_W^2\right] = -0.130 \tag{A.3g}$$

$\beta = \pm 2/\sqrt{3}$. For both signs we have

$$\Delta_L^{ij}(Z') = \frac{g}{\sqrt{3}}c_W\sqrt{f(2/\sqrt{3})}v_{3i}^* v_{3j} = 0.489\ v_{3i}^* v_{3j} \tag{A.4}$$

Next for $\beta = 2/\sqrt{3}$ we have

$$\Delta_V^{d\bar{d}}(Z') = \frac{g}{2\sqrt{3}c_W}\sqrt{f(2/\sqrt{3})}\ \left[-1 + \frac{1}{3}s_W^2\right] = -0.299\,, \tag{A.5a}$$

$$\Delta_A^{d\bar{d}}(Z') = \frac{g}{2\sqrt{3}c_W}\sqrt{f(2/\sqrt{3})}\ \left[1 - 3s_W^2\right] = 0.082\,, \tag{A.5b}$$

$$\Delta_V^{u\bar{u}}(Z') = \frac{g}{2\sqrt{3}c_W}\sqrt{f(2/\sqrt{3})}\ \left[-1 + \frac{13}{3}s_W^2\right] = 0.026\,, \tag{A.5c}$$

$$\Delta_A^{u\bar{u}}(Z') = \frac{g}{2\sqrt{3}c_W}\sqrt{f(2/\sqrt{3})}\ \left[1 + s_W^2\right] = 0.407\,, \tag{A.5d}$$

$$\Delta_L^{\nu\bar{\nu}}(Z') = \frac{g}{2\sqrt{3}c_W}\sqrt{f(2/\sqrt{3})}\,\left[1 - 3s_W^2\right] = 0.082\,, \tag{A.5e}$$

$$\Delta_V^{\mu\bar{\mu}}(Z') = \frac{g}{2\sqrt{3}c_W}\sqrt{f(2/\sqrt{3})}\ \left[1 - 7s_W^2\right] = -0.242\,, \tag{A.5f}$$

$$\Delta_A^{\mu\bar{\mu}}(Z') = \frac{g}{2\sqrt{3}c_W}\sqrt{f(2/\sqrt{3})}\ \left[-1 - s_W^2\right] = -0.407 \tag{A.5g}$$

and for $\beta = -2/\sqrt{3}$

$$\Delta_V^{d\bar{d}}(Z') = \frac{g}{2\sqrt{3}c_W}\sqrt{f(2/\sqrt{3})}\ \left[-1 + \frac{5}{3}s_W^2\right] = -0.191\,, \tag{A.6a}$$

$$\Delta_A^{d\bar{d}}(Z') = \frac{g}{2\sqrt{3}c_W}\sqrt{f(2/\sqrt{3})}\ \left[1 + s_W^2\right] = 0.407\,, \tag{A.6b}$$

$$\Delta_V^{u\bar{u}}(Z') = \frac{g}{2\sqrt{3}c_W}\sqrt{f(2/\sqrt{3})}\ \left[-1 - \frac{7}{3}s_W^2\right] = -0.515\,, \tag{A.6c}$$

$$\Delta_A^{u\bar{u}}(Z') = \frac{g}{2\sqrt{3}c_W}\sqrt{f(2/\sqrt{3})}\;\left[1-3s_W^2\right] = 0.082\,, \tag{A.6d}$$

$$\Delta_L^{\nu\bar{\nu}}(Z') = \frac{g}{2\sqrt{3}c_W}\sqrt{f(2/\sqrt{3})}\left[1+s_W^2\right] = 0.407\,, \tag{A.6e}$$

$$\Delta_V^{\mu\bar{\mu}}(Z') = \frac{g}{2\sqrt{3}c_W}\sqrt{f(2/\sqrt{3})}\;\left[1+5s_W^2\right] = 0.731\,, \tag{A.6f}$$

$$\Delta_A^{\mu\bar{\mu}}(Z') = \frac{g}{2\sqrt{3}c_W}\sqrt{f(2/\sqrt{3})}\;\left[-1+3s_W^2\right] = -0.082 \tag{A.6g}$$

These results confirm the ones seen in figure 1. For completeness we also list the formulae for $\beta = \pm\sqrt{3}$ in order to demonstrate that for $\beta = \sqrt{3}$ the couplings are too small to provide relevant NP effects, while for $\beta = -\sqrt{3}$ they are too large to be consistent with the flavour data and LEP-II bounds for $M_{Z'} < 4\,\mathrm{TeV}$, for which this model is valid because of the Landau singularities in question. In order to stay away from this singularity we give the values of couplings for $M_{Z'} = 2\,\mathrm{TeV}$, that is for $\sin^2\theta_W = 0.246$ and $g = 0.636$.

$\beta = \pm\sqrt{3}$. For both signs we have

$$\Delta_L^{ij}(Z') = \frac{g}{\sqrt{3}}c_W\sqrt{f(\sqrt{3})}v_{3i}^* v_{3j} = \;2.52\,v_{3i}^* v_{3j} \tag{A.7}$$

In the case of $\beta = \sqrt{3}$ the formulae for leptonic couplings are modified [2]. We have then

$$\Delta_V^{d\bar{d}}(Z') = \frac{g}{2\sqrt{3}c_W}\sqrt{f\sqrt{3})}\;\left[-1\right] = -1.672\,, \tag{A.8a}$$

$$\Delta_A^{d\bar{d}}(Z') = \frac{g}{2\sqrt{3}c_W}\sqrt{f(\sqrt{3})}\;\left[1-4s_W^2\right] = 0.027\,, \tag{A.8b}$$

$$\Delta_V^{u\bar{u}}(Z') = \frac{g}{2\sqrt{3}c_W}\sqrt{f(\sqrt{3})}\;\left[-1+6s_W^2\right] = 0.796\,, \tag{A.8c}$$

$$\Delta_A^{u\bar{u}}(Z') = \frac{g}{2\sqrt{3}c_W}\sqrt{f(\sqrt{3})}\;\left[1+2s_W^2\right] = 2.494\,, \tag{A.8d}$$

$$\Delta_L^{\nu\bar{\nu}}(Z') = \frac{g}{2\sqrt{3}c_W}\sqrt{f(\sqrt{3})}\left[1-4s_W^2\right] = 0.027\,, \tag{A.8e}$$

$$\Delta_V^{\mu\bar{\mu}}(Z') = \frac{3g}{2\sqrt{3}c_W}\sqrt{f(\sqrt{3})}\;\left[1-4s_W^2\right] = 0.080\,, \tag{A.8f}$$

$$\Delta_A^{\mu\bar{\mu}}(Z') = \frac{g}{2\sqrt{3}c_W}\sqrt{f(\sqrt{3})}\;\left[1-4s_W^2\right] = 0.027 \tag{A.8g}$$

and for $\beta = -\sqrt{3}$

$$\Delta_V^{d\bar{d}}(Z') = \frac{g}{2\sqrt{3}c_W}\sqrt{f\sqrt{3})}\;\left[-1+2s_W^2\right] = -0.849\,, \tag{A.9a}$$

$$\Delta_A^{d\bar{d}}(Z') = \frac{g}{2\sqrt{3}c_W}\sqrt{f(\sqrt{3})}\;\left[1+2s_W^2\right] = 2.494\,, \tag{A.9b}$$

$$\Delta_V^{u\bar{u}}(Z') = \frac{g}{2\sqrt{3}c_W}\sqrt{f(\sqrt{3})}\;\left[-1-4s_W^2\right] = -3.316\,, \tag{A.9c}$$

$$\Delta_A^{u\bar{u}}(Z') = \frac{g}{2\sqrt{3}c_W}\sqrt{f(\sqrt{3})}\ \left[1-4s_W^2\right] = 0.027\,, \tag{A.9d}$$

$$\Delta_L^{\nu\bar{\nu}}(Z') = \frac{g}{2\sqrt{3}c_W}\sqrt{f(\sqrt{3})}\left[1+2s_W^2\right] = 2.49\,, \tag{A.9e}$$

$$\Delta_V^{\mu\bar{\mu}}(Z') = \frac{g}{2\sqrt{3}c_W}\sqrt{f(\sqrt{3})}\ \left[1+8s_W^2\right] = 4.96\,, \tag{A.9f}$$

$$\Delta_A^{\mu\bar{\mu}}(Z') = \frac{g}{2\sqrt{3}c_W}\sqrt{f(\sqrt{3})}\ \left[-1+4s_W^2\right] = -0.027 \tag{A.9g}$$

SM couplings of Z. For comparison we give the couplings of Z boson that we evaluate with $g = 0.652$ and $\sin^2\theta_W = 0.23116$ as valid at M_Z. The non-diagonal couplings vanish at tree-level and the diagonal ones are given as follows:

$$\Delta_V^{d\bar{d}}(Z) = \frac{g}{2c_W}\ \left[-1+\frac{4}{3}s_W^2\right] = -0.257\,, \tag{A.10a}$$

$$\Delta_A^{d\bar{d}}(Z) = \frac{g}{2c_W} = 0.372\,, \tag{A.10b}$$

$$\Delta_V^{u\bar{u}}(Z) = \frac{g}{2c_W}\ \left[1-\frac{8}{3}s_W^2\right] = 0.143\,, \tag{A.10c}$$

$$\Delta_A^{u\bar{u}}(Z) = -\frac{g}{2c_W} = -0.372\,, \tag{A.10d}$$

$$\Delta_L^{\nu\bar{\nu}}(Z) = \frac{g}{2c_W} = 0.372\,, \tag{A.10e}$$

$$\Delta_V^{\mu\bar{\mu}}(Z) = -\frac{g}{2c_W}\ \left[1-4s_W^2\right] = -0.028\,, \tag{A.10f}$$

$$\Delta_A^{\mu\bar{\mu}}(Z) = \frac{g}{2c_W} = 0.372 \tag{A.10g}$$

B LEP-II constraints

We will list here formulae which we used to verify that the four 331 models investigated by us satisfy LEP-II constraints on $M_{Z'}$. To this end we generalized the usual SM expressions to include Z' contribution. In this context we found the presentation in the book of Burgess and Moore [83] useful.

The cross section for $e^+\mathrm{e}^- \to f\bar{f}$ where f is a lepton or quark is given in terms of helicity amplitudes A_{ij}^{ef} by

$$\sigma(e^+\mathrm{e}^- \to f\bar{f}) = \frac{\pi\alpha^2 s N_c}{3}\left(|A_{\mathrm{LL}}^{ef}(s)|^2 + |A_{\mathrm{RR}}^{ef}(s)|^2 + |A_{\mathrm{LR}}^{ef}(s)|^2 + |A_{\mathrm{RL}}^{ef}(s)|^2\right), \tag{B.1}$$

where $N_c = 3(1)$ for quarks (leptons).

For FB and LR asymmetries we have

$$\mathcal{A}_{\mathrm{FB}}(e^+\mathrm{e}^- \to f\bar{f}) = \frac{3}{4}\frac{\left(|A_{\mathrm{LL}}^{ef}(s)|^2 + |A_{\mathrm{RR}}^{ef}(s)|^2 - |A_{\mathrm{LR}}^{ef}(s)|^2 - |A_{\mathrm{RL}}^{ef}(s)|^2\right)}{\left(|A_{\mathrm{LL}}^{ef}(s)|^2 + |A_{\mathrm{RR}}^{ef}(s)|^2 + |A_{\mathrm{LR}}^{ef}(s)|^2 + |A_{\mathrm{RL}}^{ef}(s)|^2\right)} \tag{B.2}$$

and

$$\mathcal{A}_{\rm LR}(e^+e^- \to f\bar{f}) = \frac{\left(|A^{ef}_{\rm LL}(s)|^2 + |A^{ef}_{\rm LR}(s)|^2 - |A^{ef}_{\rm RR}(s)|^2 - |A^{ef}_{\rm RL}(s)|^2\right)}{\left(|A^{ef}_{\rm LL}(s)|^2 + |A^{ef}_{\rm RR}(s)|^2 + |A^{ef}_{\rm LR}(s)|^2 + |A^{ef}_{\rm RL}(s)|^2\right)}. \tag{B.3}$$

The helicity amplitudes are given for $M_{Z'} \gg \sqrt{s}$ in the Z' models generally as follows (we drop the argument s)

$$A^{ef}_{ij} = A^{\rm SM}_{ij} + A^{\rm NP}_{ij}, \qquad i,j = {\rm L},{\rm R} \tag{B.4}$$

Defining then

$$\eta^{ef}_{ij}(Z') = -\Delta^{e\bar{e}}_i(Z')\Delta^{f\bar{f}}_j(Z'), \tag{B.5}$$

where the minus sign comes from Z' propagator but

$$\eta^{ef}_{ij}(Z) = \Delta^{e\bar{e}}_i(Z)\Delta^{f\bar{f}}_j(Z), \tag{B.6}$$

without this minus sign ($\sqrt{s} > M_Z$) we have

$$A^{\rm SM}_{ij} = \frac{Q_e Q_f}{s} + \frac{1}{4\pi\alpha}\left[\frac{\eta^{ef}_{ij}(Z)}{s - M_Z^2}\right], \qquad A^{\rm NP}_{ij} = \frac{1}{4\pi\alpha}\left[\frac{\eta^{ef}_{ij}(Z')}{M^2_{Z'}}\right]. \tag{B.7}$$

Here the first term in the SM contribution represents photon contribution. Note that for the values of $M_{Z'}$ considered, s in the Z' propagator can be neglected, while for $\sqrt{s} = 200\,\text{GeV}$ one has $\sqrt{s - M_Z^2} = 178\,\text{GeV}$.

One can define the shift in the cross section due to NP contributions simply as follows:

$$\Delta\sigma^{\rm NP} = \sigma(e^+e^- \to f\bar{f}) - \sigma^{\rm SM}. \tag{B.8}$$

In view of small NP effects only the interference between NP and SM matters and we find

$$\sigma^{\rm SM} = \frac{\pi\alpha^2 s N_c}{3}\left(|A^{\rm SM}_{\rm LL}|^2 + |A^{\rm SM}_{\rm RR}|^2 + |A^{\rm SM}_{\rm LR}|^2 + |A^{\rm SM}_{\rm RL}|^2\right) \tag{B.9}$$

and

$$\Delta\sigma^{\rm NP} = 2\frac{\pi\alpha^2 s N_c}{3}\left(A^{\rm SM}_{\rm LL}A^{\rm NP}_{\rm LL} + A^{\rm SM}_{\rm RR}A^{\rm NP}_{\rm RR} + A^{\rm SM}_{\rm LR}A^{\rm NP}_{\rm LR} + A^{\rm SM}_{\rm RL}A^{\rm NP}_{\rm RL}\right). \tag{B.10}$$

Analogous formulae can be derived for corrections to FB and LR asymmetries.

C The $\beta = \pm\sqrt{3}$ models

Here we list the problems of $\beta = \pm\sqrt{3}$ models which originate in the value of the coupling g_X which is not free but for a fixed β is given in terms of g and $\sin^2\theta_W$ as follows:

$$g_X^2 = g^2 \frac{6\sin^2\theta_W}{1 - (1+\beta^2)\sin^2\theta_W}. \tag{C.1}$$

This formula implies for $\beta = \pm\sqrt{3}$ a Landau singularity for $\sin^2\theta_W = 0.25$ and this value is reached through the renormalization group evolution of the SM couplings for

$M_{Z'}$ typically around 4 TeV [28, 84].[10] Therefore these models as they stand, even if $V_L \neq V_{\rm CKM}$, can only be valid for $M_{Z'} < 4\,\text{TeV}$. Although in principle some new dynamics entering around these scales could shift the Landau singularity to higher scales, in particular supersymmetry [66, 67], one should realize that even at $\mu = 80\,\text{GeV}$ the coupling would be as large as $\alpha_X \approx 0.6$ that is much larger than all couplings of the SM. At the relevant scales of order few TeV $\alpha_X \geq 2.5$ implying that perturbative calculations cannot be trusted even in the presence of a large $M_{Z'}$. This is not the problem for other four models discussed by us, where at $\mu = 3\,\text{TeV}$, the coupling α_X equals approximately 0.07 and 0.11 for $\beta = \pm 1/\sqrt{3}$ and $\beta = \pm 2/\sqrt{3}$, respectively.

The related problems are as follows

- Noting that the masses of the new charged gauge bosons V and Y are related within 1% accuracy to $M_{Z'}$ through

$$M_V = M_Y = M_{Z'}\sqrt{1-(1+\beta^2)s_W^2}, \tag{C.2}$$

  we find for $|\beta| = \sqrt{3}$ and $s_W^2 = 0.24-0.25$, valid for $M_{Z'}$ in the ballpark of a few TeV, the masses of other heavy gauge bosons $M_V = M_Y \leq M_{Z'}/5$. This is basically ruled out by the LHC for $M_{Z'} \leq 4\,\text{TeV}$. However, a dedicated study would be necessary in order to put this statement on the firm footing. This is not a problem for $|\beta| = 1/\sqrt{3}$ and $|\beta| = 2/\sqrt{3}$, where we find $M_V = M_Y \approx 0.8\,M_{Z'}$ and $M_V = M_Y \approx 0.7\,M_{Z'}$, respectively.

- With the matrix V_L equal to the CKM matrix we find that even for values of $M_{Z'} = (5-7)\,\text{TeV}$ as considered in [14] the mass differences ΔM_s and ΔM_d are enhanced at least by a factor of two ($C_{B_{s,d}} \approx 2$) relative to the SM values. In our view it is unlikely that the future lattice values of $\sqrt{\hat{B}_{B_s}}F_{B_s}$ and $\sqrt{\hat{B}_{B_d}}F_{B_d}$ would change so much to allow for a satisfactory description of the data for $\Delta M_{s,d}$ in this model. While choosing $V_L \neq V_{\rm CKM}$ would remove this problem, this does not help because of the last difficulty.

- It turns out that the size of predicted coupling $\Delta_V^{\mu\bar\mu}(Z')$ in this model implies through LEP-II data a lower bound on $M_{Z'}$ of order of 10 TeV when RG effects in $\sin^2\theta_W$ are taken into account.[11] This value is outside the validity of the model unless complicated new dynamics is introduced at scales of few TeV.

[10] In fact we confirmed Frampton's result that at one-loop level the singularity is reached precisely at $M_{Z'} = 4\,\text{TeV}$ and this result is practically unchanged at NLO. We thank David Straub for checking this.

[11] We thank Francois Richard for pointing out the inconsistency of the model in [14] with the LEP-II data even in the absence of RG effects. We refer to his analysis of 331 models in [80], where the prospects for testing 331 models at the future ILC are presented.

References

[1] A.J. Buras and J. Girrbach, *Towards the Identification of New Physics through Quark Flavour Violating Processes*, arXiv:1306.3775 [INSPIRE].

[2] A.J. Buras, F. De Fazio, J. Girrbach and M.V. Carlucci, *The Anatomy of Quark Flavour Observables in 331 Models in the Flavour Precision Era*, JHEP **02** (2013) 023 [arXiv:1211.1237] [INSPIRE].

[3] M. Blanke, A.J. Buras, B. Duling, S. Recksiegel and C. Tarantino, *FCNC Processes in the Littlest Higgs Model with T-Parity: a 2009 Look*, *Acta Phys. Polon.* **B 41** (2010) 657 [arXiv:0906.5454] [INSPIRE].

[4] LHCb collaboration, *Measurement of the $B_s^0 \to \mu^+\mu^-$ branching fraction and search for $B^0 \to \mu^+\mu^-$ decays at the LHCb experiment*, *Phys. Rev. Lett.* **111** (2013) 101805 [arXiv:1307.5024] [INSPIRE].

[5] CMS collaboration, *Measurement of the $B_s \to \mu^+\mu^-$ branching fraction and search for B0 to $\mu^+\mu^-$ with the CMS Experiment*, *Phys. Rev. Lett.* **111** (2013) 101804 [arXiv:1307.5025] [INSPIRE].

[6] CMS collaboration, *Combination of results on the rare decays $B^0_{(s)} \to \mu^+\mu^-$ from the CMS and LHCb experiments*, CMS-PAS-BPH-13-007 (2013).

[7] LHCb collaboration, *Differential branching fraction and angular analysis of the decay $B^0 \to K^{*0}\mu^+\mu^-$*, JHEP **08** (2013) 131 [arXiv:1304.6325] [INSPIRE].

[8] LHCb collaboration, *Measurement of form-factor independent observables in the decay $B^0 \to K^{*0}\mu^+\mu^-$*, *Phys. Rev. Lett.* **111** (2013) 191801 [arXiv:1308.1707] [INSPIRE].

[9] CMS collaboration, *Angular analysis and branching fraction measurement of the decay $B^0 \to K^{*0}\mu^+\mu^-$*, *Phys. Lett.* **B 727** (2013) 77 [arXiv:1308.3409] [INSPIRE].

[10] S. Descotes-Genon, J. Matias and J. Virto, *Understanding the $B \to K^*\mu^+\mu^-$ Anomaly*, *Phys. Rev.* **D 88** (2013) 074002 [arXiv:1307.5683] [INSPIRE].

[11] W. Altmannshofer and D.M. Straub, *New physics in $B \to K^*\mu\mu$?*, *European Physical Journal* **C 73** (November 2013) [arXiv:1308.1501] [INSPIRE].

[12] R. Gauld, F. Goertz and U. Haisch, *On minimal Z' explanations of the $B \to K^*\mu^+\mu^-$ anomaly*, *Phys. Rev.* **D 89** (2014) 015005 [arXiv:1308.1959] [INSPIRE].

[13] A.J. Buras and J. Girrbach, *Left-handed Z' and Z FCNC quark couplings facing new $b \to s\mu^+\mu^-$ data*, JHEP **12** (2013) 009 [arXiv:1309.2466] [INSPIRE].

[14] R. Gauld, F. Goertz and U. Haisch, *An explicit Z'-boson explanation of the $B \to K^*\mu^+\mu^-$ anomaly*, JHEP **01** (2014) 069 [arXiv:1310.1082] [INSPIRE].

[15] F. Beaujean, C. Bobeth and D. van Dyk, *Comprehensive Bayesian Analysis of Rare (Semi)leptonic and Radiative B Decays*, arXiv:1310.2478 [INSPIRE].

[16] A. Datta, M. Duraisamy and D. Ghosh, *Explaining the $B \to K^*\mu^+\mu^-$ anomaly with scalar interactions*, arXiv:1310.1937 [INSPIRE].

[17] R.R. Horgan, Z. Liu, S. Meinel and M. Wingate, *Calculation of $B^0 \to K^{*0}\mu^+\mu^-$ and $B_s^0 \to \phi\mu^+\mu^-$ observables using form factors from lattice QCD*, arXiv:1310.3887 [INSPIRE].

[18] S. Descotes-Genon, J. Matias and J. Virto, *Optimizing the basis of $B \to K^*\ell^+\ell^-$ observables and understanding its tensions*, arXiv:1311.3876 [INSPIRE].

JHEP02(2014)112

[19] A.J. Buras, F. De Fazio and J. Girrbach, *The Anatomy of Z' and Z with Flavour Changing Neutral Currents in the Flavour Precision Era*, JHEP **02** (2013) 116 [arXiv:1211.1896] [INSPIRE].

[20] A. Khodjamirian, T. Mannel, A. Pivovarov and Y.-M. Wang, *Charm-loop effect in $B \to K^{(*)}\ell^+\ell^-$ and $B \to K^*\gamma$*, JHEP **09** (2010) 089 [arXiv:1006.4945] [INSPIRE].

[21] M. Beylich, G. Buchalla and T. Feldmann, *Theory of $B \to K^{(*)}\ell^+\ell^-$ decays at high q^2: OPE and quark-hadron duality*, Eur. Phys. J. **C 71** (2011) 1635 [arXiv:1101.5118] [INSPIRE].

[22] J. Matias, *On the S-wave pollution of $B \to K * \ell^+\ell^-$ observables*, Phys. Rev. **D 86** (2012) 094024 [arXiv:1209.1525] [INSPIRE].

[23] S. Jäger and J. Martin Camalich, *On $B \to V\ell\ell$ at small dilepton invariant mass, power corrections and new physics*, JHEP **05** (2013) 043 [arXiv:1212.2263] [INSPIRE].

[24] C. Hambrock, G. Hiller, S. Schacht and R. Zwicky, *$B \to K^*$ Form Factors from Flavor Data to QCD and Back*, arXiv:1308.4379 [INSPIRE].

[25] A.J. Buras, *Relations between $\Delta M_{s,d}$ and $B_{s,d} \to \mu^+\mu^-$ in models with minimal flavor violation*, Phys. Lett. **B 566** (2003) 115 [hep-ph/0303060] [INSPIRE].

[26] F. Pisano and V. Pleitez, *An* SU(3) × U(1) *model for electroweak interactions*, Phys. Rev. **D 46** (1992) 410 [hep-ph/9206242] [INSPIRE].

[27] P. Frampton, *Chiral dilepton model and the flavor question*, Phys. Rev. Lett. **69** (1992) 2889 [INSPIRE].

[28] D. Ng, *The Electroweak theory of* SU(3) × U(1), Phys. Rev. **D 49** (1994) 4805 [hep-ph/9212284] [INSPIRE].

[29] R.A. Diaz, R. Martinez and F. Ochoa, *The Scalar sector of the* SU(3)*(c) x* SU(3)*(L)* × U(1)*(X) model*, Phys. Rev. **D 69** (2004) 095009 [hep-ph/0309280] [INSPIRE].

[30] J.T. Liu and D. Ng, *Lepton flavor changing processes and CP-violation in the 331 model*, Phys. Rev. **D 50** (1994) 548 [hep-ph/9401228] [INSPIRE].

[31] R.A. Diaz, R. Martinez and F. Ochoa, $SU(3)(c) \times SU(3)(L) \times U(1)(X)$ *models for beta arbitrary and families with mirror fermions*, Phys. Rev. **D 72** (2005) 035018 [hep-ph/0411263] [INSPIRE].

[32] J.T. Liu, *Generation nonuniversality and flavor changing neutral currents in the 331 model*, Phys. Rev. **D 50** (1994) 542 [hep-ph/9312312] [INSPIRE].

[33] J.A. Rodriguez and M. Sher, *FCNC and rare B decays in 3-3-1 models*, Phys. Rev. **D 70** (2004) 117702 [hep-ph/0407248] [INSPIRE].

[34] C. Promberger, S. Schatt and F. Schwab, *Flavor Changing Neutral Current Effects and CP-violation in the Minimal 3-3-1 Model*, Phys. Rev. **D 75** (2007) 115007 [hep-ph/0702169] [INSPIRE].

[35] J. Agrawal, P.H. Frampton and J.T. Liu, *The Decay $b \to s\gamma$ in the 3-3-1 model*, Int. J. Mod. Phys. **A 11** (1996) 2263 [hep-ph/9502353] [INSPIRE].

[36] A. Carcamo Hernandez, R. Martinez and F. Ochoa, *Z and Z' decays with and without FCNC in 331 models*, Phys. Rev. **D 73** (2006) 035007 [hep-ph/0510421] [INSPIRE].

[37] C. Promberger, S. Schatt, F. Schwab and S. Uhlig, *Bounding the Minimal 331 Model through the Decay $B \to X_s\gamma$*, Phys. Rev. **D 77** (2008) 115022 [arXiv:0802.0949] [INSPIRE].

[38] Particle Data Group collaboration, J. Beringer et al., *Review of Particle Physics (RPP)*, *Phys. Rev.* **D 86** (2012) 010001 [INSPIRE].

[39] P. Gambino and C. Schwanda, *Inclusive semileptonic fits, heavy quark masses and V_{cb}*, *Phys. Rev.* **D 89** (2014) 014022 [arXiv:1307.4551] [INSPIRE].

[40] Heavy Flavor Averaging Group collaboration, Y. Amhis et al., *Averages of B-Hadron, C-Hadron and tau-lepton properties as of early 2012*, arXiv:1207.1158 [INSPIRE].

[41] ETM collaboration, N. Carrasco et al., *B-physics from Nf=2 tmQCD: the Standard Model and beyond*, arXiv:1308.1851 [INSPIRE].

[42] LHCb collaboration, *Measurement of CP violation and the B_s^0 meson decay width difference with $B_s^0 \to J/\psi K^+K^-$ and $B_s^0 \to J/\psi\pi^+\pi^-$ decays*, *Phys. Rev.* **D 87** (2013) 112010 [arXiv:1304.2600] [INSPIRE].

[43] K. De Bruyn et al., *Probing New Physics via the $B_s^0 \to \mu^+\mu^-$ Effective Lifetime*, *Phys. Rev. Lett.* **109** (2012) 041801 [arXiv:1204.1737] [INSPIRE].

[44] R. Fleischer, *On Branching Ratios of B_s Decays and the Search for New Physics in $B_s^0 \to \mu^+\mu^-$*, *Nucl. Phys. Proc. Suppl.* **241-242** (2013) 135 [arXiv:1208.2843] [INSPIRE].

[45] A.J. Buras, R. Fleischer, J. Girrbach and R. Knegjens, *Probing New Physics with the $B_s \to \mu^+\mu^-$ Time-Dependent Rate*, *JHEP* **1307** (2013) 77 [arXiv:1303.3820] [INSPIRE].

[46] C. Bobeth et al., *$B_{s,d} \to \ell^+\ell^-$ in the Standard Model*, arXiv:1311.0903 [INSPIRE].

[47] C. Bobeth, M. Gorbahn and E. Stamou, *Electroweak Corrections to $B_{s,d} \to \ell^+\ell^-$*, arXiv:1311.1348 [INSPIRE].

[48] T. Hermann, M. Misiak and M. Steinhauser, *Three-loop QCD corrections to $B_s \to \mu^+\mu^-$*, *JHEP* **12** (2013) 097 [arXiv:1311.1347] [INSPIRE].

[49] A.J. Buras, J. Girrbach, D. Guadagnoli and G. Isidori, *On the Standard Model prediction for BR(Bs,d to $\mu^+\mu^-$)*, *Eur. Phys. J.* **C 72** (2012) 2172 [arXiv:1208.0934] [INSPIRE].

[50] M. Misiak, *Rare B-Meson Decays*, arXiv:1112.5978 [INSPIRE].

[51] A.J. Buras, *Weak Hamiltonian, CP-violation and rare decays*, hep-ph/9806471 [INSPIRE].

[52] J. Brod, M. Gorbahn and E. Stamou, *Two-Loop Electroweak Corrections for the $K- > \pi\nu\bar{n}u$ Decays*, *Phys. Rev.* **D 83** (2011) 034030 [arXiv:1009.0947] [INSPIRE].

[53] F. Beaujean, C. Bobeth, D. van Dyk and C. Wacker, *Bayesian Fit of Exclusive $b \to s\bar{\ell}\ell$ Decays: The Standard Model Operator Basis*, *JHEP* **08** (2012) 030 [arXiv:1205.1838] [INSPIRE].

[54] C. Bobeth, G. Hiller and D. van Dyk, *General Analysis of $\bar{B} \to \bar{K}^{(*)}\ell^+\ell^-$ Decays at Low Recoil*, *Phys. Rev.* **D 87** (2013) 034016 [arXiv:1212.2321] [INSPIRE].

[55] Particle Data Group collaboration, K. Nakamura et al., *Review of particle physics*, *J. Phys.* **G 37** (2010) 075021 [INSPIRE].

[56] G. Colangelo et al., *Review of lattice results concerning low energy particle physics*, *Eur. Phys. J.* **C 71** (2011) 1695 [arXiv:1011.4408] [INSPIRE].

[57] HPQCD collaboration, R. Dowdall, C. Davies, R. Horgan, C. Monahan and J. Shigemitsu, *B-Meson Decay Constants from Improved Lattice Nonrelativistic QCD with Physical u, d, s and c Quarks*, *Phys. Rev. Lett.* **110** (2013) 222003 [arXiv:1302.2644] [INSPIRE].

JHEP02(2014)112

[58] J. Laiho, E. Lunghi and R.S. Van de Water, *Lattice QCD inputs to the CKM unitarity triangle analysis*, Phys. Rev. **D 81** (2010) 034503 [arXiv:0910.2928] [INSPIRE].

[59] K. Chetyrkin et al., *Charm and Bottom Quark Masses: An Update*, Phys. Rev. **D 80** (2009) 074010 [arXiv:0907.2110] [INSPIRE].

[60] A.J. Buras, M. Jamin and P.H. Weisz, *Leading and Next-to-leading QCD Corrections to ϵ Parameter and $B^0 - \bar{B}^0$ Mixing in the Presence of a Heavy Top Quark*, Nucl. Phys. **B 347** (1990) 491 [INSPIRE].

[61] CDF Collaboration, D0 collaboration, T. Aaltonen et al., *Combination of the top-quark mass measurements from the Tevatron collider*, Phys. Rev. **D 86** (2012) 092003 [arXiv:1207.1069] [INSPIRE].

[62] A.J. Buras and D. Guadagnoli, *Correlations among new CP-violating effects in $\Delta F = 2$ observables*, Phys. Rev. **D 78** (2008) 033005 [arXiv:0805.3887] [INSPIRE].

[63] A.J. Buras, D. Guadagnoli and G. Isidori, *On ϵ_K beyond lowest order in the Operator Product Expansion*, Phys. Lett. **B 688** (2010) 309 [arXiv:1002.3612] [INSPIRE].

[64] J. Brod and M. Gorbahn, *Next-to-Next-to-Leading-Order Charm-Quark Contribution to the CP-violation Parameter ϵ_K and ΔM_K*, Phys. Rev. Lett. **108** (2012) 121801 [arXiv:1108.2036] [INSPIRE].

[65] J. Brod and M. Gorbahn, *ϵ_K at Next-to-Next-to-Leading Order: The Charm-Top-Quark Contribution*, Phys. Rev. **D 82** (2010) 094026 [arXiv:1007.0684] [INSPIRE].

[66] A.G. Dias, *Evading the few TeV perturbative limit in 3-3-1 models*, Phys. Rev. **D 71** (2005) 015009 [hep-ph/0412163] [INSPIRE].

[67] A.G. Dias, R. Martinez and V. Pleitez, *Concerning the Landau pole in 3-3-1 models*, Eur. Phys. J. **C 39** (2005) 101 [hep-ph/0407141] [INSPIRE].

[68] C. Bouchard, G.P. Lepage, C. Monahan, H. Na and J. Shigemitsu, *Standard Model predictions for $B \to Kll$ with form factors from lattice QCD*, Phys. Rev. Lett. **111** (2013) 162002 [arXiv:1306.0434] [INSPIRE].

[69] C. Bouchard, G.P. Lepage, C. Monahan, H. Na and J. Shigemitsu, *Rare decay $B \to Kll$ form factors from lattice QCD*, Phys. Rev. **D 88** (2013) 054509 [arXiv:1306.2384] [INSPIRE].

[70] W. Altmannshofer, A.J. Buras, D.M. Straub and M. Wick, *New strategies for New Physics search in $B \to K^*\nu\bar{\nu}$, $B \to K\nu\bar{\nu}$ and $B \to X_s\nu\bar{\nu}$ decays*, JHEP **04** (2009) 022 [arXiv:0902.0160] [INSPIRE].

[71] G. Buchalla and A.J. Buras, *The rare decays $K \to \pi\nu\bar{\nu}$, $B \to X\nu\bar{\nu}$ and $B \to \ell^+\ell^-$: An Update*, Nucl. Phys. **B 548** (1999) 309 [hep-ph/9901288] [INSPIRE].

[72] P. Colangelo, F. De Fazio, P. Santorelli and E. Scrimieri, *Rare $B \to K^{(*)}$ neutrino anti-neutrino decays at B factories*, Phys. Lett. **B 395** (1997) 339 [hep-ph/9610297] [INSPIRE].

[73] G. Buchalla, G. Hiller and G. Isidori, *Phenomenology of nonstandard Z couplings in exclusive semileptonic $b \to s$ transitions*, Phys. Rev. **D 63** (2000) 014015 [hep-ph/0006136] [INSPIRE].

[74] C. Bouchiat and P. Fayet, *Constraints on the parity-violating couplings of a new gauge boson*, Phys. Lett. **B 608** (2005) 87 [hep-ph/0410260] [INSPIRE].

[75] W. Marciano and A. Sirlin, *Constraint on Additional Neutral Gauge Bosons From Electroweak Radiative Corrections*, Phys. Rev. **D 35** (1987) 1672 [INSPIRE].

[76] H. Davoudiasl, H.-S. Lee and W.J. Marciano, *Muon Anomaly and Dark Parity Violation*, *Phys. Rev. Lett.* **109** (2012) 031802 [arXiv:1205.2709] [INSPIRE].

[77] ALEPH, DELPHI, L3, OPAL, LEP Electroweak collaborations, S. Schael et al., *Electroweak Measurements in Electron-Positron Collisions at W-Boson-Pair Energies at LEP*, *Phys. Rept.* **532** (2013) 119 [arXiv:1302.3415] [INSPIRE].

[78] E. Eichten, K.D. Lane and M.E. Peskin, *New Tests for Quark and Lepton Substructure*, *Phys. Rev. Lett.* **50** (1983) 811 [INSPIRE].

[79] CMS collaboration, *Search for Resonances in the Dilepton Mass Distribution in pp Collisions at $\sqrt{s} = 8$ TeV*, CMS-PAS-EXO-12-061.

[80] F. Richard, *A Z-prime interpretation of $B_d \to K^* \mu^+ \mu^-$ data and consequences for high energy colliders*, arXiv:1312.2467 [INSPIRE].

[81] Y. Coutinho, V. Salustino Guimarães and A. Nepomuceno, *Bounds on Z' from 3-3-1 model at the LHC energies*, *Phys. Rev.* **D 87** (2013) 115014 [arXiv:1304.7907] [INSPIRE].

[82] S. Profumo and F.S. Queiroz, *Constraining the Z' Mass in 331 Models using Direct Dark Matter Detection*, arXiv:1307.7802 [INSPIRE].

[83] C. Burgess and G. Moore, *The standard model: A primer*, Cambridge University Press, Cambridge, U.K. (2007) [ISBN-9780521860369].

[84] P.H. Frampton, *Strong electroweak unification at about 4-TeV*, *Mod. Phys. Lett.* **A 18** (2003) 1377 [hep-ph/0208044] [INSPIRE].